The Role of Thioredoxin-Interacting Protein (TXNIP) in Mediating the Effects of Phenformin and Torin1 on Glucose Uptake and Cell Proliferation

Kristofferson Tandoc

Division of Experimental Medicine
McGill University, Montreal
December 15, 2019

A thesis submitted to McGill University in partial fulfillment of the requirements of the degree of Master of Science

Abstract

Biguanides (e.g. metformin) are commonly used for type 2 diabetes mellitus (T2DM) treatment and have been reported to have anti-neoplastic activity. Systemic effects of biguanides are chiefly mediated by its effects in the liver, leading to decrease in gluconeogenesis and consequent reduction in insulinemia. However, compelling evidence shows that the anti-neoplastic effects of biguanides occur at least in part on a cell-autonomous manner by likely targeting complex I of the mitochondria. This results in inhibition of oxidative phosphorylation and leads to a compensatory increase in cellular glucose uptake. Biguanides also repress the mammalian/mechanistic target of rapamycin (mTOR). We have previously shown that metformin and mTOR inhibitors (PP242 and rapamycin) affect translation of a number of overlapping mRNAs. Unexpectedly, we identified thioredoxin-interacting protein (TXNIP) to be translationally repressed by metformin, but not by direct mTOR inhibitors. Independent of its role in cellular redox homeostasis, TXNIP functions as a negative regulator of glucose uptake in part by directly binding and internalizing GLUT1 and GLUT4. We hypothesize that the mTOR-independent suppression of TXNIP expression and subsequent increase in glucose uptake play a major role of adaptation of cancer cells to biguanide-induced energy stress. We show in MCF7 cells that phenformin (a more potent biguanide than metformin) increases glucose uptake and decreases TXNIP expression, while torin1 (active-site mTOR inhibitor) shows the opposite effects. Of note, both drugs decrease cell proliferation. Inhibition of oxidative phosphorylation by phenformin raises AMP/ATP ratio which, in turn, activates AMP-activated protein kinase (AMPK). In human, it has been shown that TXNIP residue Ser-308 is phosphorylated by AMPK, and as a result increases TXNIP degradation which is mediated by E3 ubiquitin ligase ITCH. In

this study, we aim to link TXNIP expression to the effects of phenformin and torin1 on glucose uptake and cell proliferation. To date, we have generated MCF7 cells that constitutively express wild-type and Ser-308-Ala mutant TXNIP constructs lacking endogenous promoter and 5' and 3' untranslated regions (UTRs). In this, we confirmed that a Ser-308-Ala mutation increases stability of TXNIP protein. Indeed, Ser-308-Ala TXNIP mutant was more stable than TXNIP wild-type in phenformin treated cells. This was paralleled by a ~20% reduction in glucose uptake in cells expressing the mutant vs. wild-type form of the protein. Since the overexpressed TXNIP constructs were devoid of endogenous transcriptional and translational regulatory elements, these finding suggests that phenformin suppression of TXNIP expression occurs at least in part at the level of protein stability, and that TXNIP degradation may mediate phenformin-induced increase in glucose uptake. We also generated CRISPR/Cas9-mediated TXNIP-deficient MCF7 cells that show increase in glucose uptake relative to control cells, confirming previous studies of TXNIP, a suppressor of glucose uptake. Deletion of TXNIP in MCF7 cells attenuates the effects of torin1 on glucose uptake. Since glucose metabolism plays a major role in cancer, these results suggest that TXNIP may play a central role in mediating the effects of biguanides and mTOR inhibitors on cancer metabolism.

Le résumé

Les biguanides (par exemple, la metformine) sont couramment utilisés pour le traitement du diabète de type 2 et ont été associes à des activités antinéoplasiques. Les effets systémiques des biguanides, observés principalement dans le foie, mènent à une diminution de la gluconéogenèse et de l'insulinémie. Cependant, il a été montré que les effets antinéoplasiques des biguanides agissent directement au niveau cellulaire en ciblant le complexe I de la mitochondrie, inhibant ainsi la phosphorylation oxydative. Cela mène a une augmentation compensatoire de l'absorption de glucose. Ce processus n'est pas encore bien compris, car la plupart des cancers présentent une augmentation de la glycolyse en aérobie (L'effet Warburg) en restant dépendants de la phosphorylation oxydative. Cela soulève également des aspects sous-explorés de la dérégulation du métabolisme du glucose dans le cancer. Nous avons précédemment montré que les inhibiteurs de la metformine et de mTOR (PP242 et rapamycine) perturbent le traductome en régulant la traduction de groupes d'ARNm qui se chevauchent. De manière inattendue, nous avons identifié que la protéine d'interaction de la thiorédoxine (TXNIP) est réprimée de manière traductionnelle par la metformine, mais non par les inhibiteurs de mTOR. Indépendamment de son rôle dans l'homéostasie d'oxydo-réduction cellulaire, TXNIP agit en tant que régulateur négatif de l'absorption du glucose, en partie en se liant et en intériorisant directement GLUT1 et GLUT4. Nous émettons l'hypothèse que les biguanides induisent une reprogrammation métabolique via une suppression de l'expression de TXNIP indépendante de mTOR, ce que mène à une augmentation ultérieure de l'absorption de glucose. Nous montrons que la phenformine (un biguanide plus puissant que la metformine) augmente l'absorption de glucose et diminue l'expression de TXNIP, tandis que torin1 (inhibiteur du site actif de mTOR) montre les effets opposés. Il est à noter que

les deux molécules convergent vers l'inhibition de la voie mTOR et de la prolifération cellulaire. L'inhibition de la phosphorylation oxydative par la phénformine augmente le rapport AMP / ATP qui, à son tour, active la protéine kinase activée par l'AMP (AMPK). Il a été démontré que le résidu TXNIP Ser-308 est phosphorylé par l'AMPK, ce qui augmente la dégradation de TXNIP via l'ubiquitine ligase ITCH E3. Dans cette étude, nous visons à associer l'expression de TXNIP aux effets de la phenformine et de la torine1 sur l'absorption du glucose et la prolifération cellulaire. À ce jour, nous avons généré des cellules qui expriment TXNIP (non-muté) ou le mutant Ser-308-Ala. Nous avons également généré des cellules MCF7 déficientes en TXNIP médiées par CRISPR / Cas9, qui montrent une augmentation de l'absorption de glucose par rapport aux cellules controles, confirmant les études sur TXNIP, un suppresseur d'absorption de glucose. Les cellules MCF7 traitées par Torin1 dépourvues de TXNIP montrent une augmentation de l'absorption du glucose, annulant les effets de torin1. Ici, nous montrons que la phenformine peut moduler la stabilité de TXNIP, ce qui devrait avoir un impact sur les effets anti-néoplasiques des biguanides.

Table of Contents

List of Figures

List of Abbreviations

18F-FDG	18f-Fluorodeoxyglucose
AKT	Protein Kinase B
AMPK	Amp-Activated Protein Kinase
ASK-1	Apoptosis Signal-Regulating Kinase 1
ATF4	Activating Transcription Factor 4
ATP	Adenosine Triphosphate
CaMKK	Calcium/Calmodulin Dependent Protein Kinase Kinase
CHORE	Carbohydrate Response Element
EIF4E	Eukaryotic Translation Initiation Factor 4e
EIF4EBP	Eukaryotic Translation Initiation Factor 4e Binding Protein
EIF4F	Eukaryotic Translation Initiation Factor 4f
EIF4G	Eukaryotic Translation Initiation Factor 4g
EMT	Epithelial-Mesenchymal Transition
ER	Endoplasmic Reticulum
FADH2	Flavin Adenine Dinucleotide
FBP	Fructose-1,6-Bisphosphate
FKBP12	Fk506-Binding Protein 12
FOXO1	Forkhead Box O1
G3P	Glyceraldehyde-3-Phosphate
G6P	Glucose 6-Phosphate
GLUT1	Glucose Transporter Type 1
GLUT10	Glucose Transporter Type 10

GLUT11	Glucose Transporter Type 11
GLUT12	Glucose Transporter Type 12
GLUT2	Glucose Transporter Type 2
GLUT3	Glucose Transporter Type 3
GLUT4	Glucose Transporter Type 4
GLUT5	Glucose Transporter Type 5
GLUT6	Glucose Transporter Type 6
GLUT7	Glucose Transporter Type 7
GLUT8	Glucose Transporter Type 8
GLUT9	Glucose Transporter Type 9
GTP	Guanosine Triphosphate
HER2	Human Epidermal Growth Factor 2
HIF1α	Hypoxia Inducible Factor 1 Subunit Alpha
IRE1α	Inositol-Requiring Enzyme 1 Alpha
LKB1	Liver Kinase B1
MAPK	Mitogen-Activated Protein Kinase
MTOR	Mechanistic/Mammalian Target Of Rapamycin
mTORC1	Mechanistic/Mammalian Target Of Rapamycin Complex 1
mTORC2	Mechanistic/Mammalian Target Of Rapamycin Complex 2
NADH	Nicotinamide Adenine Dinucleotide
NADPH	Nicotinamide Adenine Dinucleotide Phosphate
NLPR3	NLR Family Pyrin Domain Containing 3
OCT1	Organic Cation Transporter 1

PDPK1	3-Phosphoinositide Dependent Protein Kinase 1
PERK	Protein Kinase R (PKR)-Like Endoplasmic Reticulum Kinase
PFK	Phosphofructokinase
PI3K	Phosphoinositide 3-Kinase
PIP2	Phosphatidyl Inositol-4,5biphosphate
PIP3	Phosphatidyl Inositol-3,4,5-Triphosphate
PJS	Peutz-Jeghers Syndrome
PTEN	Phosphatase And Tensin Homolog
REDD1	Protein Regulated In Development And DNA Damage Response 1
RHEB	Ras Homolog Enriched In Brain
ROS	Reactive Oxygen Species
SLC2A	Solute Carrier Family 2
STAT3	Signal Transducer And Activator Of Transcription 3
TBC1D7	TBC1 Domain Family Member 7
TGF-β	Transforming Growth Factor Beta 1
TRX	Thioredoxin
TSC1	Tuberous Sclerosis Complex Subunit 1
TSC2	Tuberous Sclerosis Complex Subunit 1
TSG	Tumour Suppressor Gene
TXNIP	Thioredoxin-Interacting Protein
UPR	Unfolded Protein Response
VDUP1	Vitamin D3 Upregulated Protein 1

Acknowledgements

I would like to thank both of my supervisors and mentors Dr. Ivan Topisirovic and Dr. Michael Pollak for giving me the opportunity to work in their labs. Dr. Topisirovic has been very patient and understanding during my learning experience. His generosity has allowed me to participate in numerous exciting studies in collaboration with other labs. With his expertise in oncology at a clinical standpoint, Dr. Pollak has helped me understand better the clinical relevance of my findings. With both Dr. Topisirovic and Dr. Pollak's whole-hearted support, I learned and received proper training in research with so much to take away and for that I'm grateful. Lastly, I would like to extend my gratitude to all the members of the collaborative labs of Dr. Topisirovic and Dr. Pollak, as they too have been very supportive and provided me with a suitable work environment for learning.

Contribution of Authors

All experiments were designed and conducted by me with the guidance of my supervisors Dr. Ivan Topisirovic and Dr. Michael Pollak. Previous preliminary data that were used as guidelines for my current experiments were conducted by Marie Cargnello, Laura Hulea, Sophie Guenin, and Shannon Mclaughlan. Figures presented in this thesis were generated by me.

1 – INTRODUCTION

1.1. Glycolysis

Glucose is the central carbon source for cellular energetics and generation of building blocks such as nucleotides, amino acids and lipids (Burgess, 2011). Glycolysis is the reversible process of breaking down glucose to generate 2 ATP molecules along with 2 NADH and 2 pyruvate molecules in the cytoplasm (Berg JM, 2002). This metabolic process can occur in normoxia (aerobic) or anoxia (anaerobic). Under anoxic conditions, the breakdown of glucose to pyruvate produces lactate by NADH-dependent reduction of pyruvate to lactate by lactate dehydrogenase (LDH) (Goldblatt and Cameron, 1953), as the end-product. However, in normoxia, pyruvate is produced and converted to acetyl-coA for entry into the TCA cycle (Bacci et al., 1985). The glycolytic pathway is crucial for the brain due to its dependence on glucose as macronutrient for energy. In addition, this metabolic pathway produces intermediates that are linked to biosynthetic pathways for nucleotides, amino acids and lipids (Berg JM, 2002).

Upon entry into the cytoplasm, hexokinase or glucokinases initiate ATP and Mg^{2+}-dependent phosphorylation of glucose into glucose 6-phosphate (G6P) (Veramendi et al., 2002). G6P is utilized in the pentose phosphate pathway to generate ribose-5-phosphate for nucleotide synthesis along with nicotinamide adenine dinucleotide phosphate (NADPH) that scavenges reactive oxygen species (ROS) (Riganti et al., 2012). G6P is then converted to fructose-6-phosphate by phosphohexose isomerase and phosphorylated by phosphofructokinase-1 to produce fructose-1,6-bisphosphate (FBP), while consuming 1 ATP molecule. Aldolase enzymes then initiate cleavage of 6-carbon phosphate FBP to two 3-carbon sugar phosphates to form glyceraldehyde-3-phosphate (G3P) and dihydroxyacetone phosphate. Glyceraldehyde-3-phosphate dehydrogenase enzymes

convert two G3P intermediates into two 1,3-Bisphosphoglycerate molecules along with two NADHs. Consequently, two 1,3-Bisphosphoglycerate intermediates are converted to two 3-phosphoglycerates by phosphoglycerate kinases and generating two ATPs. Two 3-phosphoglycerate intermediates are then converted to two 2-phosphoglycerates by phosphoglycerate mutase, which is then converted to two phosphoenolpyruvates along with two molecules of water. Finally, the phosphoenolpyruvate intermediates are converted into two pyruvates along with 2 more ATPs (Berg JM, 2002).

1.2. The Warburg Effect

In 1924, Otto Warburg noted that the amount of glucose consumed by tumours is elevated relative to normal tissues and that this is correlated by the consequent production of lactic acid in normoxia (Warburg et al., 1927). The glycolytic pathway generates only 2 ATPs per molecule of glucose, however oxidative phosphorylation produces 36-38 ATPs per one glucose molecule (Flier et al., 1987). This raises the question of why a less efficient metabolism, at least in terms of ATP production, would be preferred by proliferating cells. This observation posed an interesting question concerning the supposedly enormous need for ATP in tumours and its overuse of the glycolytic pathway. Warburg proposed that cancer cells intensively utilize glycolysis as a compensatory mechanism due to defective mitochondria and impaired oxidative phosphorylation. Consequently, Warburg and his colleagues arrived at the conclusion that deprivation of oxygen, in addition to glucose starvation, could be a potential approach in preventing cancer growth (Warburg et al., 1927).

In 1929, Warburg's work was extended by Herbert Crabtree confirming Warburg's findings of increased glycolytic flux in tumours. However, Crabtree also discovered that tumours exhibited significant levels of respiration (Crabtree, 1929) and that cancer cells are intensively breaking down glucose in the presence of oxygen (aerobic glycolysis). This phenomenon was later coined as the "Warburg Effect" by Efraim Racker (Racker, 1972). Racker and his colleagues eventually found that the Warburg Effect is regulated by aberrant growth factor signaling, leading to the discovery of oncogenes. And thus, Warburg's initial findings and other works by Crabtree and Racker have revolutionized cancer biology (Birnbaum et al., 1987; Boerner et al., 1985; Flier et al., 1987; Hiraki et al., 1988). More recently, studies conclusively showed that the Warburg Effect was required for tumor growth (Fantin et al., 2006; Shim et al., 1998) and raised possibility of the potential of targeting both aerobic glycolysis and oxidative phosphorylation (Birsoy et al., 2015; Flaveny et al., 2015; Sullivan et al., 2015; Viale et al., 2014). Aerobic glycolysis is thought of as inefficient means to generate ATP and thus the significance of the Warburg Effect is still not fully understood, although it is postulated that this mode of metabolic reprogramming serves cancer cells to provide sufficient building blocks to support neoplastic growth, while protecting them from ROS (REF.. you can add any DeBerardinis review).

1.3. PI3K-AKT-mTOR signaling

1.3.1. PI3K

The phosphatidylinositol-4,5-biphosphate 3-kinase (PI3K)-AKT-mTOR signaling pathway is the central node that regulates metabolism and cell proliferation among many other essential processes (Kauffmann-Zeh et al., 1997; Laplante and Sabatini, 2009; Yao and Cooper, 1995) Dysregulation of the PI3K-AKT-mTOR signaling pathway has been associated with

pathological states (e.g. cancer and diabetes) (Laplante and Sabatini, 2012; Porta et al., 2014). The activation of PI3K/AKT signaling pathway is initiated by insulin and/or growth factors binding to insulin or insulin-like growth factor receptors resulting in intracellular phosphorylation of adaptor proteins such insulin receptor substrates (IRS1, IRS2, and IRS4) on its tyrosine residues (Haeusler et al., 2018). IRS1-2 are predominantly found in most cell types, but in human, IRS4 was found to be expressed in brain, thymus, kidney, and liver (Shaw, 2011). The phosphorylated tyrosine residues of adaptor proteins recruit the lipid kinase PI3K to the membrane (Domchek et al., 1992). PI3K are divided into three classes (I, II, and III). PI3K classes I, II and III phosphorylate the 3′-OH group of the D-myo-inositol head group to generate specific phosphoinositide forms. All three PI3K classes can generate phosphatidylinositol-3-phosphate (PIP), however, only class I can generate phosphatidylinositol-(3,4,5)-trisphosphate (PIP_3) (Jean and Kiger, 2014). Class I PI3K consists of four catalytic p110 subunits (p110α, p110β, p110γ, and p110δ) that catalyze the generation of PIP_3. The PI3K regulatory p85 subunits (p85, p55, p50) contain src-homology 2 (SH2) domains that bind to phosphorylated tyrosine residues of IRS proteins, consequently allowing association of PI3K class IA catalytic subunits (p110α, p110β, and p110δ) (Fruman et al., 2017). At the membrane PI3K generates phosphatidyl inositol-3,4,5-triphosphate (PIP_3) by phosphorylation of phosphatidyl inositol-4,5biphosphate (PIP_2) (Cantley, 2002). Forming PIP_3 serves as a messenger to recruit AKT to the cell membrane to be activated by phosphorylation by PDPK1 (3-phosphoinositide dependent protein kinase 1) (Alessi et al., 1997; Fresno Vara et al., 2004). In human tumours, the most common *PIK3CA* mutations responsible for hyperactivated PI3K signaling are identified as H1047R and E542K/E545K (Burke et al., 2012; Burke and Williams, 2015).

1.3.2. AKT/protein kinase B

Protein kinase B/AKT is a serine/threonine kinase downstream of PI3K that regulates pivotal cellular processes including metabolism, proliferation and survival (Myers and Cantley, 2010; Wan et al., 2007). The tumour suppressor PTEN (phosphatase and tensin homolog) acts to block AKT activation by catalyzing dephosphorylation of PIP_3 to PIP_2 (Stambolic et al., 1998). In cancer, AKT activity is often bolstered due to hyperactivation of PI3K, increased expression of *AKT1* gene, or abrogated PTEN activity (Cheng et al., 2005; Malanga et al., 2008). AKT mediates the translocation of glucose transporter GLUT1 and GLUT4 to the cell membrane and promotes expression of *Glut1* mRNA to the plasma membrane (Barthel et al., 1999; Kohn et al., 1996; Wieman et al., 2007). AKT also promotes hexokinase activity to phosphorylate internalized glucose molecules, thereby inhibiting their efflux to the extracellular space (Gottlob et al., 2001). The enzyme that catalyzes a crucial irreversible glycolytic process, phosphofructokinase (PFK), is also potentiated by AKT (Deprez et al., 1997). Tumours monitored by 18F-FDG-PET intensity signals show direct correlation with PI3K/AKT signaling activity and can be reversed by PI3K inhibitors (Benz et al., 2010; Lheureux et al., 2013). In addition, AKT inhibits forkhead box O1 (FOXO1) transcription factor by phosphorylation thereby inhibiting gluconeogenesis (Accili and Arden, 2004). AKT-mediated phosphorylation deactivates glycogen synthase kinase isoforms (GSK3α and GSK3β) indirectly causing glycogen production (Manning and Toker, 2017). Further, AKT signaling can mediate glucose uptake in physiological settings whereby targeted deletion of *AKT1* in the mouse mammary gland attenuates lactation-induced increase in glucose uptake, thereby preventing milk production (Boxer et al., 2006).

1.3.3. mTOR

The mechanistic/mammalian target of rapamycin (mTOR) is a serine/threonine kinase that forms the catalytic subunit of two distinct multiprotein complexes (mTORC1 and mTORC2) to regulate key cellular processes including metabolism, survival, growth and proliferation (Saxton and Sabatini, 2017). mTOR complex 1 (mTORC1) regulates both initiation and elongation in the mRNA translation processes (Roux and Topisirovic, 2018) by phosphorylating eukaryotic translation initiation factors 4E binding proteins (EIF4EBP1-3 in mammals) to prevent EIF4EBPs from binding EIF4E thereby allowing EIF4F complex to be formed and proceed to the initiation step of mRNA translation (Brunn et al., 1997; Gingras et al., 2001; Sonenberg and Hinnebusch, 2009). When mTORC1 is inhibited, EIF4EBPs are unphosphorylated and readily bind EIF4E to prevent EIF4F complex formation via blocking EIF4E association with EIF4G (Pause et al., 1994).

In addition, the mTOR pathway mediates upstream signaling cues from the PI3K/AKT signaling cascade to regulate metabolic reprogramming. AKT is activated by phosphorylation of both PDK1 and mTORC2 and, upon activation, phosphorylates TSC complex subunit 2 (TSC2) to form a complex with TSC complex subunit 1 (TSC1) and TBC1 domain family member 7 (TBC1D7) (Zech et al., 2016). This, in turn, leads to the inhibition of the TSC complex and increased levels of GTP-bound RHEB allowing for mTORC1 activation (Long et al., 2005; Sancak et al., 2007). Known functions of mTORC2 include regulation of cytoskeleton and survival via phosphorylation of AGC protein kinases (Saxton and Sabatini, 2017). More recently mTORC2 was implicated in systemic regulation of glucose and lipid metabolism and degradation of newly synthesized polypeptides (ADD REF.. recent review from Jachinto maybe, but check whether this is mentioned). Mutations in the components of the PI3K-AKT-mTOR pathway have been associated

with familial cancer syndromes such as tuberous sclerosis complex (*TSC1/2* mutation)(Martin et al., 2017), Cowden disease or PTEN hamartoma tumour syndrome (*PTEN* mutation)(Eissing et al., 2019), and Proteus Syndrome (*AKT1* mutation)(Lindhurst et al., 2011). Herein, mTORC1 promotes translation of mRNAs such as *HIF1A* and *MYC*, transcription factors that promote glucose uptake and glucose metabolism via transcription of genes such as the facilitative glucose transporter 1 (GLUT1), lactate dehydrogenase, hexokinase, and pyruvate kinase M2 (PKM2) (Kim et al., 2007; Osthus et al., 2000; Shim et al., 1997). The PI3K-AKT-mTOR signaling pathway is not the only mechanistic route in facilitating glucose uptake. Ras has been demonstrated to promote transcription of *GLUT1* mRNA to increase glucose influx and consumption (Murakami et al., 1992). Indeed, aberration of growth factor signaling cascades presents an increase in ability to facilitate internalization of glucose, a central macronutrient for energy source.

1.4. Glucose uptake in cancer

Acquiring extracellular nutrients is the mechanism that allows for the fulfillment of biosynthetic requirements of cells during proliferation whereby glucose represents one of the principal macronutrient for energy supply. The catabolism of glucose fuels the cell with NADH (generated in glycolysis) and $FADH_2$ (generated through the TCA cycle) in the electron transport chain to generate ATP and synthesize macromolecules that are necessary for growth and proliferation. Nearly 100 years since the discovery of the "Warburg Effect", the increased uptake of glucose by tumours has been actively utilized for clinical diagnosis and staging of tumours using positron emission tomography-based imaging of the uptake of a radioactive fluorine-labeled non-hydrolysable glucose analog, 18F-fluorodeoxyglucose (18F-FDG) (Almuhaideb et al., 2011). However, the question remains unanswered: Why do cancer cells internalize elevated amounts of

glucose? Nutrient internalization is regulated by signaling of growth factors (e.g. epidermal growth factor [EGF], insulin-like growth factor [IGF]) and hormones (e.g. insulin) (Thompson, 2011). During growth factor starvation, consumption of glucose is inhibited despite copious amount of glucose in the culture media in stem cells and neurons and, thereby restricting cellular energy needs for growth and proliferation (Lindsten et al., 2003; Rathmell et al., 2000). In addition, glucose uptake remains inhibited following overexpression of facilitative glucose transporter GLUT1 and hexokinase when growth factors are withdrawn in the presence of abundant glucose. (Rathmell et al., 2003). These observations suggest that glucose uptake is driven by growth factor signaling input. In cancer, cells acquire genetic mutations that alter activity of upstream kinase signaling regulators that result in the independence from extracellular stimuli-driven glucose uptake (Hanahan and Weinberg, 2000)

1.5. Glucose transporters

Since Warburg's observation that tumours consume enormous amounts of glucose relative to non-cancerous surrounding tissues, the role of glucose transporters in glucose metabolism is highlighted as rate-limiting in facilitating internalization of glucose molecules from the extracellular matrix and across the plasma membrane. Transformed cells via sarcoma virus infection acquire increased rates of glucose uptake relative to normal cells, and, in turn, causes glucose-induced expression of glucose transporters (Hatanaka, 1974). Facilitative glucose transporters (GLUTs) require no energy to allow glucose molecules across the hydrophobic cell membrane. In mammals, facilitative glucose transporters belong to the solute carrier 2A family (SLC2A) and are divided into three classes (Joost et al., 2002; Joost and Thorens, 2001). Each of

the glucose transporter proteins possesses different affinities for glucose and other hexoses such as fructose.

1.5.1. *Class I*

Class I of GLUTS is composed of GLUT1, GLUT2, GLUT3, and GLUT4. In addition to GLUT1, GLUT3, and GLUT4 having high glucose affinities, increased transport activity of GLUT1 has been reported to be due to glycosylation of the protein (Asano et al., 1991; Burant and Bell, 1992; Keller et al., 1989). GLUT1 is proposed as the main facilitative glucose transporter for glucose uptake and its level of expression varies in different tissues (Birnbaum et al., 1986; Fukumoto et al., 1988). GLUT2 expression is found in the liver, intestine, kidney, pancreatic beta-cells, and as well as in neurons (Thorens, 2015). The glucose transporter isoform GLUT3 has five-fold higher affinity to glucose than GLUT1 and, as glucose is the main carbon source of the brain, GLUT3 is predominantly and preferentially expressed in the brain (Flavahan et al., 2013). GLUT4 is localized in intracellular compartments and is translocated to the cell membrane of muscle and fat cells upon insulin stimulation (Rea and James, 1997). GLUT2 has a relatively lower glucose affinity among Class I GLUTs as fructose can also serve as its substrate or transport (Colville et al., 1993).

1.5.2. Class II

Class II is comprised of the fructose transporter GLUT5 and glucose transporters GLUT7, GLUT9, and GLUT11. In human, GLUT5 is the main transporter for fructose and therefore has weaker affinity for glucose and possesses high affinity for fructose in the small intestine (Burant et al., 1992). GLUT7 expression in human is reported to be in the small intestine and colon and has a high affinity (<0.5 mM) for glucose and fructose. However, GLUT7 is localized along the

small intestine where glucose and fructose are not readily available for transport and therefore suggest possibility of other substrates (Cheeseman, 2008). GLUT9 expression is reported to be exclusively in kidney and liver in humans (Phay et al., 2000) and presently lack sufficient studies on its activity. In human tissues, GLUT11 expression has been shown to be exclusively located in skeletal muscles and the heart and has a glucose affinity and activity that is suppressed by fructose presence. This suggests that GLUT11 is dominantly a fructose transporter. Further studies are presently lacking on regulation of GLUT11 expression and this may be of interest as exclusive expression of GLUT11 in heart and muscle may hint towards glucose metabolism and homeostasis in these tissues (Joost and Thorens, 2001).

1.5.3. Class III

Class III is composed of GLUT6, GLUT8, GLUT10, and GLUT12. These are facilitative glucose transports variedly expressed in different tissues in human. GLUT6 is predominantly expressed in the brain, spleen and peripheral leukocytes (Doege et al., 2000a) in human. Glucose transport activity of GLUT6 is poorly characterized but previous evidence shows weak affinity for glucose (Doege et al., 2000a). GLUT12 has been previously reported to mediate facilitative glucose transport in Xenopus laevis (African clawed frog) oocyte (Rogers et al., 2003). In human, expression of GLUT8 is mostly found in testis (Doege et al., 2000b; Ibberson et al., 2000), while GLUT10 expression is found in liver and pancreas predominantly (McVie-Wylie et al., 2001). In normal adult tissues, GLUT12 expression was detected in insulin-sensitive tissues, skeletal muscle, heart, and fat (Rogers et al., 2002) and was discovered in human breast cancer cell lines (Rogers et al., 2002). Presently, class III glucose transporters lack sufficient studies to characterize function and regulation of expression.

Ras and sarcoma virus-transformed rat fibroblasts were observed to have increased rates in glucose influx and GLUT1 expression (Birnbaum et al., 1987; Flier et al., 1987). In addition, src and ras-transformed mouse fibroblasts were reported to induce GLUT1 expression via enhancer elements binding to the promoter (Murakami et al., 1992). In ras and polyoma middle-T-transformed Caco-2cells (human colon carcinoma), GLUT1 and GLUT3 (high glucose affinity) expression were found to be increased with subsequent increase in glucose uptake, while GLUT2 and GLUT5 (low glucose affinity) (Baron-Delage et al., 1996). Breast cancer cell lines represent the most extensively used model in GLUT expression studies. GLUT1 represents the predominantly expressed GLUT in breast cancer cell lines, in addition to low levels of GLUT2-GLUT5 expression (Binder et al., 1997; Grover-McKay et al., 1998; Zamora-Leon et al., 1996). Moreover, increased GLUT1 expression and activity were also shown to correlate with tumour invasiveness (Grover-McKay et al., 1998). Initial studies in GLUT class II and III transporters report glucose affinity and uptake in *Xenopus laevis* oocytes (GLUT8 and GLUT10) and in transfected COS-7 cells (GLUT6, GLUT8, and GLUT11) (Dawson et al., 2001; Doege et al., 2000a; Doege et al., 2000b; Ibberson et al., 2000).

1.6. Pharmacological inhibitors of PI3K-AKT-mTOR pathway

Targeting metabolic vulnerabilities in cancer using kinase inhibitors is of high interest (Vander Heiden et al., 2009). Drugs that suppress PI3K-AKT-mTOR signaling have been reported to inhibit glucose uptake, a main phenotype denoted by the "Warburg Effect" (Pirola et al., 2003; Russell et al., 1999).

1.6.1. PI3K inhibitors

LY294002 and wortmannin have been extensively used in studies and are considered as first PI3K antagonists. Wortmannin is an extract from *Penicillium wortmannin* and exhibits irreversible inhibition of PI3K by targeting catalytic site. The synthetic PI3K inhibitor, LY294002, also targets catalytic site but can bind to PI3K reversibly. Both inhibitors contributed to many studies regarding significance of PI3K function due to their effective inhibition of PI3K activity, but are highly toxic to animals and have weak selectivity for PI3K isoforms (Knight et al., 2006; Marone et al., 2008). LY294002 and wortmannin have also paved the way for the following new PI3K inhibitors used in clinical trials: BEZ235, BGT226, BKM120, XL765, XL147, GDC0941, SF1126, PX-866, CAL-101. Dual PI3K-mTOR inhibitors BEZ235 (targets class I PI3K isoforms), BGT226, XL765 (solid tumour treatment), and SF1126 (low toxicity LY294002-derivative for solid tumour treatment) have entered Phase I clinical trials (Garcia-Echeverria and Sellers, 2008; Garlich et al., 2008; Marone et al., 2008; Serra et al., 2008)**.** GDC0941 has been reported to exhibit potent inhibition of tumorigenesis in patients with advanced solid tumours and is under Phase I clinical trials. Class I PI3K isoform-selective inhibitors BKM120, PX-866 (inhibits p110α, p110δ and p110γ), and CAL-101

(selectively targets p110γ) are also under Phase I clinical trials (Ihle et al., 2005; Maira et al., 2008).

1.6.2. AKT inhibitors

AKT inhibitors that have potent anti-tumour effects are categorized into three groups: lipid-based phosphatidylinositol analogs, allosteric, and ATP-competitive inhibitors. The clinically promising lipid-based phosphatidylinositol analogs include perifosine (D-21266) and PX316 (Gills and Dennis, 2004; Hilgard et al., 1997). Perifosine inhibits AKT activation by binding to phosphatidyl inositol-3,4,5-triphosphate (PIP3) and is currently under clinical trials (Hilgard et al., 1997). PX316 hold promising anti-proliferative results in tumour cells with high PI3K-AKT signaling activity (Gills et al., 2006). The inhibitory effects of both perifosine and PX316 non-selectively targets all isoforms of AKT. GSK690693 is a non-selective ATP-competitive AKT inhibitor with working doses at nanomolar concentrations conveying low toxicity effects. Both lipid-based phosphatidylinositol analogs and ATP-competitive AKT inhibitors display non-selective AKT inhibition as their limitations. Allosteric-binding AKT inhibitors have been developed to address this limitation and some of the drugs in clinical trials include: AKTi-1/2, MK-2206, and triciribine (Lindsley et al., 2008). AKTi-1/2 is an allosteric inhibitor of AKT1 and AKT2 isoforms that has shown encouraging anti-tumour effects (Chandarlapaty et al., 2011; Puglisi et al., 2014). An analog of AKTi-1/2, MK2206, has passed through Phase I clinical trials for treatments in patients with solid tumours. Finally, triciribine, a small cell-permeable nucleotide and allosteric inhibitor of AKT isoforms AKT1, AKT2, and AKT3 has been reported to exhibit potent anti-proliferative effects and induced apoptosis in cancer cells with altered PTEN activity and hyperactivated AKT (Yang et al., 2004). Triciribine

is also used in studies to overcome drug-resistant ovarian cancer cell and has entered phase I of clinical trials (Yang et al., 2008).

1.6.3. mTOR inhibitors

In the PI3K-AKT-mTOR signaling cascade, the mTOR pathway is the first to be targeted with the discovery of rapamycin (sirolimus), a bacteria derived antifungal agent and the first mTOR inhibitor used in research (Vezina et al., 1975). The potential of rapamycin was its immunosuppressive properties and anti-tumour effects (Faivre et al., 2006; Guertin and Sabatini, 2007; Hay, 2005; Sabatini, 2006; Yatscoff et al., 1993). Rapamycin is an allosteric inhibitor of mTORC1, which at least acutely does not affect mTORC2 (Sabatini, 2006 #388). Rapamycin associates with FK506-binding protein 12 (FKBP12) and binds to FKBP12-rapamycin binding (FRB) domain on mTOR preventing phosphorylation of mTOR downstream substrates (Saxton and Sabatini, 2017). However, mTORC2 is insensitive to rapamycin (unless exposure is prolonged) because mTORC2 cannot be bound and inhibited by the FKBP12-rapamycin complex due to structural placement of SIN1, one of the defining components of mTORC2 (Stuttfeld et al., 2018). Rapamycin analogs (rapalogs), everolimus and temsirolimus, mechanistically inhibit mTOR like rapamycin but have been reported to have improved results in cancer treatment (e.g. renal cell carcinoma) relative to rapamycin (Pal and Quinn, 2013). However, these allosteric mTOR inhibitors exhibit low dose response to advanced breast cancer and glioma (Faivre et al., 2006). In human, S6K has been shown to inhibit insulin signaling by directly phosphorylating IRS1 on Ser-270 (Zhang et al., 2008). In this, rapamycin-induced inhibition of mTORC1, not only inhibits S6K-IRS1 feedback, but also negates inhibitory Ser-639 on IRS1 in addition to decreased activation of IRS1 inhibitory Ser-789. Ultimately, this

allows for increased AKT activity that may reduce anti-neoplastic activity of rapamycin (Zakikhani et al., 2010). More recently, it has been demonstrated that rapamycin and rapalogs incompletely inhibit some of the mTORC1 outputs (see below), whereby their inability to fully inhibit phosphorylation of EIF4EBPs has been linked to their relatively modest anti-proliferative effects (Dowling et al., 2010).

ATP-competitive mTOR inhibitors, TORKinibs such as torin1, INK128 and Ku-0063794 show inhibition of both mTORC1 and mTORC2 and present promising anti-neoplastic effects. The dual inhibition of mTORC1 and mTORC2 by TORkinibs and torin1 is considered of interest as mTORC2 plays a key role in the full activation of AKT via phosphorylation of Ser-473 and thus necessary for the PI3K-AKT pathway (Sarbassov et al., 2005). Therefore, mTOR inhibitors that target both complexes of mTOR can also effectively target PI3K-AKT signaling by hindering AKT activation. Relative to rapamycin, and TORKinibs have been reported to exhibit more effective inhibition of cell growth and proliferation in cancer due to their enhanced inhibition of mTORC1 activity (in particular EIF4EBPs) and cap-dependent translation (Feldman et al., 2009; Thoreen et al., 2009). Allosteric and ATP-competitive mTOR inhibitors have paved the way for the third generation mTOR inhibitor called rapalink-1. Rapalink-1 is a mTOR inhibitor that inhibits mTOR allosterically, but also in an ATP-competitive manner (Roux and Topisirovic, 2018). Third generation mTOR inhibitors can efficiently suppress AKT signaling in addition to inhibition of mTOR-mediated phosphorylation of downstream substrates (Benjamin et al., 2011).

1.7. Biguanides

French lilac extracts that were traditionally used for diabetes treatment in Europe (Hu et al., 2001), were found to be rich in guanidine, which is a toxic compound, and was consequently discontinued due to the widespread use of insulin (Fryer et al., 2002; Zhou et al., 2001). The application of biguanides continued in the 1950s with metformin (Saha et al., 2004), phenformin (Carlson and Kim, 1973) and buformin (Beg et al., 1973) as anti-hyperglycemia agents, but buformin intake was lesser relative to the widely adopted phenformin (Ingebritsen et al., 1978; Zhou et al., 2001). Phenformin is more potent than metformin but was eventually withdrawn from use due to rare but serious adverse effects of lactic acidosis (Carling et al., 1987; Munday et al., 1988), while metformin thrived and became one of the most widely used agents in the treatment of type II diabetes (Pollak, 2017).

Interestingly, previous reports have also shown that type 2 diabetic patients subject to metformin treatment presented lower cancer risks relative to the use of other anti-diabetic agents in retrospective epidemiological studies (Bowker et al., 2006; Evans et al., 2005). Other reports presented decrease in cancer incidence and cancer-related mortality in adult diabetic patients taking metformin regularly (Bowker et al., 2006; Decensi et al., 2010; Evans et al., 2005; Landman et al., 2010; Libby et al., 2009; Monami et al., 2009). However, while these retrospective studies led to increased research related to biguanides as potential antineoplastic agents, not all follow-up studies agreed with the early findings (Suissa, 2017). In addition to retrospective studies, clinical trials have also been performed in non-diabetic patients where they show anti-proliferative effects of metformin in colonic epithelium (Hosono et al., 2010). Furthermore, metformin has low chances of fatality (severe hypoglycemia or lactic acidosis) even after intake of excessive dosage with

suicidal intent (Junien et al., 1981; McLelland, 1985). AMP-activated protein kinase (AMPK) is as serine/threonine kinase responsible for sensing cellular energy status (Lin and Hardie, 2018). When nutrients are limiting, AMPK represses ATP-consuming processes for energy conservation (Lin and Hardie, 2018). Metformin has also been reported to have anti-proliferative effects in many cell and mouse tumour models wherein it is observed to activated AMPK and repress mTOR signaling (Ben Sahra et al., 2008; Buzzai et al., 2007; Cantrell et al., 2010; Dowling et al., 2007; Gotlieb et al., 2008; Isakovic et al., 2007; Zakikhani et al., 2006). Notably, metformin also induces apoptosis in a few other cancer cell lines (Cantrell et al., 2010; Isakovic et al., 2007; Liu et al., 2009). However, randomized clinical trials have not revealed clinical benefit when metformin was added to standard chemotherapy regimes for advanced cancer (Kordes et al., 2015).

It was revealed that the mitochondrial complex I may represent the chief target of biguanides. Biguanides inhibit oxidative phosphorylation by targeting complex I of the electron transport chain and binding reversibly to its hydrophilic-hydrophobic domain interface (Andrzejewski et al., 2014; Bridges et al., 2014). At a systemic level, biguanides accumulate in the liver which coincided with downregulation of oxidative phosphorylation in hepatocytes. This causes energetic stress and subsequent activation of AMPK (Foretz et al., 2010; Shaw et al., 2005), inhibition of gluconeogenesis and, as a secondary consequence, a reduction in insulinemia (Pollak, 2013). At the cellular level, metformin and other lipophilic biguanides enter cells via organic cation transporter 1 (OCT1) and therefore the bioactivity of lipophilic biguanides varies between different cells due to difference in OCT1 expression (Segal et al., 2011). Moreover, upon entry metformin is unevenly distributed in the cells where it appears to mostly accumulate in the mitochondria

(Pollak, 2013). Ultimately, biguanide-induced suppression of ATP synthesis by oxidative phosphorylation promotes compensatory increase in glucose uptake.

1.8. AMPK

The interest in AMPK initially ignited when reports showed that AMPK was activated by exercise in both rat and human skeletal muscle (Fujii et al., 2000; Winder and Hardie, 1996; Wojtaszewski et al., 2000), where AMPK activation was shown to be LBK1-dependent in conditions of decreased cellular energy (Sakamoto et al., 2005). In the absence of LKB1 during muscle contraction, AMPK remains inactive and is thus unable to repress ATP-consuming processes for energy conservation. In all eukaryotes, AMPK is formed as heterotrimeric complexes that consist of catalytic α subunits (two isoforms: α1 and α2), regulatory β subunits (two isoforms: β1 and β2) and regulatory γ subunits (three isoforms: γ1, γ2, and γ3) (Lin and Hardie, 2018). The catalytic α subunits comprises the serine/threonine kinase domains at their N termini, where the residue Thr-172 in the activation loop is located for LBK1-mediated phosphorylation. The regulatory β subunits contain a C-terminal domain (β-CTD) that interacts with regulatory γ subunits. β subunits also have carbohydrate-binding modules (β-CBM) that bind to glycogen or starch, but its physiological role is unclear. Lastly, the regulatory γ subunits contain a motif with four tandem repeats responsible for binding AMP, ADP, and ATP. In its inactive form, ATP is normally bound to the γ subunit of AMPK. When AMPK is activated, the γ subunit binds AMP/ADP allowing a conformational change to expose Thr-172 in the activation loop for LBK1-mediated phosphorylation (reviewed in (Lin, 2018 #315)).

The discovery of AMPK manifested due to acetyl-CoA carboxylase and 3-hydroxy-3-methyl (HMG)-CoA reductase inactivation in the presence of ATP (Beg et al., 1973; Carling et al., 1987; Carlson and Kim, 1973). AMPK is as serine/threonine kinase that plays a principal role in sensing cellular energy status. AMPK remains inactive unless phosphorylated by LKB1 on Thr-172 located within the activation loop on the α subunit in an AMP-dependent manner (Hardie et al., 1999; Hawley et al., 2003; Hawley et al., 1996; Shaw et al., 2004; Stein et al., 2000). LKB1 was initially identified as a mutated gene in patients with Peutz-Jeghers syndrome (PJS) (Hemminki et al., 1998; Jenne et al., 1998). It was later reported that patients with PJS correlated with increased risk of malignant tumours (Boudeau et al., 2003; Giardiello et al., 1987) and paved the way to the idea of LKB1 as a tumour suppressor. Initial investigations involved the constitutive overexpression of LKB1 in cancer cells with somatically mutated (lung adenocarcinoma) or no LKB1 expression (HeLa) and resulted in suppressed proliferation (Sanchez-Cespedes et al., 2002; Tiainen et al., 1999). These findings linked LKB1, as a tumour suppressor gene, to the role of AMPK in cancer.

Independent of LKB1, AMPK was also shown to be activated by calmodulin-dependent protein kinase kinases (CaMKKs) (Hawley et al., 1995) in HeLa cells where LKB1 is not expressed (Hawley et al., 2005; Hawley et al., 1995; Hurley et al., 2005; Woods et al., 2005). Studies that lead to identifying AMPK downstream targets (e.g. acetyl-CoA carboxylase and HMG-CoA reductase) involved the use of AICAR, an intermediate in purine biosynthesis that activates AMPK (Gadalla et al., 2004). AMPK has been shown to inhibit energy-consuming key anabolic pathways such as gluconeogenesis (Lochhead et al., 2000), fatty acid synthesis (Sullivan et al., 1994) cholesterol synthesis (Corton et al., 1995; Henin et al., 1995), and protein synthesis (Bolster et al.,

2002; Horman et al., 2002; Inoki et al., 2003; Kimura et al., 2003; Krause et al., 2002). In addition AMPK can also promote catabolic pathways such as autophagy (Lindqvist et al., 2018), fatty acid oxidation (Merrill et al., 1997; Velasco et al., 1997), as well as fatty acid uptake (Luiken et al., 2003), and glucose uptake (Barnes et al., 2002; Merrill et al., 1997). The potential use of drugs that enhance insulin sensitivity such as biguanides for treatment of type 2 diabetes (insulin-insensitive) then became attractive due to findings relating to AMPK activation (Fryer et al., 2002; Hawley et al., 2002; Saha et al., 2004; Zhou et al., 2001). LKB1 has been shown to play an important role in biguanide-induced AMPK activation (Hawley et al., 2003; Sakamoto et al., 2005). Indeed, its role as a master regulator of metabolism provided the link for AMPK to be a potential target for drugs used in type 2 diabetes treatment (Winder and Hardie, 1999). Interestingly, previous reports have also shown that type 2 diabetic patients subject to metformin treatment presented lower cancer risks relative to the use of other anti-diabetic agents (Bowker et al., 2006; Evans et al., 2005).

1.9. Thioredoxin-interacting protein (TXNIP)

1.9.1. Initial findings

Thioredoxin-interacting protein (TXNIP) was discovered in 1994 by DeLuca's group in 1,25-dihydroxyvitamin D-3-treated HL-60 cells (human promyeloblasts) and was initially named vitamin D3 upregulated protein 1 (VDUP1) (Chen and DeLuca, 1994). This study revealed that TXNIP mRNA was upregulated by 1,25-dihydroxyvitamin D3 treatment and remains elevated for 24h (Chen and DeLuca, 1994). The work of DeLuca's group was later confirmed by Yodoi's group in 1999 and reportedly added that TXNIP plays a role in an important redox system by interacting with the thioredoxin (TRX) in its reduced state. TRX is of the main components of the thiol reducing system to scavenge reactive oxygen species (ROS) (Nishiyama et al., 1999). In addition, 1,25-dihydroxyvitamin D3-induced increase in TXNIP levels in HL-60 cells and/or overexpression of TXNIP in COS-7 (SV40-transformed *Cercopithecus aethiops* fibroblasts) and HEK293 (human embryonic kidney cells) cell lines resulted in suppressed TRX activity and expression (Nishiyama et al., 1999). Other studies showed that mutation of Cys32 and Cys35 on TRX prevented its association with thereby suggesting that TXNIP interacts with TRX catalytic site (Junn et al., 2000). The molecular mechanism of the anti-oxidative function of TXNIP via its interaction with TRX was later reported as a *de novo* intermolecular interaction of TXNIP(Cys247)-TRX(Cys32) forming a disulfide bridge (Hwang et al., 2014). Moreover, TXNIP dissociates from TRX in the presence of increased levels of ROS (Hwang et al., 2014). In the cytoplasm, apoptosis signal-regulating kinase 1 (ASK-1) and TRX are normally bound to each other thereby preventing ASK-1-mediated apoptosis (Saitoh et al., 1998). Thus, in addition to TRX inhibition, TXNIP-TRX interaction also promotes ASK-1-mediated apoptotic pathways (Junn et al., 2000). TXNIP induction is triggered by H_2O_2 treatment (Junn et al., 2000) thereby suggesting

its role in mediating oxidative stress. Also, other studies showed that TXNIP induction in hyperglycemia-induced oxidative stress is mediated my p38 MAPK (Schulze et al., 2004). Altogether, these studies initially highlighted a key role of TXNIP in regulating ROS by binding to TRX, a key component of a redox system necessary for signaling, cell survival, and proliferation (Saitoh et al., 1998; Yoshihara et al., 2014).

Independent of its role in redox reactions, TXNIP plays a principal role in glucose metabolism (Chen et al., 2010; Gorgens et al., 2017; Han and Ayer, 2013; Parikh et al., 2007; Stoltzman et al., 2011; Wu et al., 2013) and is highly involved in the development of diabetes (Minn et al., 2005; Muoio, 2007). In addition, TXNIP has been reported to serve a crucial part in senescence and aging (Cadenas et al., 2010; Sharma et al., 2017; Zhuo de et al., 2010) and has been thought to exert tumour suppressive properties in certain types of cancer (Baker et al., 2008; Goldberg et al., 2003; Han et al., 2003; Morrison et al., 2014; Nishinaka et al., 2004; Sheth et al., 2006). Below is the outline of all presented findings that have introduced TXNIP as a potential therapeutic target in pathological states ranging from diabetes to cancer. In addition, we present a graphical summary orchestrating the effects of biguanides and mTOR inhibitors on TXNIP expression and its role in glucose uptake and cell proliferation.

1.9.2. The role of TXNIP in glucose metabolism

TXNIP was identified as the most upregulated glucose-induced gene in a study using DNA microarrays in human islets and showed that overexpression of TXNIP in pancreatic beta-cells induced apoptosis (Minn et al., 2005). Indeed, in diabetic/insulin-resistant mice, TXNIP was reported to have elevated expression (Minn et al., 2005) (Chen et al., 2008). In support of this

evidence, TXNIP-null Akita mice (type 1 diabetic mice) were observed to have low blood glucose levels and consequent increase in survival (Huy et al., 2018). A decrease in glucose-induced apoptosis was also observed in TXNIP-deficient islets. In addition, TXNIP function was described to promoting pancreatic β-cell apoptosis in the context of ER stress-mediated activation of NLRP3 inflammasome (Anthony and Wek, 2012). In this, TXNIP-induction by suppression of miR-17 is achieved during activation of PERK-IRE1α axis via the unfolded protein response (UPR) pathway in response to endoplasmic reticulum (ER) stress (Lerner et al., 2012). These findings suggest that TXNIP may be linked to glucose toxicity and beta-cell apoptosis in diabetes and ER-stress related human diseases such as Wolfram Syndrome (Oslowski et al., 2012). In other studies, TXNIP was shown to be transcriptionally induced by a carbohydrate response element (ChoRE) transcription factor complex MondoA-MLX suggesting that TXNIP is a glucose responsive gene and plays an important part in glucose metabolism (Yu and Luo, 2009). Interestingly, glutamine, a non-essential amino acid carbon source for energy in cell growth and survival, was demonstrated to downregulate TXNIP transcription by recruiting a histone deacetylase-dependent corepressor to associate with MondoA (Kaadige et al., 2009). However, TXNIP repression was reportedly observed in the presence of abundant glutamine and glucose promoting glucose uptake for cell growth and proliferation (Kaadige et al., 2009).

A significant finding on TXNIP revealed its role in negatively regulating insulin-dependent and insulin-independent internalization of glucose molecules from the extracellular space in human skeletal muscles (Parikh et al., 2007). Insulin-stimulated activation of AKT leads to phosphorylation and activation of downstream target FOXO1 transcription factor (Zhang et al., 2006). Intriguingly, FOXO1 transcription factor has been reported as a transrepressor factor

inhibiting *TXNIP* transcription by binding to *TXNIP* promoter in both human and mouse pancreatic β-cells (Kibbe et al., 2013). These findings support the claim that insulin stimulation suppresses hyperglycemia-induced TXNIP expression to promote glucose uptake and prevent pancreatic beta-cell apoptosis in human and mouse (Shaked et al., 2009; Wu et al., 2013). Mechanistically, it appears that TXNIP-mediated suppression of glucose uptake entails clathrin-mediated endocytosis of GLUT1 (Wu et al., 2013) and GLUT4 (Waldhart et al., 2017). It suggests thatglucose-induced TXNIP expression suppresses glucose uptake to re-establish energy homeostasis during GLUT1 and GLUT4-mediated rapid glucose influx in insulin-independent and insulin-dependent conditions respectively. *In vivo* studies of glucose metabolism using TXNIP-null mice reported cases of hypoglycemia and hypoinsulinemia relative to control littermates (Chutkow et al., 2008). Intriguingly, it has been demonstrated that TXNIP inhibits insulin transcription factor MAFA by promoting miR-204 expression via inhibition of signal transducer and activator of transcription 3 (STAT3) expression (Xu et al., 2013). Other studies showed that the transcription factor complex MondoA-MLX serves as a sensor of glucose-6-phosphate converted by hexokinases from glucose, thereby allowing translocation of MondoA-MLX into the nucleus to bind to the *TXNIP* promoter (Stoltzman et al., 2008). This suggests that TXNIP acts as a gate keeper of glycolytic flux to prevent rapid consumption of glucose in normal cells. In addition, TXNIP suppression in conditions of compromised cellular energy status in studies, using inhibitors of oxidative phosphorylation in HEK293 cells, may hint a role in mediating compensatory increase in glucose uptake for source of cellular energy (Yu et al., 2010).

Mechanisms of regulation of TXNIP expression also remain unclear. AMPK is a serine/threonine kinase that plays a principal role in detecting changes in cellular energy (Lin and Hardie, 2018).

In conditions of compromised cellular energy, AMPK is activated to suppress anabolic pathways to limit ATP consumption (Lin and Hardie, 2018) review and promote glucose uptake (Barnes et al., 2002; Kurth-Kraczek et al., 1999; Merrill et al., 1997). The mechanism behind AMPK-mediated induction of glucose uptake is linked to TXNIP suppression. It was reported that activated AMPK phosphorylates TXNIP on Ser-308 which recruits ITCH, an E3 ubiquitin ligase, for TXNIP polyubiquitination and subsequent degradation via ubiquitin-proteasome pathway (Liu et al., 2016; Ohtake et al., 2018; Wu et al., 2013). Regulation of TXNIP stability was reported to be mediated by ITCH via interaction with two PPxY motifs on TXNIP (Liu et al., 2016). In addition to AMPK-mediated TXNIP regulation, TXNIP suppression can also be mediated by AKT phosphorylation on Ser-308 promoting its proteasomal degradation during insulin-stimulated glucose uptake (Waldhart et al., 2017). In support of this evidence, TXNIP suppression was readily observed upon insulin stimulation, contrary to the dramatic TXNIP induction in response to glucose-stimulation (Parikh et al., 2007). The mechanistic/mammalian target of rapamycin (mTOR) has been extensively shown to be involved in glucose metabolism pathways (Kim et al., 2007; Osthus et al., 2000; Shim et al., 1997). Interestingly, a study has implicated mTORC1-mediated glucose uptake to *TXNIP* transcriptional regulation. In this study, MondoA was described to be sequestered by mTOR in the cytoplasm preventing its binding to TXNIP promoter whereby the inhibition of mTOR reverses this mechanism which leads to increase in TXNIP levels (Kaadige et al., 2015). Moreover, TXNIP was also reported to inhibit mTORC1 via ATF4-induced REDD1 expression in response to stress signals (Jin et al., 2011). In this, REDD1 stabilization by TXNIP inhibits mTOR by promoting assembly of TSC complex thereby inhibiting mTOR activity.

1.9.3. TXNIP in cancer

Evidence of the implication of TXNIP in cancer was initially observed with its marked downregulation in breast, lung, and stomach cancers (Han et al., 2003). TXNIP expression in many cancer cell lines have also been observed to be suppressed relative to their non-transformed counterparts (Jeon et al., 2005; Kwon et al., 2010; Masaki et al., 2012; Nishinaka et al., 2004). In different cancer cell models, ectopic TXNIP overexpression leads to increased apoptosis (Baker et al., 2008), decreased metastasis (Goldberg et al., 2003), and cell-cycle arrest at G0/G1 phase (Han et al., 2003). Moreover, in culture conditions where serum is deficient, cell-cycle arrest and suppressed cell proliferation also correlated with elevated TXNIP expression (Han et al., 2003). In addition, it has been shown that TXNIP-deficiency resulted in increased cell proliferation in human and mouse fibroblasts (Jeon et al., 2005). *In vivo* studies have also shown that TXNIP-null mice are more susceptible to diethylnitrosamine-induced hepatocarcinogenesis relative to littermate wildtype controls (Kwon et al., 2010). To corroborate this finding, TXNIP deficiency has also shown enhanced transforming growth factor beta (TGF-beta) signaling and consequently promoting epithelial-mesenchymal transition (EMT) in human cancer cell lines (Knoll et al., 2014; Masaki et al., 2012). Another evidence shows that constitutive overexpression of TXNIP in thyroid cancer cells results in a decrease in tumour size and metastasis in mouse models (Morrison et al., 2014). TXNIP expression is also correlated with better overall survival rates in breast cancer patients (Nie et al., 2015); see below).

Human epidermal growth factor receptor 2 (HER2)-driven breast cancer cell lines BT474 and SKBr3 have been presented with low levels of TXNIP expression. In this, treatment with HER-1/HER-2 inhibitors cetuximab, trastuzumab, and lapatinib resulted in increased TXNIP expression

and induced cell-cycle arrest and apoptosis (Nie et al., 2015). Notably, in triple negative breast cancer patients, MYC/TXNIP gene signature ratio has been reported as a prognostic marker for overall survival and tumour metastasis, whereby low MYC expression with high TXNIP expression results in better clinical outcome and increased survival and remains true for the contrary (high MYC/low TXNIP) (Shen et al., 2015). An important finding revealed that hyaluronidase-induced extracellular remodeling results in TXNIP suppression and consequent increase in glucose uptake highly needed for cell migration and invasion during tumorigenesis (Sullivan et al., 2018). Altogether, these findings present the significance of TXNIP expression as a putative tumour suppressor gene (TSG), which remains mechanistically poorly understood.

2 – OBJECTIVE

Biguanides (e.g. metformin) are widely used for treating type 2 diabetes and have been reported to exhibit anti-neoplastic activity (Bailey and Turner, 1996; Pollak, 2010; Zakikhani et al., 2006). Biguanides are thought to target oxidative phosphorylation by inhibiting mitochondrial complex I (Bridges et al., 2014). In turn, this leads to increase in AMP/ATP levels and activation of AMP-activated protein kinase (AMPK) (Hardie, 2011). AMPK activation downregulates energy consumption, in part by suppressing translation via mTOR (Hay and Sonenberg, 2004; Hsieh et al., 2012; Proud, 2013). Moreover, inhibition of oxidative phosphorylation by biguanides causes an energetic stress that is compensated by increased glucose uptake. However, the underpinning mechanism(s) are not clearly defined. We have previously shown that metformin and mTOR inhibitors regulate translation of a number of overlapping mRNAs (Larsson et al., 2012). Surprisingly, we also identified mRNAs, including Thioredoxin-interacting protein (TXNIP), that are translationally repressed by metformin but not by mTOR inhibitors (Larsson et al., 2012). Independent of its role in redox homeostasis, TXNIP is identified as a negative regulator of glucose uptake (Parikh et al., 2007), in part by directly binding and internalizing GLUT1 when excess glucose is present (Wu et al., 2013). The objective of this study is to understand the role of TXNIP in mediating the effects of biguanides and mTOR inhibitors on the glucose uptake and neoplastic growth as presented by the graphical summary of relevant findings (Figure 1).

Figure 1

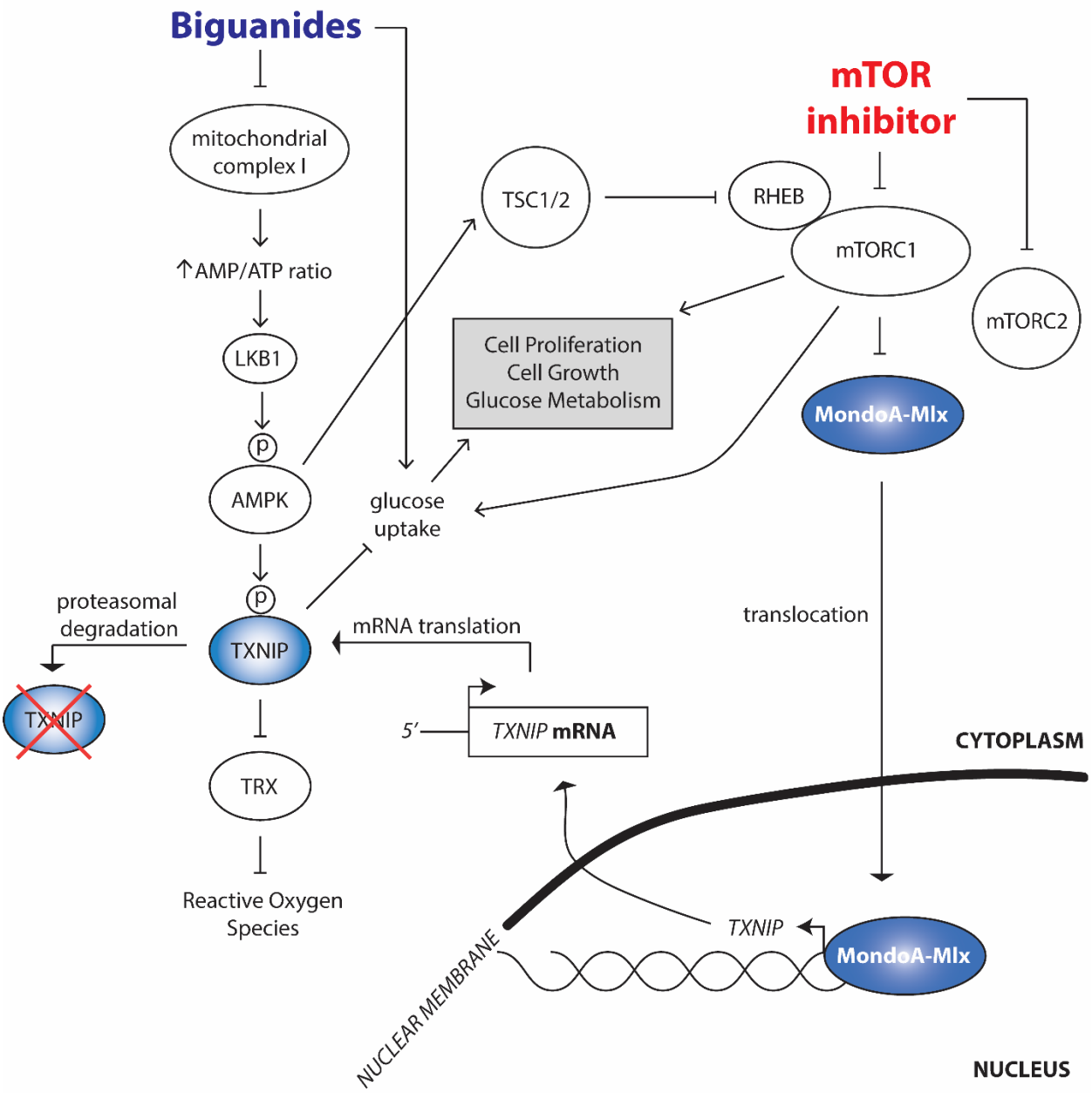
Biguanides
mitochondrial complex I
↑AMP/ATP ratio
LKB1
P
AMPK
TSC1/2
RHEB
mTOR inhibitor
mTORC1
mTORC2
Cell Proliferation
Cell Growth
Glucose Metabolism
MondoA-Mlx
glucose uptake
proteasomal degradation
P
TXNIP
TXNIP
mRNA translation
translocation
5′
TXNIP mRNA
CYTOPLASM
TRX
Reactive Oxygen Species
TXNIP
MondoA-Mlx
NUCLEAR MEMBRANE
NUCLEUS

Figure 1 – *Schematic presentation of the role of TXNIP in the effects of biguanides and mTOR inhibitors on glucose uptake.*

Biguanide-induced (e.g. phenformin) energetic stress by inhibiting mitochondrial complex I (Bridges et al., 2014) raises AMP/ATP ratio and thereby activates LKB1 to phosphorylate and activate AMPK (Hardie, 2011). The activation of AMPK occurs when resources are limiting to reduce energy-consuming processes (Lin and Hardie, 2018). This is in part achieved when activated AMPK induces TSC1/2 complex to inhibit mTOR activity and consequently reducing anabolic processes (Hay and Sonenberg, 2004; Hsieh et al., 2012; Proud, 2013). Alternatively, mTOR activity is also inhibited using allosteric (e.g. rapamycin) (Sabatini, 2006) and ATP-competitive mTOR inhibitors (e.g. torin1) (Thoreen et al., 2009). Torin1 and other active-site mTOR inhibitors target both mTOR complexes 1 (mTORC1) and 2 (mTORC2) (Sarbassov et al., 2005), while rapamycin and its analogs only inhibit mTORC1 (Pal and Quinn, 2013). The effects of both biguanides and mTOR inhibitors converge on mTOR, the central regulator of key processes for cell growth and proliferation but impinge opposing effects on TXNIP expression and consequently on glucose uptake (Figure 1). Independent of its role in regulating TRX activity in scavenging reactive oxygen species (ROS), TXNIP is a negative regulator of glucose uptake. Biguanides have been shown to downregulate TXNIP expression through ubiquitination and proteasomal degradation initiated by AMPK phosphorylation on TXNIP on Ser-308. Increased expression of TXNIP with mTOR inhibitors has been shown to be transcriptionally regulated, wherein mTOR inhibition allows the sequestered transcription factor complex MondoA-Mlx to bind to the *TXNIP* promoter. With this, the use of biguanides shows increase in glucose uptake, while mTOR inhibitors shows an opposite effect.

3 – METHODOLOGY

Cell Lines and Cell Culture Conditions

MCF7 cells were cultured in Roswell Park Memorial Institute medium (RPMI 1640; Wisent #350-000-CL), supplemented with 10% heat-inactivated fetal bovine serum (Wisent), 1% penicillin/streptomycin (Wisent; #450-201-EL) and 2mM L-Glutamine (Wisent, #609-065-EL) to obtain 4mM L-Glutamine final concentration. HEK293 (Gandin et al., 2016) and HeLa (ATCC #CCL-2) cells were cultured in Dulbecco's modified Eagle's medium (DMEM; Wisent #319-005-CL), supplemented with 10% heat-inactivated fetal bovine serum (Wisent), 1% penicillin/streptomycin (Wisent; #450-201-EL) and 2mM L-Glutamine (Wisent, #609-065-EL) to obtain 6mM L-Glutamine final concentration. Where indicated, cells were treated with phenformin hydrochloride (Sigma) and torin1 (Tocris Bioscience).

Generation of cell lines overexpressing TXNIP wildtype and mutant (SER-308-ALA)

Wild-type (Knoll et al.) and mutant (SER-308-ALA) thioredoxin-Interacting protein (TXNIP) CDS (NorClone Biotech Labs) were subcloned into neomycin-resistant lentiviral vector pLV[Exp]-Neo-CMV (by Vector Builder #VB160727-1030erw). Lentiviral supernatants were generated as described at https://portals.broadinstitute.org/gpp/public/resources/protocols. Supernatants were applied on target cells with polybrene (6 μg/mL). MCF7 cells were infected every 24 hours for 3 days (total of 3 rounds of infection), selected with G418 (1 mg/mL, Bio Basic) for 72 hours.

Proliferation and Cell Viability Assays

For the bromodeoxyuridine (BrdU) incorporation assay (Cell Proliferation ELISA BrdU Kit from Roche), MCF7 cells were seeded in 96-well plates (4000 cells/well) and maintained as indicated in the figure legends of Figure 4 for 72h. Preliminary results were performed once (n=1), including media and DMSO (vehicle) control wells, as per the manufacturer's instruction. Absorbance at 370nm (reference wavelength 492nm) was measured using a Benchmark Plus microplate reader (Bio-Rad). Viable cell count was performed as previously described (Gravel et al., 2014). Briefly, MCF7 cells were seeded in 6-well culture plates ($1.0x10^5$ cells/well), treated 24h later as indicated in figure legends of Figure 4 for 72 hours, prior to trypsinization and trypan blue staining (1:1 v/v ratio). Viable cell number were counted using an automated cell counter (Invitrogen) for the indicated samples and were normalized to those obtained for vehicle-treated cells (control cells). Data are expressed as a percentage of inhibition relative to control cells.

Reverse Transcription – Quantitative Polymerase Chain Reaction (RT-qPCR)

RNA was extracted using Trizol (Thermo Fisher Scientific) according to manufacturer's instructions. RT-qPCR was performed as previously described (Miloslavski et al., 2014). RT and qPCR were performed by SuperScript III Reverse Transcriptase and Fast SYBR Green Mastermix (Invitrogen), respectively. Experiments were done at least in 2 independent experiments (n = 2) whereby every sample was analyzed in a technical triplicate.

Analyses were carried out using relative standard curve method as described in http://www3.appliedbiosystems.com/cms/groups/mcb_support/documents/generaldocuments/cms_040980.pdf. Primers are listed in the Table 1 and the Key Resources Table.

Primer	Sequence (5'-3')
Human_*TXNIP* (FWD)	TGTTCATTCCTGATGGGCGG
Human_*TXNIP* (Gorgens et al.)	TGGCCATTGGCAAGGTAAGT
Human_*CCND3* (FWD)	CTGGATCGCTACCTGTCTTG
Human_*CCND3* (Gorgens et al.)	AGGCAGTCCACTTCAGTGC
Human_*ACTB* (FWD)	ACCACACCTTCTACAATGAGC
Human_*ACTB* (Gorgens et al.)	GATAGCACAGCCTGGATAGC
Human_*GAPDH* (FWD)	TGTTGCCATCAATGACCCCTT
Human_*GAPDH* (Gorgens et al.)	CTCCACGACGTACTCAGCG

Table 1. List of RT-qPCR primers used. Primers were designed via NCBI Primer Blast. All primer efficiencies were verified through standard curves using template cDNA generated from MCF7 cells. Primer length, melting temperature, and GC content were optimized to 20-24bp, 55-65^{o}C, and 40-60% respectively.

Western Blotting and Antibodies

Cells were washed in cold 1X PBS and were harvested on ice prior to centrifugation at 2000 RPM in 4C to pellet harvested cells. Samples on ice were resuspended in lysis buffer [50mM Tris/HCL pH 7.4, 5mM NaF, 5mM Na pyrophosphate, 1mM EDTA, 1mM EGTA, 250mM mannitol, 1% (v/v) triton x-100, 1mM DTT, 1X complete protease inhibitors (Roche), 1X PhosSTOP (Sigma-Aldrich)]. Protein concentrations in cell extracts were determined using Pierce BCA Protein Assay Kit (Thermo Fisher Scientific) and samples were prepared in 4X Laemmli buffer recipe. Proteins were resolved by SDS-PAGE, and then transferred to nitrocellulose membranes (Bio-Rad). The following primary antibodies were used: anti-TXNIP (NBP1-54578) from Novus, anti-β-actin (Clone AC-15) #A1978, anti-HA #H6908, from Sigma (Saint Louis, Missouri, USA); anti-TXNIP (D5F3E) #14715, anti-4E-BP1(53H11) #9644, anti-p-4E-BP1 (Ser65) (174A9) #9456, anti-rpS6 (5G10) #2217, anti-p-rpS6 (Ser240/244) #2215, anti-S6K (49D7) #2708, anti p-S6K (Thr389) (#9234), anti-GAPDH (14C10) #2118, all from Cell Signaling Technologies (CST) (Danvers, MA, USA); Antibodies were diluted in 5% (w/v) BSA or 5% (w/v) non-fat dry milk

(depending on the manufacturer's instructions), in 1X TBS/0.5%Tween-20, at the following dilutions: 1:1000 dilution for anti-TXNIP (D5F3E) (CST #14715, anti-HA #H6908 (Sigma), anti-p-4E-BP1 (Ser65) (174A9) (CST #9456), anti-S6K (49D7) (CST #2708), anti p-S6K (Thr389) (CST #9234); and 1:5000 dilution for anti-β-actin (Clone AC-15) (Sigma #A1978) and anti-GAPDH (14C10) (CST #2118). Membranes were incubated with antibodies overnight at 4°C. Horseradish peroxidase-conjugated anti-rabbit IgG and anti-mouse IgG antibodies were from Amersham Biosciences (Baie d'Urfé) and were used at 1:5,000 dilution in 5% (w/v) non-fat dry milk in 1XTBS/0.5%Tween 20 for 1 hour at room temperature. Signals were revealed by chemiluminescence (ECL, GE Healthcare) on Azure C300 chemiluminescent western blot imaging system (Azure Biosystems). Where possible, the membranes were stripped and re-probed.

Glucose Consumption Assay

MCF7 cells were seeded in 6-well plates and cultured in complete medium for 24h in order to obtain 80% density. Medium was replaced with 0.5 ml of indicated treatment media, and cells were cultured for 6h. Subsequently, supernatant samples were collected, and cells were counted by trypan blue exclusion. Measurement of glucose concentration in samples was done as previously described (Gravel et al., 2014). Total consumption was calculated by subtracting results from baseline glucose concentration, measured in samples from media incubated in identical conditions, without cells. Molar concentrations of glucose were multiplied by total media volume/well (0.5 ml) and normalized by cell count; data were expressed as μM glucose/μg of protein/h, or normalized relative to DMSO control.

Polysome profiles and RT-qPCR

Briefly, MCF7 cells were seeded in two 15cm Petri dish, harvested at 80% confluency and lysed in hypotonic lysis buffer (5mM Tris HCl pH7.5, 2.5mM $MgCl_2$, 1.5mM KCl, 100 µg/ml cycloheximide, 2mM DTT, 0.5% Triton, 0.5% Sodium Deoxycholate). Polysome-profiling was carried out as described (Gandin et al., 2014). Fractions were collected as described in (Gandin et al., 2014) and RNA was extracted using Trizol (Thermo Fisher Scientific) according to manufacturer's instructions. RT-qPCR was performed as previously described (Miloslavski et al., 2014). RT and qPCR were performed by SuperScript III Reverse Transcriptase and Fast SYBR Green Mastermix (Invitrogen), respectively. Experiments were done at least in independent duplicates (n=2) whereby every sample was analyzed in a technical triplicate. Analyses were carried out using relative standard curve method as described in http://www3.appliedbiosystems.com/cms/groups/mcb_support/documents/generaldocuments/cms_040980.pdf. Polysome to 80S ratios were calculated by determining integrated area under the curve of 80S (monosome) peak and comparing to the integrated area under curve corresponding to heavy polysome peaks (>3 ribosomes).

4 – RESULTS

4.1 *TXNIP expression correlates to ameliorated survival rate in different cancer types*

Kaplan-Meier plots, adapted from kmplot.com (Lanczky et al., 2016), show two populations (low and high *TXNIP*) of patients in different cancer types - cervical squamous carcinoma, kidney renal clear cell carcinoma, breast cancer, sarcoma, and uterine corpus sarcoma. Hazard ratio (HR) refers to the measure of the effect of high *TXNIP* expression on outcome (survival rate). Except for breast cancer, HR for all other cancer types were roughly 0.5 independently of the stage or cancer subtype (Figure 2). This indicates that half as many patients with high TXNIP expression will have better probability of survival. In support of these Kaplan-Meier plots, a number of studies have outlined tumor-suppressive TXNIP functions and linked its high expression with improved prognosis (Nie et al., 2015; Shen et al., 2015; Sullivan et al., 2018).

Figure 2

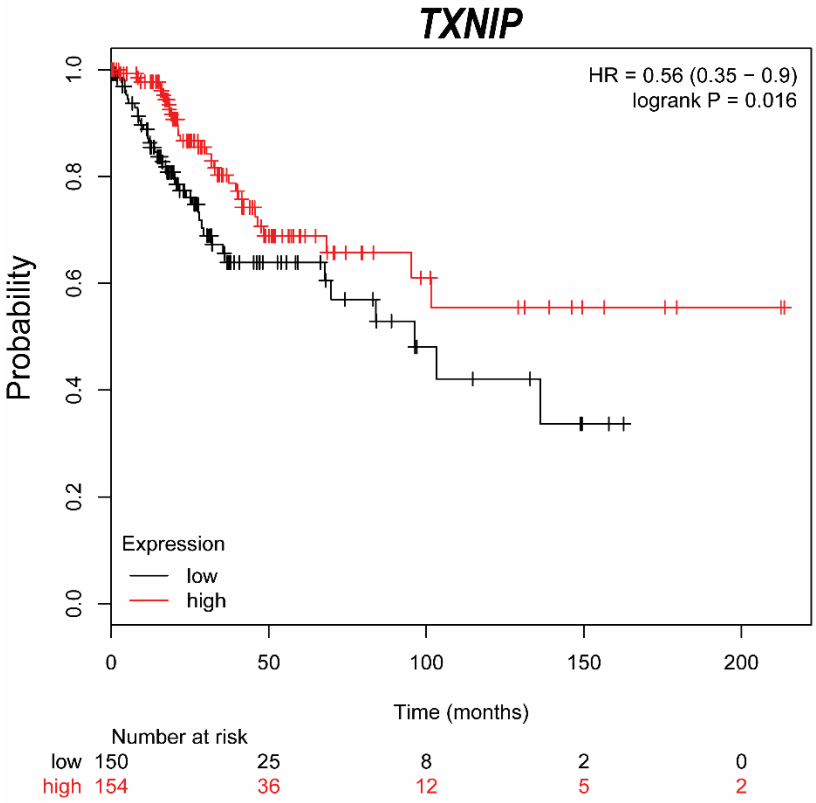

Cervical squamous carcinoma

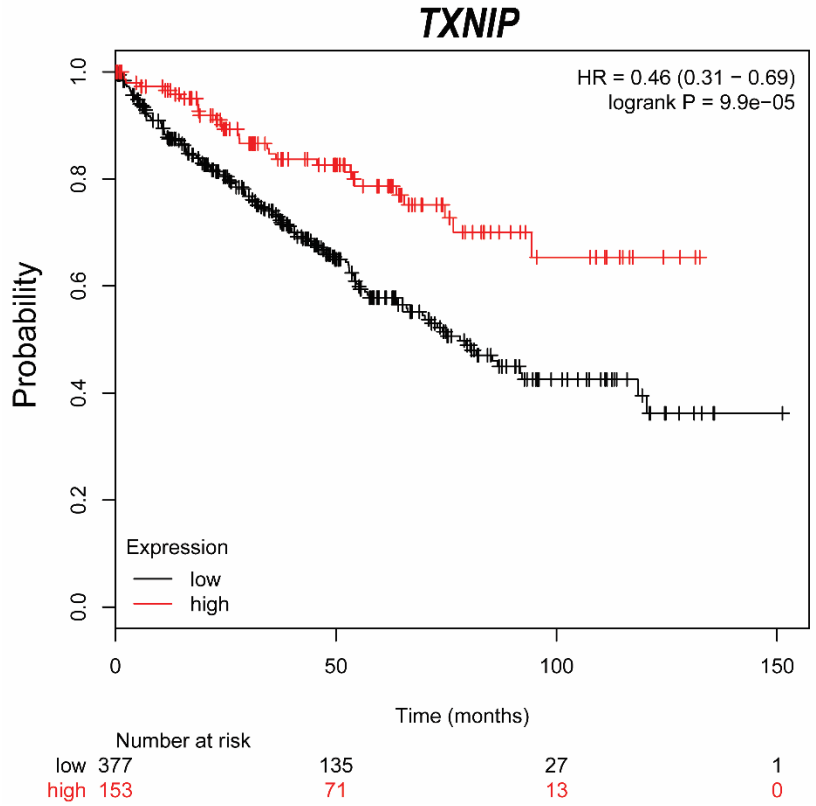

Kidney renal clear cell carcinoma

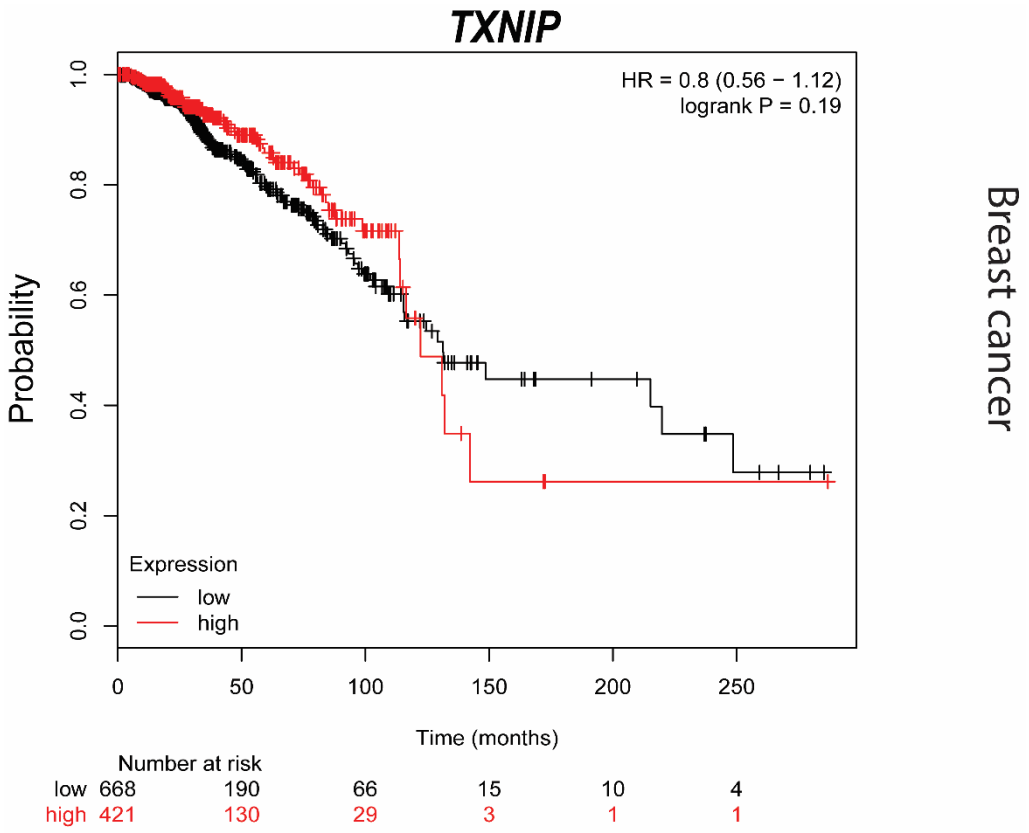

Breast cancer

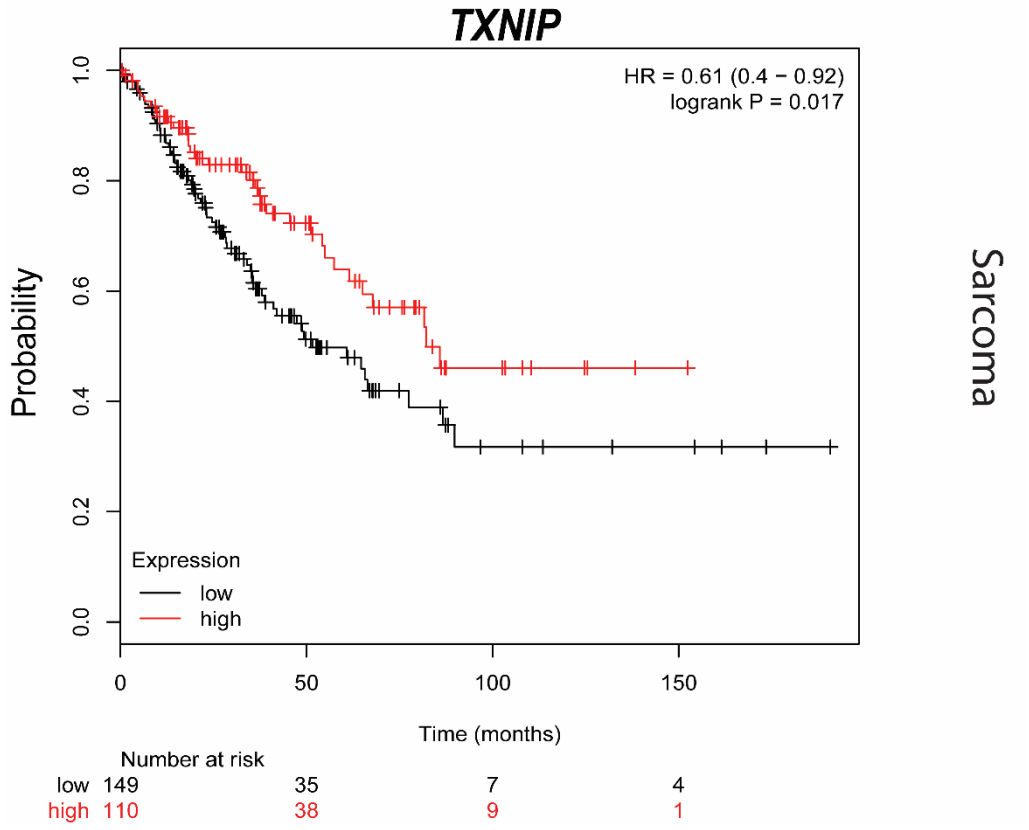

Sarcoma

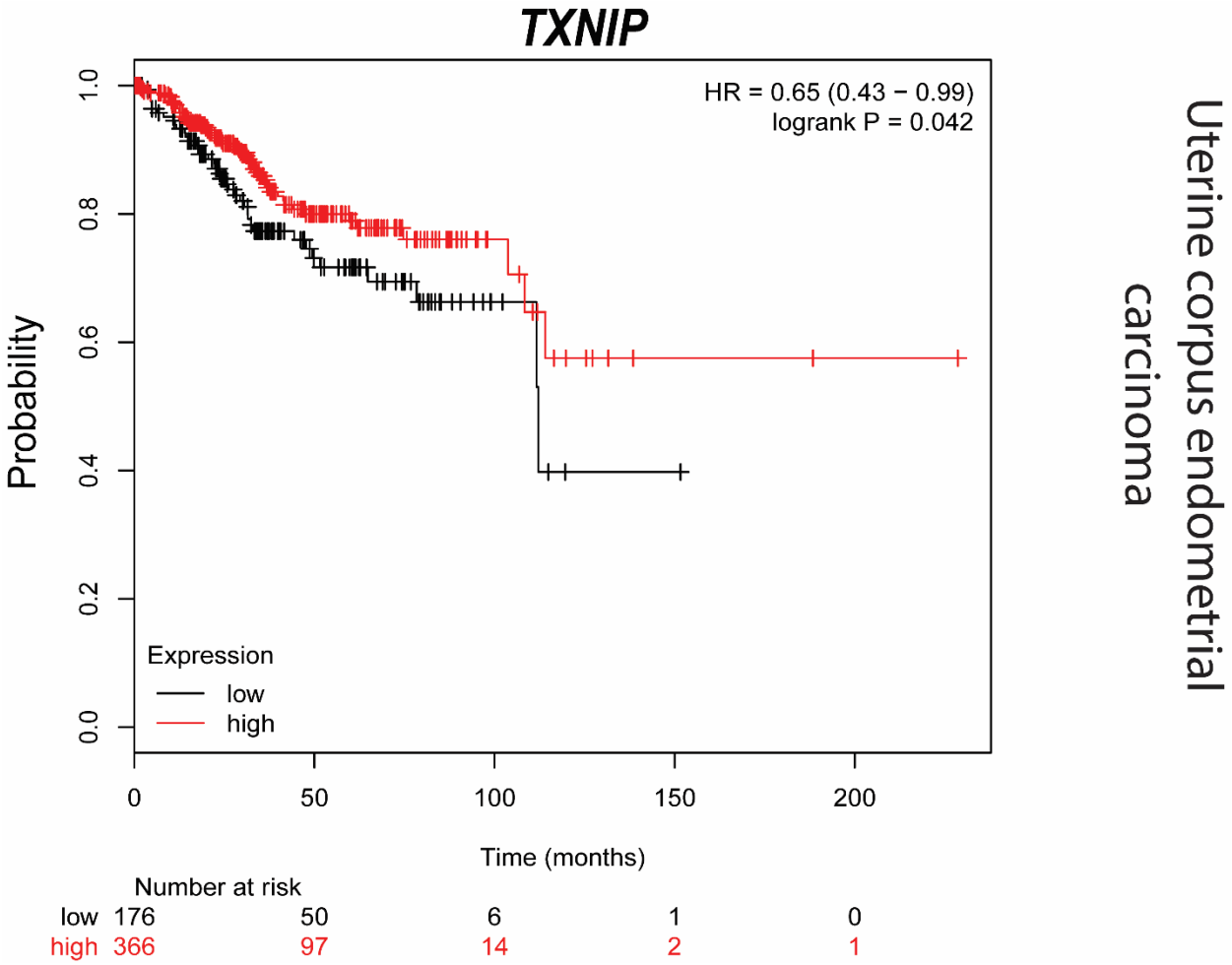

Figure 2 – *Clinical outcome of patients with different cancer types correlated to TXNIP expression.*

Kaplan-Meier plots adapted from kmplot.com (Lanczky et al., 2016) displaying survival rates for patients with tumors with high (Osthus et al.) or low (black) TXNIP expression for the indicated malignancies are shown. Corresponding hazard ratio (HR) with a 95% confidence interval are shown in the upper right corner of each plot. HR represents probability of death of patients with high TXNIP expression relative to patients with low TXNIP expression. Values plotted represent RNAseq data including patients of all races, gender, and stages of corresponding cancer type.

4.2 *TXNIP expression is suppressed by phenformin and is induced by torin1*

We next treated MCF7 cells with phenformin and torin1 for 2h and conducted RT-qPCR for total *TXNIP* RNA and 8h treatment for western blots to determine TXNIP protein levels, respectively (Figure 3A-B). In this, we note that 2h is sufficient to observe dramatic downregulation of *TXNIP* mRNA by phenformin (300μM), whereby the opposite effect was noted for torin1 (250nM) inasmuch as it induced *TXNIP* transcript levels (Figure 3A). In addition, we also monitored the effects of the drugs on TXNIP levels by western blot in other cell lines HEK293E and HeLa, in addition to MCF7 (Figure 5B). We first gather results consistent with previous findings that these drugs (phenformin and torin1) (Bridges et al., 2014; Pollak, 2013; Sarbassov et al., 2005; Thoreen et al., 2009), converge in the inhibition of mTORC1 activity ((Kalender, 2010 #354)(Thoreen et al., 2009), but interestingly show opposing effects on TXNIP expression. Ribosomal protein S6 (RPS6) is phosphorylated on Ser-240/244 via the mTORC1/S6 kinase axis (Banerjee et al., 1990). Phenformin treatments suppressed phosphorylation of RPS6 on Ser-240/244 which was the most dramatic in HEK293E cells (Figure 3B). Torin1, an ATP-competitive active-site inhibitor of mTOR complexes 1 and 2 (Thoreen et al., 2009), abolished mTORC1 activity as marked by a sharp decrease in phosphorylation of ribosomal protein S6 (RPS6) on Ser-240/244 and eukaryotic initiation factor 4E-binding protein 1 (EIF4EBP1) on Ser-65 in all three cell lines tested (Figure 3B). In this, the role of TXNIP in glucose uptake and its change in expression following phenformin and torin1 treatments may hint that TXNIP could mediate the opposing effects of these drugs on glucose uptake.

Figure 3

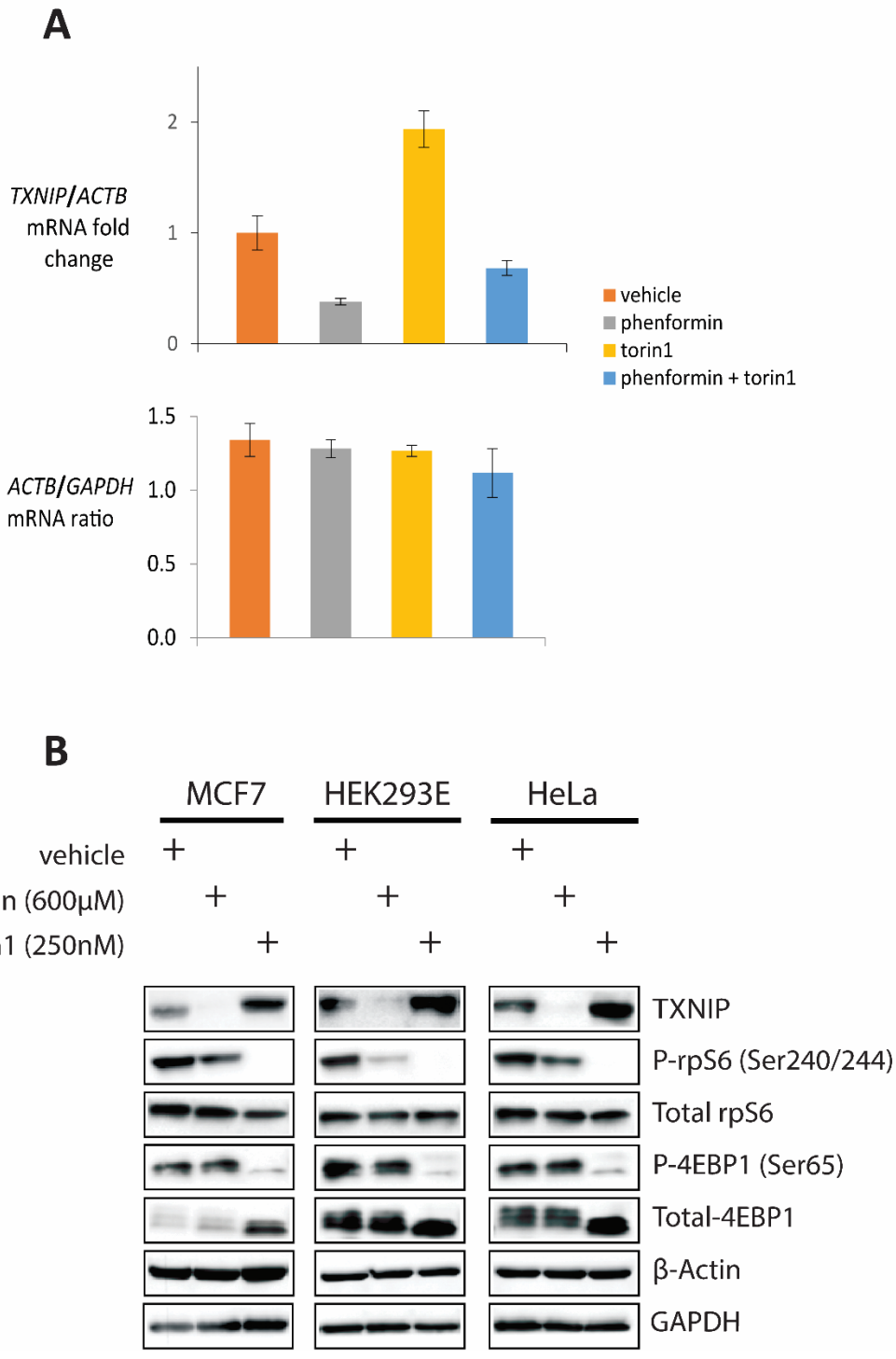
A
TXNIP/ACTB mRNA fold change
2
1
0
vehicle
phenformin
torin1
phenformin + torin1
ACTB/GAPDH mRNA ratio
1.5
1.0
0.5
0.0
B
MCF7
HEK293E
HeLa
vehicle
phenformin (600μM)
torin1 (250nM)
TXNIP
P-rpS6 (Ser240/244)
Total rpS6
P-4EBP1 (Ser65)
Total-4EBP1
β-Actin
GAPDH

Figure 3 - *Characterizing the effects of mTOR inhibitor and biguanides on TXNIP expression.*

(A) MCF7 cells were treated with 300μM phenformin, 250nM torin1, and their combination for 2h. Total *TXNIP* mRNA levels were determined by RT-qPCR and normalized to *ACTB*. *ACTB* mRNA levels normalized to *GAPDH* (*ACTB/GAPDH* ratio) are shown as additional housekeeping control. Error bars represent SD. Data are presented as fold change relative to vehicle (DMSO) and are representative of three independent replicates (n=3). **(B)** MCF7, HEK293E, and HeLa cells were treated for 8h as indicated in (A). The expression and phosphorylation status of indicated proteins were determined by western blot with β-actin as a loading control. Data presented are representative of two independent replicates (n=2).

4.3 *Torin1 induces TXNIP expression in part by upregulating translation.*

Using polysome profiling/DNA microarray approach to capture changes in translation on a genome-wide scale, we have previously identified thioredoxin-interacting protein (*TXNIP*) mRNA to be translationally repressed by metformin but not by mTOR inhibitors in MCF7 cells (Larsson et al., 2012). To validate this previous finding (Figure 4A), we treated MCF7 cells for 6h with phenformin and torin1 and subjected the cells to polysome fractionation. Polysome fractionation is based on ultracentrifugation of cytosolic extracts on 5-50% sucrose gradients which allows separation of mRNAs based on the number of ribosomes they bind (Gandin et al., 2014). Translational efficiency of mRNA is directly proportional to the number of ribosomes it associates with (Masvidal et al., 2017). Using polysome fractionation, we generated fractions corresponding to subpolysomal, light polysomal, and heavy polysomes to probe for *TXNIP, CCND3, ACTB* mRNAs by RT-qPCR. In torin1-treated cells, we showed that *TXNIP* mRNA distribution is concentrated in the fractions corresponding to heavy polysomes relative to vehicle control (Figure 4B). This signifies that *TXNIP* is translationally upregulated when treated with mTOR inhibitors relative to vehicle control (DMSO). Our previous data showed metformin-induced suppression of *TXNIP* mRNA translation (Larsson et al., 2012). Herein, however we observed that phenformin, a more potent biguanide, failed to induce a major effect on *TXNIP* mRNA translation. We used *ACTB* for negative control and *CCND3* as positive control for translational regulation in phenformin and torin1 treatments (Figure 4B), as cyclins of type D and E have been previously reported to have MTOR-dependent translation (Graff et al., 2008). Prior to loading into sucrose gradients, 10% of the total lysates were kept as input controls and were subjected to RNA extraction for RT-qPCR. Cells were also plated and treated for 6h as indicated for western blot control in parallel with cells for polysome fractionation. We showed that phenformin decreases

total *TXNIP* RNA, while torin1 increased it (Figure 4C) and the same effect can be observed at the protein level (Figure 4E).

Figure 4

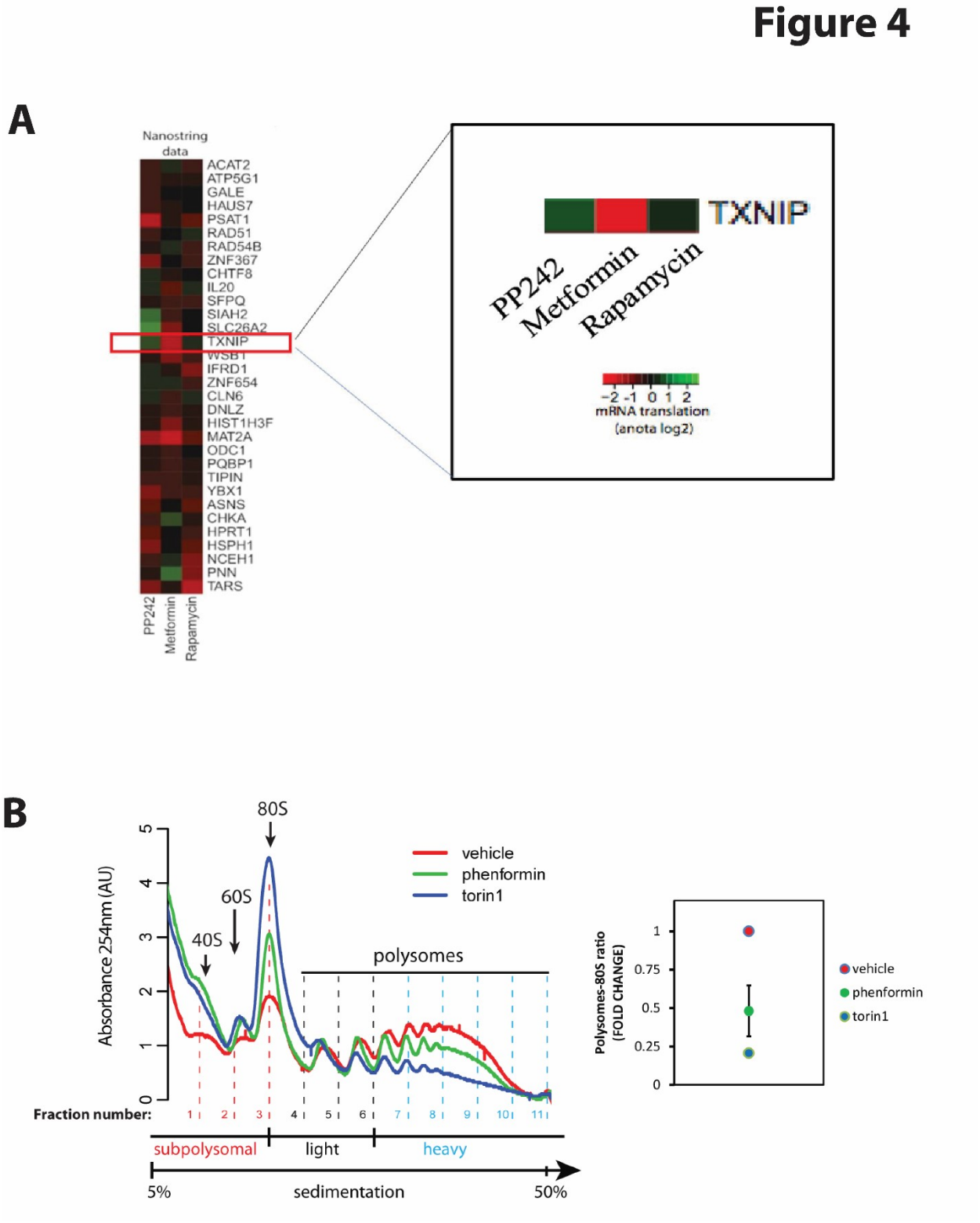
A
Nanostring data
ACAT2
ATP5G1
GALE
HAUS7
PSAT1
RAD51
RAD54B
ZNF367
CHTF8
IL20
SFPQ
SIAH2
SLC26A2
TXNIP
WSB1
IFRD1
ZNF654
CLN6
DNLZ
HIST1H3F
MAT2A
ODC1
PQBP1
TIPIN
YBX1
ASNS
CHKA
HPRT1
HSPH1
NCEH1
PNN
TARS
PP242
Metformin
Rapamycin
TXNIP
PP242
Metformin
Rapamycin
−2 -1 0 1 2
mRNA translation
(anota log2)
B
80S
60S
40S
vehicle
phenformin
torin1
polysomes
Absorbance 254nm (AU)
0
1
2
3
4
5
Fraction number:
1
2
3
4
5
6
7
8
9
10
11
subpolysomal
light
heavy
5%
sedimentation
50%
Polysomes-80S ratio
(FOLD CHANGE)
0
0.25
0.5
0.75
1
vehicle
phenformin
torin1

C

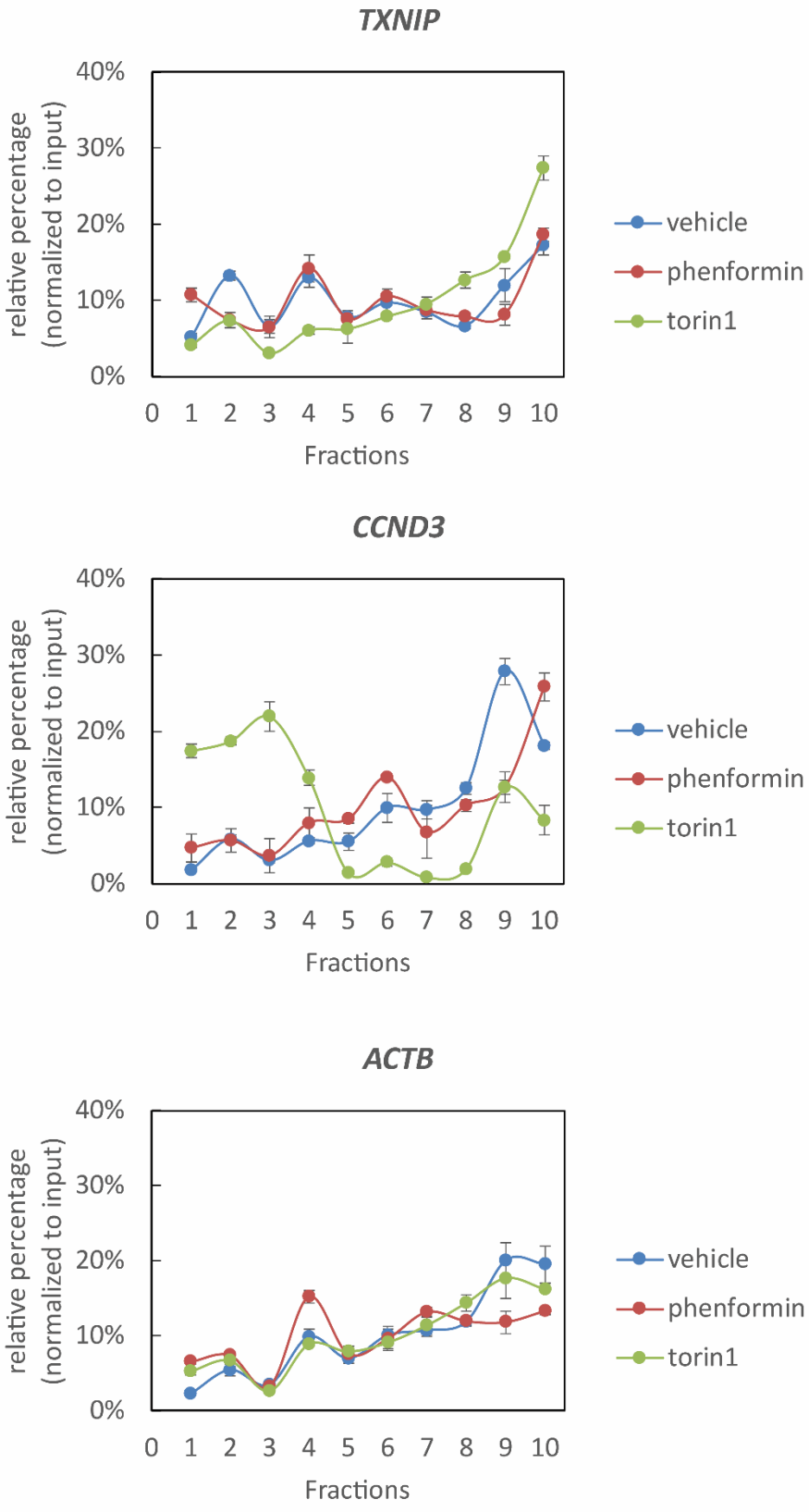
TXNIP
relative percentage (normalized to input)
40%
30%
20%
10%
0%
0 1 2 3 4 5 6 7 8 9 10
Fractions
vehicle
phenformin
torin1
CCND3
relative percentage (normalized to input)
40%
30%
20%
10%
0%
0 1 2 3 4 5 6 7 8 9 10
Fractions
vehicle
phenformin
torin1
ACTB
relative percentage (normalized to input)
40%
30%
20%
10%
0%
0 1 2 3 4 5 6 7 8 9 10
Fractions
vehicle
phenformin
torin1

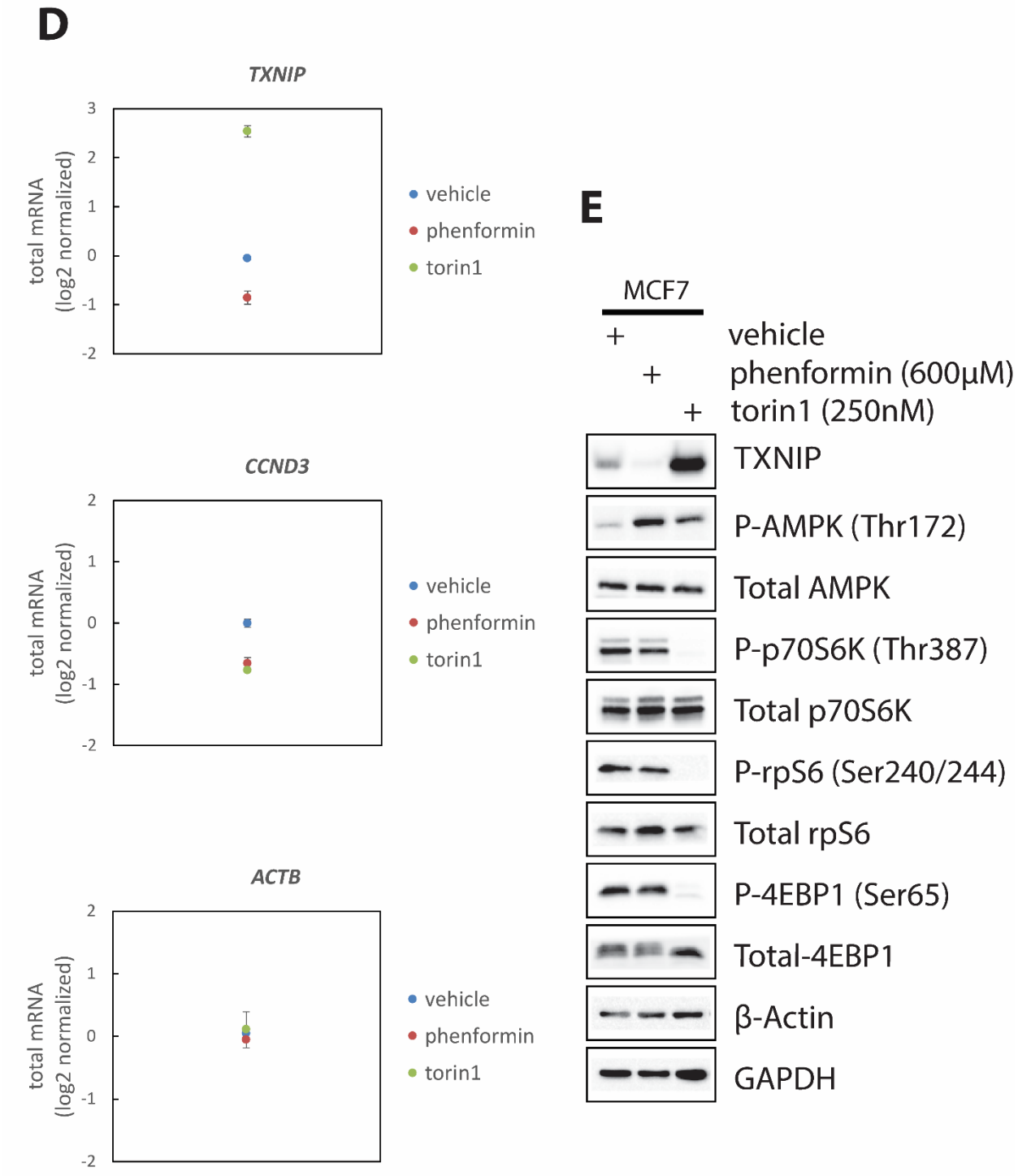
D
TXNIP
total mRNA (log2 normalized)
3
2
1
0
-1
-2
vehicle
phenformin
torin1
CCND3
total mRNA (log2 normalized)
2
1
0
-1
-2
vehicle
phenformin
torin1
ACTB
total mRNA (log2 normalized)
2
1
0
-1
-2
vehicle
phenformin
torin1
E
MCF7
+ vehicle
+ phenformin (600μM)
+ torin1 (250nM)
TXNIP
P-AMPK (Thr172)
Total AMPK
P-p70S6K (Thr387)
Total p70S6K
P-rpS6 (Ser240/244)
Total rpS6
P-4EBP1 (Ser65)
Total-4EBP1
β-Actin
GAPDH

Figure 4 – *Translational regulation of TXNIP expression in MCF7 cells.*

(A) Nanostring analysis of translational activity following treatment with metformin, PP242 (active-site mTOR inhibitor), and rapamycin (allosteric mTOR inhibitor) in MCF7 cells - adapted from (Larsson et al., 2012). The heatmap represents expression of mRNAs regulated at the translational level following treatment with inhibitors. Values are presented as fold change in log2 relative to vehicle control (DMSO). Brightest green represents the highest fold increase while brightest red represents the highest fold decrease in translation **(B-D)** MCF7 cells were treated with a vehicle (DMSO), 600uM phenformin, and 250nM torin1 for 6h. Subpolysomal, light, and heavy polysome fractions were obtained by ultracentrifugation using 5%–50% sucrose gradients. Placements of 40S and 60S ribosomal subunits, monosome (80S), and polysomes in the absorbance profiles (254 nm) are shown (**B**). The percentage distribution of indicated mRNAs in the fractionated lysates (**C**) and the corresponding total mRNA levels (input) **(D)** were determined by RT-qPCR. **(E)** MCF7 cells were plated and treated in parallel to the conditions in **B-D.** Levels of indicated proteins were determined by western blot. Data in all panels are representative of two independent replicates (n=2).

4.4 *Phenformin and Torin1 suppress cell proliferation, but have opposite effects on glucose uptake*

Phenformin and torin1 are indirect and direct mTOR inhibitors, respectively and have been previously shown to inhibit cell proliferation (Thoreen et al., 2009; Zakikhani et al., 2006) but have opposite effects on glucose uptake (Iversen et al., 2017; Kaadige et al., 2015). As expected, phenformin treatment increases glucose uptake, while torin1 decreases it (Figure 5A). In support of previous studies (Thoreen et al., 2009; Zakikhani et al., 2006), we showed, using trypan blue exclusion/cell counting method, that phenformin (Figure 5B) and torin1 (Figure 5C) treatment in increasing concentration have effectively inhibited cell proliferation after 72h of treatment. These results have been validated by BrdU method.

Figure 5

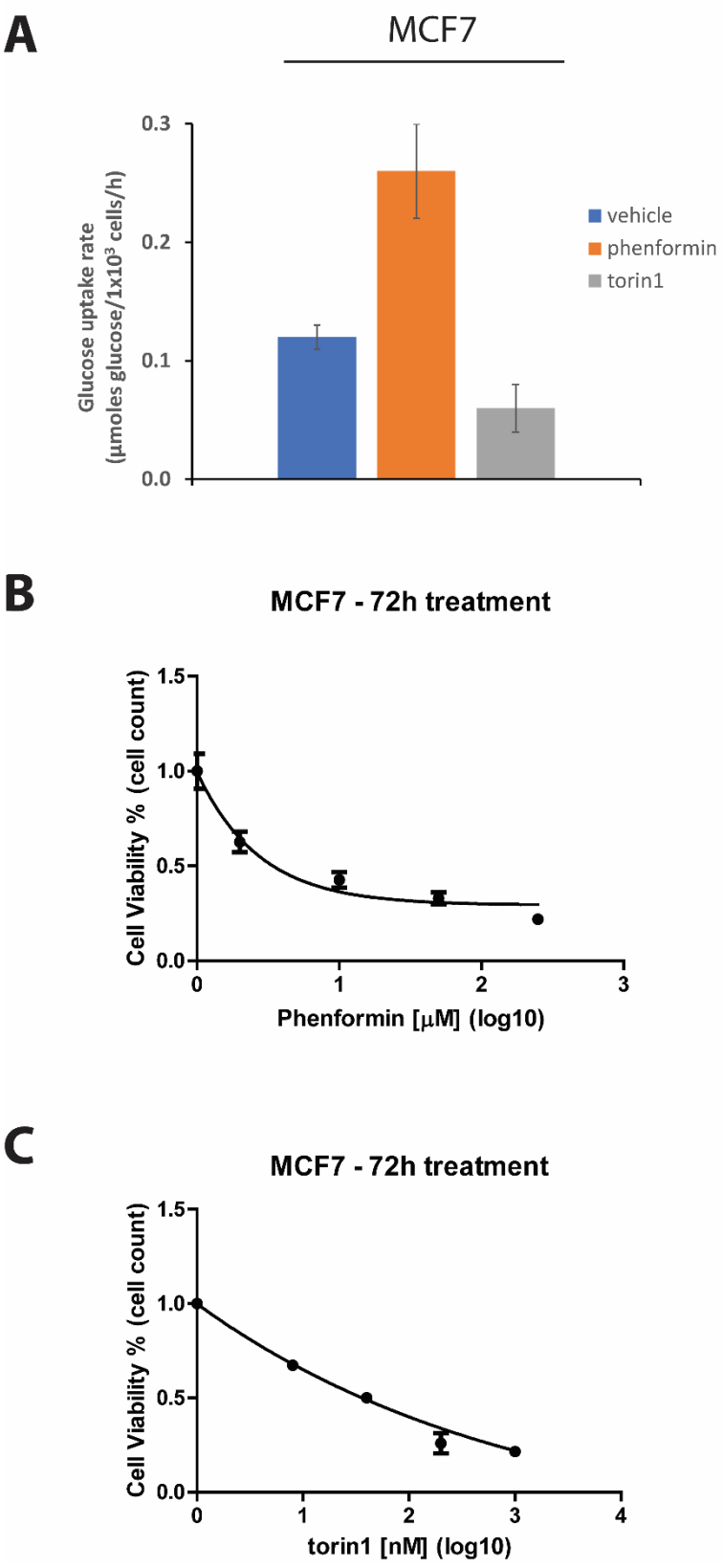
A
MCF7
Glucose uptake rate
(µmoles glucose/1x10³ cells/h)
0.3
0.2
0.1
0.0
vehicle
phenformin
torin1
B
MCF7 - 72h treatment
Cell Viability % (cell count)
1.5
1.0
0.5
0.0
0
1
2
3
Phenformin [µM] (log10)
C
MCF7 - 72h treatment
Cell Viability % (cell count)
1.5
1.0
0.5
0.0
0
1
2
3
4
torin1 [nM] (log10)

Figure 5 - *Effects of torin1 and phenformin on glucose uptake and cell proliferation.*

(A) MCF7 cells were treated with a vehicle (DMSO), 600uM phenformin, and 250nM torin1 for 6h. Glucose uptake rate was determined by monitoring the change in glucose concentration in media with cells versus cell-free media and normalized to vehicle (DMSO). Data are presented as mean ± SD (n=2). **(B)** MCF7 cells were treated with a vehicle (H_2O) and increasing concentration of phenformin (20, 100, 500, 2500 μM; presented in log10) for 72h. Viable cells were counted by trypan blue exclusion and presented as percentage inhibition relative to vehicle control (n=2). **(C)** MCF7 cells were treated with a vehicle (DMSO) and increasing concentration of torin1 (10, 50, 250, 1250 nM; presented in log10) for 72h. Viable cells were counted by trypan blue exclusion and presented as percentage inhibition relative to vehicle control (n=2).

4.5 *Suppression of TXNIP expression, partly by reducing stability, may be required for phenformin-induced increase in glucose uptake*

Phenformin causes energetic stress by inhibiting mitochondrial complex I, thereby increasing AMP/ATP ratio which leads to the induction of AMPK (Hardie, 2011). TXNIP expression is reported to be regulated at the level of protein stability, whereby activated AMPK phosphorylates TXNIP on Ser-308 for ubiquitination by E3 ubiquitin ligase ITCH and subsequent proteasomal degradation (Wu et al., 2013). Consistent with these findings, we treated MCF7 cells with phenformin and induced AMPK activation as illustrated by the increase in phosphorylation on Thr-172 which was paralleled by a modest decrease TXNIP (Figure 6A). TXNIP expression can also be transcriptionally regulated by mTOR, whereby mTOR sequesters MondoA-Mlx transcription factor and preventing its binding to the TXNIP promoter. Hence, mTOR inhibition leads to an increase in TXNIP transcript levels (Chau et al., 2017; Kaadige et al., 2015). However, post-transcriptional regulation of TXNIP expression remains underexplored.

To investigate TXNIP expression control by phenformin and torin1, we next generated MCF7 cells that constitutively express empty vector control, wild-type TXNIP, and Ser-308-Ala mutant TXNIP via lentiviral transduction. These HA-tagged constructs lack endogenous promoters and UTR's (devoid of 5' and 3' UTR's), which facilitates investigating the effects of drugs on TXNIP stability, because it is not expected that these constructs will be affected at the level of transcription or translation. We starved MCF7 cells with constitutive TXNIP expression (WT and Ser-308-Ala) of glucose or serum for 24h. Post-starvation, we stimulated the cells with fresh media containing glucose or FBS with the addition of a vehicle (DMSO), phenformin, or torin1 for 6h and extracted

proteins (Figure 6). Remarkably, the levels of exogenous Ser-308-Ala mutant TXNIP is about 2-fold higher than the exogenous wild-type construct, suggesting that the Ser-308-Ala mutation on TXNIP increased its stability (Figure 6A-C). Moreover, we observed that TXNIP is upregulated in serum-starved cells which is reversed by serum stimulation (Figure 6A and 5C). We also noted that TXNIP is reduced in glucose-starved cells and is induced upon glucose stimulation (Figure 6B). Here we show that phenformin treatment may allow for a reduction in exogenous wild-type TXNIP similar to its effects on endogenous TXNIP, however the Ser-308-Ala mutant TXNIP levels appears to remain largely unaltered (Figure 6A-C). Torin1 treatment increased endogenous TXNIP (Figure 6A-B) but did not show any changes to the exogenous constructs. In brief, this suggests that phenformin does, at least in part, regulate stability of TXNIP protein and that torin1 requires endogenous promoters and UTRs to regulate TXNIP expression.

Previously, we presented results showing phenformin treatment increases glucose uptake, while torin1 decreases it (Figure 5A). To determine whether TXNIP mediates the effects of phenformin-induced increase in glucose uptake, we measured the change in glucose levels in the media post-treatment with phenformin in MCF7 cells with constitutive exogenous TXNIP expression (WT and Ser-308-Ala mutant). Cells that constitutively express wild-type TXNIP show no difference in phenformin-induced glucose uptake relative to control cells (vector control) (Figure 6D). In cells expressing Ser-308-Ala mutant TXNIP, however, glucose uptake induction by phenformin seems to be attenuated by roughly ~20% (Figure 6D). This suggests that phenformin-induced increase in glucose uptake may require suppression of TXNIP expression. Moreover, in torin1-treated Ser-308-Ala TXNIP mutant-expressing cells, we observe no notable difference in glucose uptake rate relative to wildtype TXNIP-expressing cells (Figure 6D). Notably, we have also shown

that phenformin inhibits cell proliferation (Figure 4B). Of note, the effects of the attenuated glucose uptake in Ser-308-Ala TXNIP mutant-expressing cells following phenformin treatment were observed in cell proliferation. In this, cells with Ser-308-Ala TXNIP mutant potentiates the inhibitory effects of phenformin on cell proliferation (Figure 6E).

Figure 6

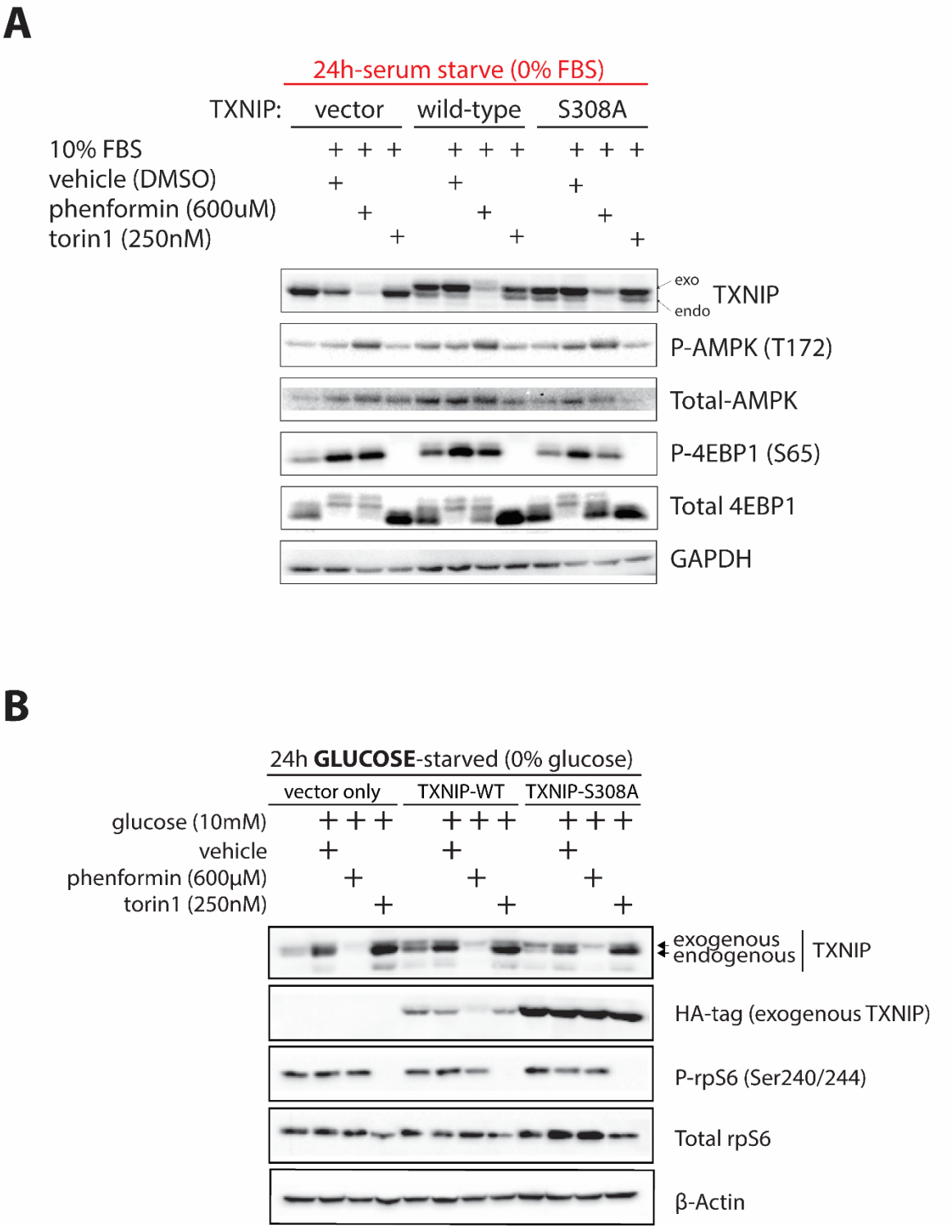
A
24h-serum starve (0% FBS)
TXNIP: vector wild-type S308A
10% FBS
vehicle (DMSO)
phenformin (600uM)
torin1 (250nM)
exo
endo
TXNIP
P-AMPK (T172)
Total-AMPK
P-4EBP1 (S65)
Total 4EBP1
GAPDH
B
24h GLUCOSE-starved (0% glucose)
vector only
TXNIP-WT
TXNIP-S308A
glucose (10mM)
vehicle
phenformin (600μM)
torin1 (250nM)
exogenous
endogenous
TXNIP
HA-tag (exogenous TXNIP)
P-rpS6 (Ser240/244)
Total rpS6
β-Actin

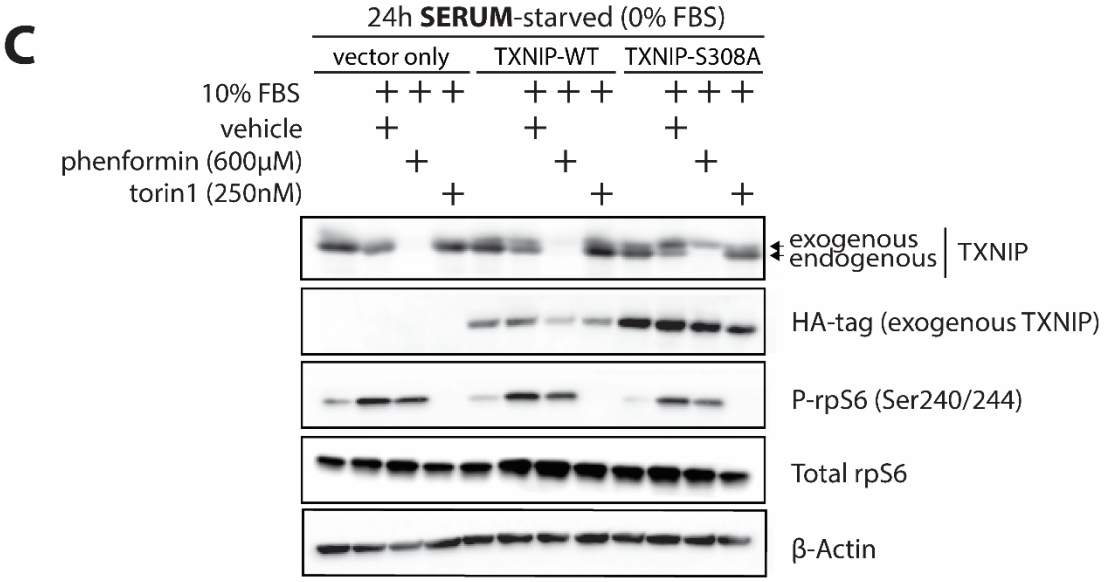
C
24h SERUM-starved (0% FBS)
vector only
TXNIP-WT
TXNIP-S308A
10% FBS
vehicle
phenformin (600μM)
torin1 (250nM)
exogenous
endogenous
TXNIP
HA-tag (exogenous TXNIP)
P-rpS6 (Ser240/244)
Total rpS6
β-Actin

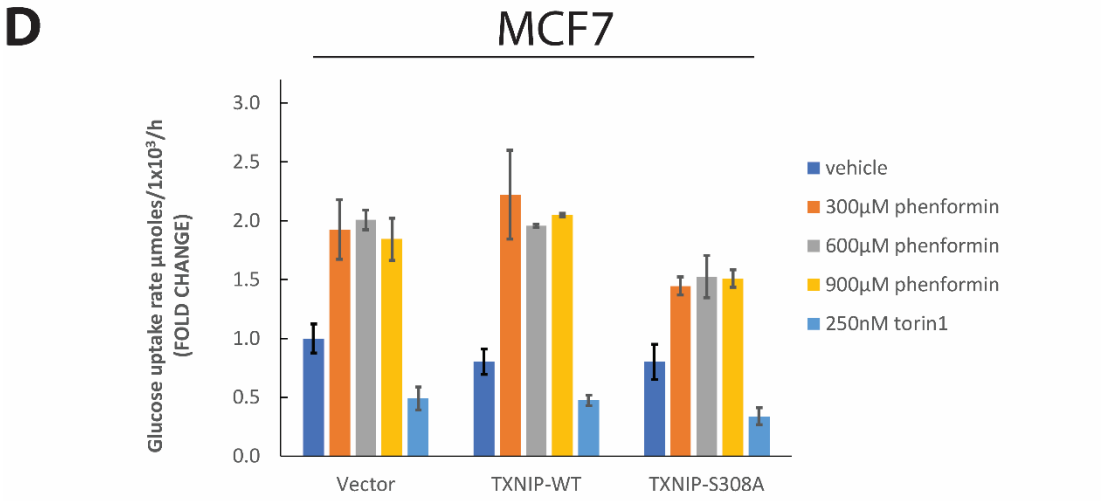
D
MCF7
Glucose uptake rate μmoles/1x10³/h
(FOLD CHANGE)
3.0
2.5
2.0
1.5
1.0
0.5
0.0
Vector
TXNIP-WT
TXNIP-S308A
vehicle
300μM phenformin
600μM phenformin
900μM phenformin
250nM torin1

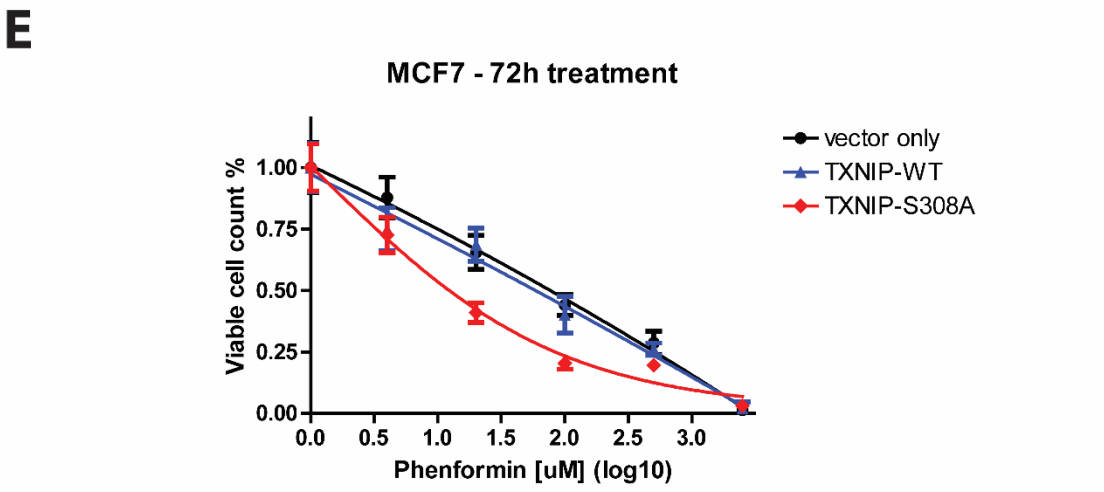
E
MCF7 - 72h treatment
Viable cell count %
1.00
0.75
0.50
0.25
0.00
0.0
0.5
1.0
1.5
2.0
2.5
3.0
Phenformin [uM] (log10)
vector only
TXNIP-WT
TXNIP-S308A

Figure 6 - *Determining the regulation of TXNIP expression and its role in mediating the effects of phenformin on glucose uptake and cell proliferation.*

MCF7 cells with constitutively overexpressed TXNIP (WT and SER-308-ALA) were starved of **(A)** glucose (0.5mM glucose, 10%FBS) or **(B)** serum (10mM glucose, 0% FBS) for 24h and stimulated with fresh media supplemented with 10mM glucose (**A**) or 10%FBS (**B**) and containing a vehicle (DMSO), 600uM phenformin, or 250nM torin1 for 6h. Protein levels were determined by western blot. Data are representative of two independent replicates (n=2). TXNIP antibody (mouse host) used is from NOVUS (NBP1-54578). **(C)** MCF7 cells with constitutive TXNIP expression were starved, stimulated, and treated as in A. The expression and phosphorylation status of indicated proteins were determined by western blot with β-Actin as loading control. Data presented are representative of three independent replicates (n=2). TXNIP antibody (rabbit host) used is from Cell Signaling Technology (CST) (#14715)**. (D)** MCF7 cells constitutively expressing wild-type and SER-308-ALA mutant TXNIP were treated as indicated for 6h. Glucose uptake rate was determined by monitoring the change in glucose concentration in media with cells versus cell-free media and normalized to vehicle (DMSO). Data are presented as mean ± SD (n=2). **(E)** MCF7 cells were treated with a vehicle (H_2O) and increasing concentration of phenformin (20, 100, 500, 2500 μM; presented in log10) for 72h. Viable cells were counted by trypan blue exclusion and presented as percentage inhibition relative to vehicle control (n=2).

4.6 *Investigating the potential role of TXNIP in mediating effects of inhibitors of the PI3K-AKT-MTOR pathway on glucose uptake and proliferation in MCF7 cells.*

Phenformin and torin1 are indirect and direct mTOR inhibitors, respectively, and have been previously shown to inhibit cell proliferation (Thoreen et al., 2009; Zakikhani et al., 2006) but have opposite effects on glucose uptake (Iversen et al., 2017; Kaadige et al., 2015). In support of previous studies (Thoreen et al., 2009; Zakikhani et al., 2006), we showed that phenformin and torin1 treatment in increasing concentration have effectively inhibited cell proliferation via trypan blue exclusion after 72h of treatment (Figure 4B-C). Torin1 is an ATP-competitive mTOR inhibitor that targets both mTORC1 and mTORC2 (Thoreen et al., 2009). The significance of this finding allows us to understand torin1-induced disruption of the PI3K-AKT signaling as full AKT activation requires phosphorylation on both T308 (by PDPK1) and S473 by mTORC2. Previous studies have shown TXNIP upregulation when treated with PI3K-AKT pathway inhibitors (Hong et al., 2016). In support of this finding, we show that, in addition to torin1, inhibitors of the PI3K-AKT-MTOR pathway promotes increase in TXNIP expression (Figure 7A). In this, we use MK-2206, a dual AKT1/AKT2 inhibitor, and GDC-0941, a PI3K inhibitor, to perturb signaling in the PI3K-AKT-MTOR pathway.

To determine whether TXNIP mediates the effects of torin1-induced suppression of glucose uptake and cell proliferation, we measured the change in glucose levels in the media and cell proliferation post-treatment with torin1 in CRISPR/Cas9 TXNIP-knockout MCF7 cells (clones 6 and 11) relative to control cells (CTR). We observed that TXNIP-deficient (clone 11) cells have increased rates of glucose uptake relative to control cells (Figure 7B). More importantly, we suggest that torin1-induced suppression of glucose uptake may not mediated by TXNIP (Figure 7B) and that

TXNIP also does not mediate the effects of torin1 on cell proliferation (Figures 6C). However, these experiments need to be repeated for a solid claim and temporarily remains as suggestive rather than conclusive due to inefficient number of replicates and potential escape of TXNIP expressing cells. In addition, the inhibitory effects of AKT inhibitors on cell proliferation may also not TXNIP-mediated, despite induction of TXNIP following treatment with MK-2206 (Figure 7D). Intriguingly, the effects of GDC-0941 on cell proliferation were exacerbated in TXNIP-deficient MCF7 cells (Figure 7E). Moreover, we sought to answer whether TXNIP deficiency-induced increase in glucose uptake offers an advantage in phenformin-treated inhibition of mitochondrial complex I and subsequent suppression of cell proliferation. In this, we show negative data suggesting no changes in cell proliferation in TXNIP-deficient cells (clone 11) versus control cells, when treated with phenformin (Figure 7F). To confirm our negative findings on TXNIP mediating the effects of torin1 on cell proliferation (Figure 7C), we sought to investigate if the findings were reproducible using a different clone for TXNIP-deficient MCF7 cells (clone 6). We note that, in TXNIP-deficient (clone 6) MCF7 cells, the effects of mTOR inhibitors, in addition to torin1, on cell proliferation seem to remain unchanged relative to wild-type control MCF7 cells (Figures 6G, 6I, 6J). We also show negative results in Figure 7F suggesting no differences in cell proliferation in TXNIP knockout cells (clone 6) versus control cells, when treated with phenformin (Figure 7H). Altogether, data generated from these experiments remain suggestive and are highly required to be repeated to determine statistical significance and claim conclusive statements.

Figure 7

A

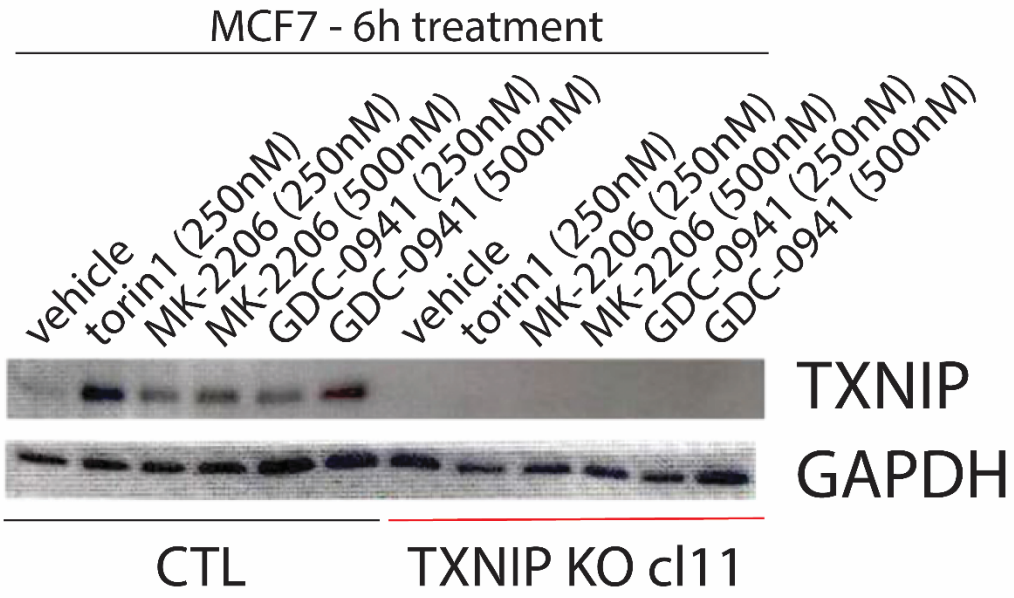
MCF7 - 6h treatment
vehicle
torin1 (250nM)
MK-2206 (250nM)
MK-2206 (500nM)
GDC-0941 (250nM)
GDC-0941 (500nM)
vehicle
torin1 (250nM)
MK-2206 (250nM)
MK-2206 (500nM)
GDC-0941 (250nM)
GDC-0941 (500nM)
TXNIP
GAPDH
CTL
TXNIP KO cl11

B

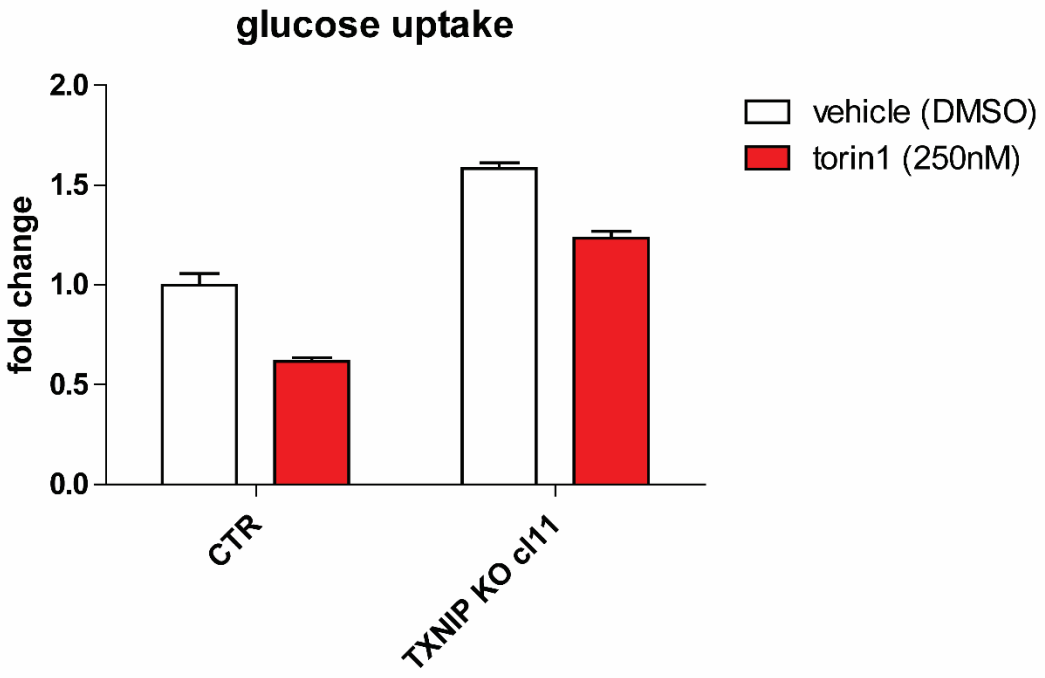
glucose uptake
fold change
2.0
1.5
1.0
0.5
0.0
vehicle (DMSO)
torin1 (250nM)
CTR
TXNIP KO cl11

C

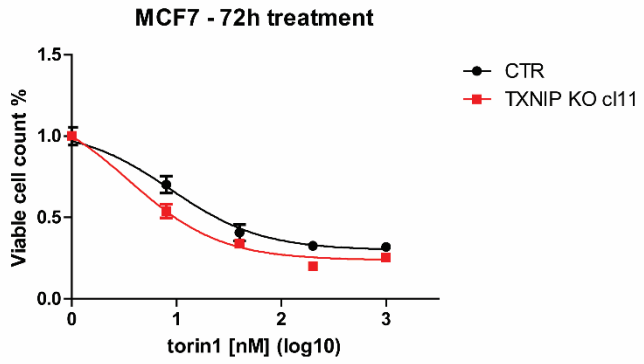
MCF7 - 72h treatment
Viable cell count %
1.5
1.0
0.5
0.0
0
1
2
3
torin1 [nM] (log10)
CTR
TXNIP KO cl11

D

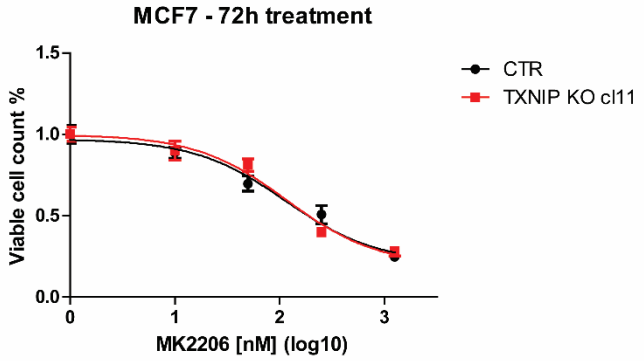
MCF7 - 72h treatment
Viable cell count %
1.5
1.0
0.5
0.0
0
1
2
3
MK2206 [nM] (log10)
CTR
TXNIP KO cl11

E

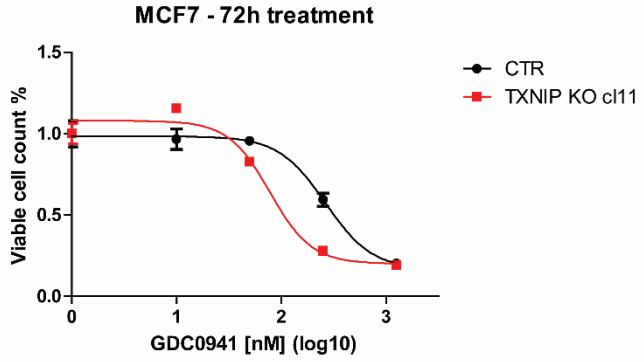
MCF7 - 72h treatment
Viable cell count %
1.5
1.0
0.5
0.0
0
1
2
3
GDC0941 [nM] (log10)
CTR
TXNIP KO cl11

F

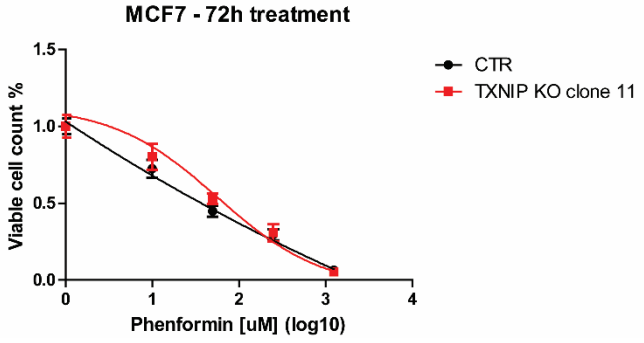
MCF7 - 72h treatment
Viable cell count %
1.5
1.0
0.5
0.0
0
1
2
3
4
Phenformin [uM] (log10)
CTR
TXNIP KO clone 11

G

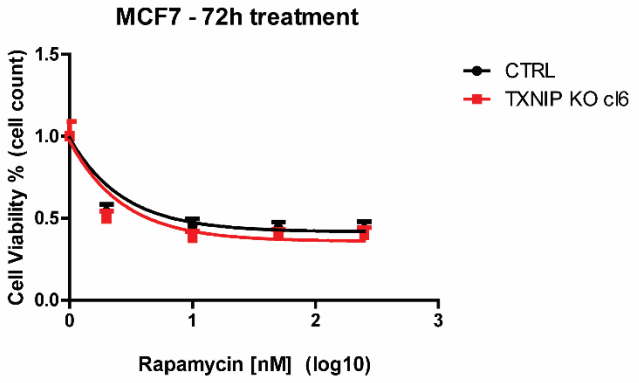
MCF7 - 72h treatment
CTRL
TXNIP KO cl6
Cell Viability % (cell count)
1.5
1.0
0.5
0.0
0
1
2
3
Rapamycin [nM] (log10)

H

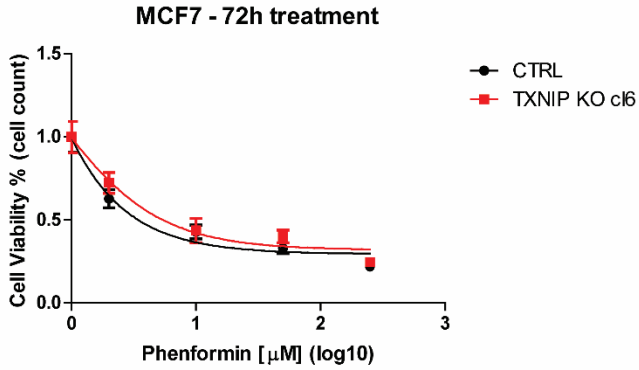
MCF7 - 72h treatment
CTRL
TXNIP KO cl6
Cell Viability % (cell count)
1.5
1.0
0.5
0.0
0
1
2
3
Phenformin [μM] (log10)

I

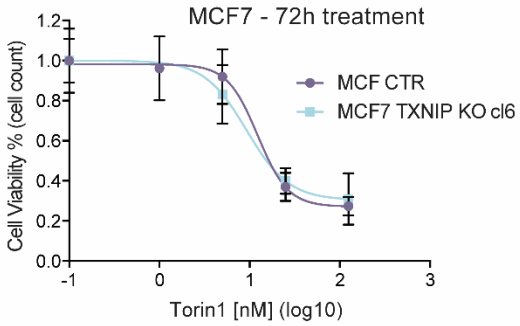
MCF7 - 72h treatment
MCF CTR
MCF7 TXNIP KO cl6
Cell Viability % (cell count)
1.2
1.0
0.8
0.6
0.4
0.2
0.0
-1
0
1
2
3
Torin1 [nM] (log10)

J

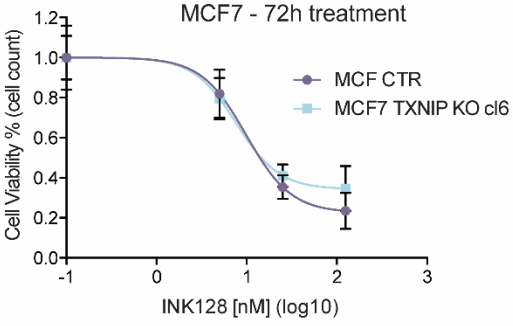
MCF7 - 72h treatment
MCF CTR
MCF7 TXNIP KO cl6
Cell Viability % (cell count)
1.2
1.0
0.8
0.6
0.4
0.2
0.0
-1
0
1
2
3
INK128 [nM] (log10)

Figure 7 - *The role of TXNIP in mediating effects of mTOR inhibitors (rapamycin, torin1, and INK128), AKT inhibitor MK-2206, and PI3K inhibitor GDC-0941 on cell proliferation.*

(A) MCF7 control (CTR) and TXNIP-KO (clone 11) cells were treated with torin1, MK-2206, and GDC-0941 as indicated for 6h. Protein levels were determined by western blot (n=2). **(B)** MCF7 control (CTR) and TXNIP-KO (clone 11) cells were treated with torin1 (250nM) for 6h. Glucose uptake rate was determined by monitoring the change in glucose concentration in media with versus cell-free media and normalized to vehicle (DMSO). Data are presented as mean ± SD (n=2). **(C-F)** MCF7 cells were treated with increasing concentration of torin1 **(C)**, MK-2206 **(D)**, GDC-0941 **(E)**, and phenformin **(F)**, as indicated for 72h. Viable cells were counted by trypan blue exclusion and presented as percentage inhibition of CTR and TXNIP KO (clone 11) cells relative to vehicle control (n=2). MCF7 cells were treated as indicated with increasing concentration of phenformin **(G)**, rapamycin (allosteric mTOR inhibitor) **(H)**, INK128 (active-site mTOR inhibitor) **(I)**, and torin1 **(J)** for 72h. Viable cells were counted by trypan blue exclusion and presented as percentage inhibition of CTR and TXNIP KO (clone 6) cells relative to vehicle control (n=2). Figure panels **H-K** are representative of one replicate of clone 6 cells to validate results obtained from clone 11 (n=1). Proliferation curves are presented in semi-log (log10).

5 – DISCUSSION

Warburg's observation that tumours have increased glucose uptake relative to surrounding tissues formulated conclusions of dysfunctional mitochondria and oxidative phosphorylation, ultimately promoting compensatory glucose influx for cellular energy needs (Warburg et al., 1927). Since then, many studies confirmed Warburg's findings, but also reported that oxidative phosphorylation in cancer was not dysfunctional, contrary to Warburg's conclusions (Crabtree, 1929). Altogether, these findings suggest unexplored areas of glucose metabolism in cancer. The interest of TXNIP initially came to light due to its downregulation in cancers relative to normal tissues (Han et al., 2003). Intriguingly, these initial findings brought light to the idea of the role of TXNIP as a tumour suppressor gene. TXNIP was first reported as a negative regulator of thioredoxin activity, a major anti-oxidant (Nishiyama et al., 1999). However, independent of its role in redox systems, a significant finding presented the role of TXNIP in negatively regulating glucose influx (Parikh et al., 2007). Therefore, high expression of TXNIP and its role suppressing glucose uptake may provide a link to understand glucose metabolism in cancer. We aimed to elucidate the role of TXNIP in mediating the effects of biguanides (phenformin) and mTOR inhibitors (torin1) on glucose uptake and cell proliferation, and ultimately on neoplastic growth. The particular choice to study TXNIP function in phenformin and torin1 treatment conditions was due to previously reported study by our group that TXNIP was translationally suppressed by metformin but upregulated by mTOR inhibitors, rapamycin (allosteric) and PP242 (active-site) (Larsson et al., 2012). Notably, this suggests that both inhibitors can regulate TXNIP expression at the mRNA translation level. In support of our previous study, we addressed this question by conducting polysome fractionation experiments on MCF7 cells treated with phenformin and torin1 to determine changes on the TXNIP mRNA distribution in between treatments across the

subpolysomal, light, and heavy polysome fractions (>3 ribosomes). In this, we report that TXNIP was not translationally suppressed by phenformin, but TXNIP translation was indeed upregulated by torin1. The latter finding validates our previous nanostring data of the translatome showing TXNIP upregulation by mTOR inhibitors. Overall, TXNIP expression appears to be regulated at multiple levels, via mTOR-dependent and independent mechanisms.

TXNIP is induced by glucose stimulation and has been shown to be highly expressed among hyperglycemic mice models (Koenen et al., 2011; Parikh et al., 2007). Previous studies on TXNIP reported its expression to be transcriptionally suppressed when oxidative phosphorylation is inhibited (Yu et al., 2010). Phenformin induces energetic stress by inhibiting mitochondrial complex I, thereby increasing AMP/ATP ratio (Bridges et al., 2014) and consequently suppressing TXNIP levels. Consistent with previous reports (Waldhart et al., 2017; Wu et al., 2013), we show that in addition to transcriptional suppression, phenformin also in part suppresses TXNIP at the level of protein stability. The protein level difference between HA-tagged wild-type and Ser-308-Ala mutant TXNIP constructs appears to be barely 2-folds between control (DMSO) conditions, indicating that Ser-308-Ala mutation on TXNIP could confer increased protein stability. We also provide evidence that a Ser-308-Ala mutation on TXNIP attenuates phenformin-induced TXNIP suppression observed in overexpressed wild-type TXNIP constructs in phenformin treated vs. control, vehicle (DMSO) treated cells. As previously reported, AMPK phosphorylates TXNIP on Ser-308 which targets it for ubiquitination by E3 ubiquitin ligase ITCH and subsequent degradation by proteasome (Wu et al., 2013). To address whether AMPK is linked to TXNIP phosphorylation on Ser-308 for increased proteasomal degradation, we will determine the effects of phenformin treatment on TXNIP expression using AMPK1/2 knock-out mouse embryonic

fibroblast (MEF) cells previously used in (Laderoute et al., 2006). It is important to note, however, that in HeLa cells phenformin still decreases TXNIP levels in the absence of the LKB1 (Figure 5B) which is a kinase thought to be necessary for AMPK activation by phenformin (Shaw et al., 2004). Independent of AMPK, this signifies that TXNIP may be linked to another regulatory pathway in biguanide-induced compromised cellular energy status. TXNIP expression can also be transcriptionally regulated, whereby mTOR sequesters MondoA-Mlx transcription factor preventing its binding to the *TXNIP* promoter (Chau et al., 2017; Kaadige et al., 2015). Hence, mTOR inhibition leads to an increase in TXNIP mRNA levels. To validate past studies, we provide evidence that torin1 induces TXNIP mRNA and that TXNIP expression cannot be regulated by torin1 when devoid of endogenous promoters and UTRs. HA-tagged wild-type and Ser-308-Ala mutant TXNIP levels in MCF7 cells were not altered by torin1 treatment.

Biguanides have been shown to have anti-proliferative effects in cancer cells and these effects are potentiated with low glucose availability (Algire et al., 2011). The mechanistic/mammalian target of rapamycin (mTOR) is a master regulator of growth and proliferation, hence its inhibition by mTOR inhibitors (torin1) leads to a decrease in cell proliferation (Shimobayashi and Hall, 2014; Thoreen et al., 2009). In support of previous studies, we also provide evidence of the anti-proliferative effects of biguanides and mTOR inhibitors. Biguanides induce energetic stress via inhibition of mitochondrial complex I leading to an ATP deficit (Bridges et al., 2014). In addition to complex I, biguanides may also target and inhibit complex II and IV as shown by using phenformin in isolated rat liver mitochondria (Drahota et al., 2014). This biguanide-induced suppression of mitochondrial ATP production is compensated by an increase in glucose uptake necessary to fuel proliferation. The molecular underpinnings of this biguanide-induced

compensatory mechanism and torin1-induced, however, remain elusive. Moreover, inhibition of mTOR by torin1 causes suppression of ATP-consuming processes but induces TXNIP expression and consequently suppresses glucose uptake. It is notable that the effects of both inhibitors on glucose uptake correlate with phenformin and torin1-regulated TXNIP expression, as TXNIP is a negative regulator of glucose uptake. In this, we suggest that phenformin-induced compensatory increase in glucose uptake is in part achieved by suppressing TXNIP. In addition, induction of TXNIP levels may also play a role in the downregulation of glucose uptake by torin1. Accordingly, we demonstrate that a biguanide-insensitive TXNIP (Ser-308-Ala mutant) attenuates the effects of phenformin-induced glucose uptake increase, suggesting that TXNIP partly mediates the effects of the drugs on glucose uptake. Considering that cancer cells utilize glucose to fuel neoplastic growth, this attenuation in phenformin-induced glucose uptake beckons the question whether TXNIP play may a role in mediating the anti-neoplastic effects of biguanides. To address this question, we looked at the effects of phenformin on cell proliferation in cells expressing Ser-308-Ala TXNIP mutant and noted that the biguanide-insensitive TXNIP potentiates the inhibitory effects of phenformin on cell proliferation. Furthermore, we generated TXNIP-deficient MCF7 cells via CRISPR/Cas9 genome editing and observed that depletion of TXNIP increases glucose influx, consistent with previous findings (Kaadige et al., 2015).

In contrast to phenformin, cells overexpressing TXNIP do not display further decrease in glucose uptake after exposure to torin1. This outcome is anticipated due to the limitations that this MCF7 model comes with. It may be reasonable to presume that further increasing TXNIP levels by overexpression, in addition to torin1-induced expression, will not decrease glucose uptake further due to the saturation of the system. These limitations may be explained by the mechanism behind

the role of TXNIP as negative regulator of glucose uptake. TXNIP prevents glucose entry into the cell by binding to GLUT1 and GLUT4 facilitative glucose transporters for endocytosis internalization (Waldhart et al., 2017; Wu et al., 2013) but will eventually reach stoichiometry under which TXNIP levels will not be limiting. Furthermore, despite TXNIP function as a negative regulator of glucose uptake, we suspect that the difference in TXNIP levels may also explain the absence of notable glucose uptake suppression in untreated cells with overexpressed TXNIP constructs relative to vector control. To this end, we generated TXNIP-deficient MCF7 cells via CRISPR/Cas9 genome editing and observed that depletion of TXNIP increases glucose influx, consistent with previous findings (Kaadige et al., 2015). We anticipate that torin1-induced suppression of glucose uptake will be reversed in TXNIP-null cells which, in addition, may potentially also reverse torin1 inhibition of cell proliferation. However, we addressed the role of TXNIP in mediating the effects of mTOR inhibitors on glucose uptake and other PI3K-AKT inhibitors on cell proliferation in TXNIP depleted cells. In this, we report that TXNIP does not appear to play a role in the suppression of glucose uptake and cell proliferation by mTOR inhibitors Surprisingly, the effects of PI3K inhibitors on cell proliferation seem to be potentiated in TXNIP deficient cells.

The findings gathered in this study point more towards a suggestive possibility that requires validation rather than a conclusive outcome. The interest in the role of TXNIP in dysregulated glucose metabolism in cancer was initially presented when malignant tissues were observed to have decreased TXNIP expression, relative to control, which hinted to its tumour suppressor-like property. The significance of these findings may pave the way to understanding glucose uptake regulation in normal physiological conditions as well as in pathological diseases such as diabetes

and cancer. However, it is important that we recognize the controversy of our results and the possibility that TXNIP may play an irrelevant role in the effects of the inhibitors used in this study. In fact, our study in the role of TXNIP in mediating the effects of biguanides and mTOR inhibitors on glucose uptake and cell proliferation is largely limited to MCF7 cells. Further investigation is necessary to understand the implication of TXNIP expression in other cancer cell lines that may be more sensitive to changes in glucose influx and metabolism, whereby its regulation in stressed and stimulated conditions may also play a role in neoplastic growth. More importantly, we also recognize the limitations of the experimental systems designed for this study. The use of cell lines largely constitutes the limitations of our findings because conducting experiments in closed systems shielded from environmental influences may indeed identify causal factors between variables carefully selected by the scientist, but causal knowledge generated from this system may also be invalid. Herein, the use of mice models should also be considered in addition to cell lines.

6 – CONCLUSION

Interesting findings have noted repressed TXNIP expression in cancerous tissues in human and thus outlined potential tumor-suppressive function of TXNIP. Our group has previously generated data on the translatome in MCF7 cells treated with metformin, rapamycin and PP242 and identified *TXNIP* to be translationally repressed by metformin while surprisingly being induced by mTOR inhibitors. We aimed to validate these findings and suggest that TXNIP is translationally upregulated by active site mTOR inhibitors (torin1), but phenformin, a more potent biguanide, did not appear to suppress *TXNIP* mRNA translation. In this study, we investigate the implication of TXNIP, a negative regulator of glucose uptake, in mediating the effects of biguanides and mTOR inhibitors on glucose uptake and cell proliferation. Consistent with previous studies, we report that phenformin increases glucose uptake, while torin1 suppresses it. Both inhibitors regulate TXNIP expression accordingly with their effects on glucose uptake. Despite opposing effects on glucose uptake, we also show that both drugs converge in inhibiting cell proliferation and mTORC1 signaling, albeit with different potencies. Importantly, we show that phenformin-induced increase in glucose uptake is mediated by TXNIP suppression in part by alterations in protein stability in MCF7. Abrogating phosphorylation of Ser-308 confers increased TXNIP stability and potentiates the phenformin-induced suppression of cell proliferation. Furthermore, we also point out that TXNIP may not play a role in the downregulation of glucose uptake by inhibitors of the PI3K-AKT-MTOR pathway in TXNIP-depleted MCF7 cells. Altogether, our findings gather suggestive implications of TXNIP in the context of glucose uptake and cell proliferation in biguanide and mTOR inhibitor treatments in MCF7 cells. To this end, further experimentation is still required to establish a solid overarching conclusion.

7 – OTHER WORKS/CONTRIBUTIONS

7.1 Co-authored publications

1. **Sept 2018 – METTL13 methylation of eEF1A increases tumorigenesis by increasing translational output** (Cell. PMID: 30612740)

   This paper shows that methyltransferase-like 13 dimethylation of eukaryotic elongation factor 1A lysine 55 is utilized by Ras-driven cancers to increase translational activity and promote tumorigenesis in vivo. In collaboration with Dr. Or Gozani's lab from Stanford USA, I contributed in generating data showing that perturbing translational output of ras-driven human cancer cell lines (HT1080, PaTu8902, T3M4, Colo-357) using EIF4A inhibitor (SDS-1-021) and show that it inhibits proliferation of these cancer cell lines relative to normal human fibroblasts (IMR90).

2. **Nov 2017 – Cross-talk between protein synthesis, energy metabolism, and autophagy in cancer** (Curr Opin Genet. PMID: 29179096)

   In this review, in a collaborative effort with Dr. Lisa Lindqvist and Dr. Luc Furic from Victoria AU, we gather findings that highlight novel aspects of signaling between protein synthesis, autophagy, and energy homeostasis in cancer.

3. **Nov 2018 – Translational Reprogramming Marks Adaptation to Asparagine Restriction in Cancer** (NCB. PMID: 31740775)

   In collaboration with Dr. Ze'ev Ronai's lab from San Diego USA, we show that MAPK pathway inhibition maximizes efficacy of asparagine restriction-focused therapies, highlighting a novel cellular adaptive response to amino acid restriction. I contributed in generating polysome-associated fractions for RT-qPCR to determine translational regulation of ATF4, a stress-induced gene, in conditions of asparagine limitation and MAPK inhibition.

4. **Nov 2017 – An ErbB2/c-Src axis drives mammary tumourigenesis through metabolically directed translational regulation of Polycomb Repressor Complex 2** (PMID: 31263101)

   In collaboration with Dr. William Muller's lab from Montreal CA, we show that c-Src controls ATP synthesis by upregulating mTORC1 activity and consequently increases mRNA translation of polycomb repressor complex 2 (PRC2) subunits SUZ12 and EZH2. These results reveal mechanistic action for ErbB2-driven carcinogenesis. My contribution involved generating polysome-associated fractions for RT-qPCR in c-Src knockout vs. wildtype ErbB2-driven mouse-derived cell lines.

7.2 Co-authored manuscripts (submitted)

1. **March 2018 - Translational control of breast cancer plasticity** (submitted to NatComms)

   In collaboration with Dr. Lynne Postovit's lab from Edmonton CA, we demonstrate that cancer cell plasticity undergoes translational reprogramming of breast cancer stem cell (BCSC)-associated genes such as NANOG, SNAIL and NODAL in response to stresses like hypoxia and chemotherapy despite mTOR suppression. In consequence, this represents a challenge in cancer treatment. I contributed in generating polysome-associated fractions in embryonic stem cell lines (H1 and H9) and breast cancer cell line (T47D) in conditions of hypoxia and normoxia. https://www.biorxiv.org/content/10.1101/596544v1

2. **May 2017 - Enhanced and selective translation expands the lysosome size and promotes antigen presentation during phagocyte activation** (submitted to PLoS Bio)

   In collaboration with Dr. Roberto Botelho's lab from Toronto CA, we show mTORC1-dependent lysosome remodeling via increased translation of lysosomal mRNAs. I generated polysome-associated fractions for RT-qPCR and RNAseq using RAW264.7 cells to determine translational regulation of lysosomal mRNAs LAMP1 and V-ATPase subunits, genes required for antigen presentation by dendritic cells. https://www.biorxiv.org/content/10.1101/260257v2

REFERENCES

Accili, D., and K.C. Arden. 2004. FoxOs at the crossroads of cellular metabolism, differentiation, and transformation. *Cell*. 117:421-426.

Alessi, D.R., S.R. James, C.P. Downes, A.B. Holmes, P.R. Gaffney, C.B. Reese, and P. Cohen. 1997. Characterization of a 3-phosphoinositide-dependent protein kinase which phosphorylates and activates protein kinase Balpha. *Curr Biol*. 7:261-269.

Algire, C., L. Amrein, M. Bazile, S. David, M. Zakikhani, and M. Pollak. 2011. Diet and tumor LKB1 expression interact to determine sensitivity to anti-neoplastic effects of metformin in vivo. *Oncogene*. 30:1174-1182.

Almuhaideb, A., N. Papathanasiou, and J. Bomanji. 2011. 18F-FDG PET/CT imaging in oncology. *Ann Saudi Med*. 31:3-13.

Andrzejewski, S., S.P. Gravel, M. Pollak, and J. St-Pierre. 2014. Metformin directly acts on mitochondria to alter cellular bioenergetics. *Cancer Metab*. 2:12.

Anthony, T.G., and R.C. Wek. 2012. TXNIP switches tracks toward a terminal UPR. *Cell Metab*. 16:135-137.

Asano, T., H. Katagiri, K. Takata, J.L. Lin, H. Ishihara, K. Inukai, K. Tsukuda, M. Kikuchi, H. Hirano, Y. Yazaki, and et al. 1991. The role of N-glycosylation of GLUT1 for glucose transport activity. *J Biol Chem*. 266:24632-24636.

Bacci, G., R. Capanna, M. Orlandi, I. Mancini, G. Bettelli, D. Dallari, and M. Campanacci. 1985. Prognostic significance of serum lactic acid dehydrogenase in Ewing's tumor of bone. *Ric Clin Lab*. 15:89-96.

Bailey, C.J., and R.C. Turner. 1996. Metformin. *N Engl J Med*. 334:574-579.

Baker, A.F., M.Y. Koh, R.R. Williams, B. James, H. Wang, W.R. Tate, A. Gallegos, D.D. Von Hoff, H. Han, and G. Powis. 2008. Identification of thioredoxin-interacting protein 1 as a hypoxia-inducible factor 1alpha-induced gene in pancreatic cancer. *Pancreas*. 36:178-186.

Banerjee, P., M.F. Ahmad, J.R. Grove, C. Kozlosky, D.J. Price, and J. Avruch. 1990. Molecular structure of a major insulin/mitogen-activated 70-kDa S6 protein kinase. *Proc Natl Acad Sci U S A*. 87:8550-8554.

Barnes, K., J.C. Ingram, O.H. Porras, L.F. Barros, E.R. Hudson, L.G. Fryer, F. Foufelle, D. Carling, D.G. Hardie, and S.A. Baldwin. 2002. Activation of GLUT1 by metabolic and osmotic stress: potential involvement of AMP-activated protein kinase (AMPK). *J Cell Sci*. 115:2433-2442.

Baron-Delage, S., L. Mahraoui, A. Cadoret, D. Veissiere, J.L. Taillemite, E. Chastre, C. Gespach, A. Zweibaum, J. Capeau, E. Brot-Laroche, and G. Cherqui. 1996. Deregulation of hexose transporter expression in Caco-2 cells by ras and polyoma middle T oncogenes. *Am J Physiol*. 270:G314-323.

Barthel, A., S.T. Okino, J. Liao, K. Nakatani, J. Li, J.P. Whitlock, Jr., and R.A. Roth. 1999. Regulation of GLUT1 gene transcription by the serine/threonine kinase Akt1. *J Biol Chem*. 274:20281-20286.

Beg, Z.H., D.W. Allmann, and D.M. Gibson. 1973. Modulation of 3-hydroxy-3-methylglutaryl coenzyme A reductase activity with cAMP and wth protein fractions of rat liver cytosol. *Biochem Biophys Res Commun*. 54:1362-1369.

Ben Sahra, I., K. Laurent, A. Loubat, S. Giorgetti-Peraldi, P. Colosetti, P. Auberger, J.F. Tanti, Y. Le Marchand-Brustel, and F. Bost. 2008. The antidiabetic drug metformin exerts an

antitumoral effect in vitro and in vivo through a decrease of cyclin D1 level. *Oncogene*. 27:3576-3586.
Benjamin, D., M. Colombi, C. Moroni, and M.N. Hall. 2011. Rapamycin passes the torch: a new generation of mTOR inhibitors. *Nat Rev Drug Discov*. 10:868-880.
Benz, A.H., M. Shajari, N. Peruzki, F. Dehghani, and E. Maronde. 2010. Early growth response-1 induction by fibroblast growth factor-1 via increase of mitogen-activated protein kinase and inhibition of protein kinase B in hippocampal neurons. *Br J Pharmacol*. 160:1621-1630.
Berg JM, T.J., Stryer L. 2002. Section 16.2, The Glycolytic Pathway Is Tightly Controlled. *In* Biochemistry. W H Freeman, New York.
Binder, C., L. Binder, D. Marx, A. Schauer, and W. Hiddemann. 1997. Deregulated simultaneous expression of multiple glucose transporter isoforms in malignant cells and tissues. *Anticancer Res*. 17:4299-4304.
Birnbaum, M.J., H.C. Haspel, and O.M. Rosen. 1986. Cloning and characterization of a cDNA encoding the rat brain glucose-transporter protein. *Proc Natl Acad Sci U S A*. 83:5784-5788.
Birnbaum, M.J., H.C. Haspel, and O.M. Rosen. 1987. Transformation of rat fibroblasts by FSV rapidly increases glucose transporter gene transcription. *Science*. 235:1495-1498.
Birsoy, K., T. Wang, W.W. Chen, E. Freinkman, M. Abu-Remaileh, and D.M. Sabatini. 2015. An Essential Role of the Mitochondrial Electron Transport Chain in Cell Proliferation Is to Enable Aspartate Synthesis. *Cell*. 162:540-551.
Boerner, P., R.J. Resnick, and E. Racker. 1985. Stimulation of glycolysis and amino acid uptake in NRK-49F cells by transforming growth factor beta and epidermal growth factor. *Proc Natl Acad Sci U S A*. 82:1350-1353.
Bolster, D.R., S.J. Crozier, S.R. Kimball, and L.S. Jefferson. 2002. AMP-activated protein kinase suppresses protein synthesis in rat skeletal muscle through down-regulated mammalian target of rapamycin (mTOR) signaling. *J Biol Chem*. 277:23977-23980.
Boudeau, J., G. Sapkota, and D.R. Alessi. 2003. LKB1, a protein kinase regulating cell proliferation and polarity. *FEBS Lett*. 546:159-165.
Bowker, S.L., S.R. Majumdar, P. Veugelers, and J.A. Johnson. 2006. Increased cancer-related mortality for patients with type 2 diabetes who use sulfonylureas or insulin. *Diabetes Care*. 29:254-258.
Boxer, R.B., D.B. Stairs, K.D. Dugan, K.L. Notarfrancesco, C.P. Portocarrero, B.A. Keister, G.K. Belka, H. Cho, J.C. Rathmell, C.B. Thompson, M.J. Birnbaum, and L.A. Chodosh. 2006. Isoform-specific requirement for Akt1 in the developmental regulation of cellular metabolism during lactation. *Cell Metab*. 4:475-490.
Bridges, H.R., A.J. Jones, M.N. Pollak, and J. Hirst. 2014. Effects of metformin and other biguanides on oxidative phosphorylation in mitochondria. *Biochem J*. 462:475-487.
Brunn, G.J., C.C. Hudson, A. Sekulic, J.M. Williams, H. Hosoi, P.J. Houghton, J.C. Lawrence, Jr., and R.T. Abraham. 1997. Phosphorylation of the translational repressor PHAS-I by the mammalian target of rapamycin. *Science*. 277:99-101.
Burant, C.F., and G.I. Bell. 1992. Mammalian facilitative glucose transporters: evidence for similar substrate recognition sites in functionally monomeric proteins. *Biochemistry*. 31:10414-10420.

Burant, C.F., J. Takeda, E. Brot-Laroche, G.I. Bell, and N.O. Davidson. 1992. Fructose transporter in human spermatozoa and small intestine is GLUT5. *J Biol Chem*. 267:14523-14526.

Burgess, D.J. 2011. Metabolism: choose your carbon source. *Nat Rev Cancer*. 11:80.

Burke, J.E., O. Perisic, G.R. Masson, O. Vadas, and R.L. Williams. 2012. Oncogenic mutations mimic and enhance dynamic events in the natural activation of phosphoinositide 3-kinase p110alpha (PIK3CA). *Proc Natl Acad Sci U S A*. 109:15259-15264.

Burke, J.E., and R.L. Williams. 2015. Synergy in activating class I PI3Ks. *Trends Biochem Sci*. 40:88-100.

Buzzai, M., R.G. Jones, R.K. Amaravadi, J.J. Lum, R.J. DeBerardinis, F. Zhao, B. Viollet, and C.B. Thompson. 2007. Systemic treatment with the antidiabetic drug metformin selectively impairs p53-deficient tumor cell growth. *Cancer Res*. 67:6745-6752.

Cadenas, C., D. Franckenstein, M. Schmidt, M. Gehrmann, M. Hermes, B. Geppert, W. Schormann, L.J. Maccoux, M. Schug, A. Schumann, C. Wilhelm, E. Freis, K. Ickstadt, J. Rahnenfuhrer, J.I. Baumbach, A. Sickmann, and J.G. Hengstler. 2010. Role of thioredoxin reductase 1 and thioredoxin interacting protein in prognosis of breast cancer. *Breast Cancer Res*. 12:R44.

Cantley, L.C. 2002. The phosphoinositide 3-kinase pathway. *Science*. 296:1655-1657.

Cantrell, L.A., C. Zhou, A. Mendivil, K.M. Malloy, P.A. Gehrig, and V.L. Bae-Jump. 2010. Metformin is a potent inhibitor of endometrial cancer cell proliferation--implications for a novel treatment strategy. *Gynecol Oncol*. 116:92-98.

Carling, D., V.A. Zammit, and D.G. Hardie. 1987. A common bicyclic protein kinase cascade inactivates the regulatory enzymes of fatty acid and cholesterol biosynthesis. *FEBS Lett*. 223:217-222.

Carlson, C.A., and K.H. Kim. 1973. Regulation of hepatic acetyl coenzyme A carboxylase by phosphorylation and dephosphorylation. *J Biol Chem*. 248:378-380.

Chandarlapaty, S., A. Sawai, M. Scaltriti, V. Rodrik-Outmezguine, O. Grbovic-Huezo, V. Serra, P.K. Majumder, J. Baselga, and N. Rosen. 2011. AKT inhibition relieves feedback suppression of receptor tyrosine kinase expression and activity. *Cancer Cell*. 19:58-71.

Chau, G.C., D.U. Im, T.M. Kang, J.M. Bae, W. Kim, S. Pyo, E.Y. Moon, and S.H. Um. 2017. mTOR controls ChREBP transcriptional activity and pancreatic beta cell survival under diabetic stress. *J Cell Biol*. 216:2091-2105.

Cheeseman, C. 2008. GLUT7: a new intestinal facilitated hexose transporter. *Am J Physiol Endocrinol Metab*. 295:E238-241.

Chen, J., G. Saxena, I.N. Mungrue, A.J. Lusis, and A. Shalev. 2008. Thioredoxin-interacting protein: a critical link between glucose toxicity and beta-cell apoptosis. *Diabetes*. 57:938-944.

Chen, J.L., D. Merl, C.W. Peterson, J. Wu, P.Y. Liu, H. Yin, D.M. Muoio, D.E. Ayer, M. West, and J.T. Chi. 2010. Lactic acidosis triggers starvation response with paradoxical induction of TXNIP through MondoA. *PLoS Genet*. 6:e1001093.

Chen, K.S., and H.F. DeLuca. 1994. Isolation and characterization of a novel cDNA from HL-60 cells treated with 1,25-dihydroxyvitamin D-3. *Biochim Biophys Acta*. 1219:26-32.

Cheng, J.Q., C.W. Lindsley, G.Z. Cheng, H. Yang, and S.V. Nicosia. 2005. The Akt/PKB pathway: molecular target for cancer drug discovery. *Oncogene*. 24:7482-7492.

Chutkow, W.A., P. Patwari, J. Yoshioka, and R.T. Lee. 2008. Thioredoxin-interacting protein (Txnip) is a critical regulator of hepatic glucose production. *J Biol Chem*. 283:2397-2406.

Colville, C.A., M.J. Seatter, T.J. Jess, G.W. Gould, and H.M. Thomas. 1993. Kinetic analysis of the liver-type (GLUT2) and brain-type (GLUT3) glucose transporters in Xenopus oocytes: substrate specificities and effects of transport inhibitors. *Biochem J*. 290 (Pt 3):701-706.

Corton, J.M., J.G. Gillespie, S.A. Hawley, and D.G. Hardie. 1995. 5-aminoimidazole-4-carboxamide ribonucleoside. A specific method for activating AMP-activated protein kinase in intact cells? *Eur J Biochem*. 229:558-565.

Crabtree, H.G. 1929. Observations on the carbohydrate metabolism of tumours. *Biochem J*. 23:536-545.

Dawson, P.A., J.C. Mychaleckyj, S.C. Fossey, S.J. Mihic, A.L. Craddock, and D.W. Bowden. 2001. Sequence and functional analysis of GLUT10: a glucose transporter in the Type 2 diabetes-linked region of chromosome 20q12-13.1. *Mol Genet Metab*. 74:186-199.

Decensi, A., M. Puntoni, P. Goodwin, M. Cazzaniga, A. Gennari, B. Bonanni, and S. Gandini. 2010. Metformin and cancer risk in diabetic patients: a systematic review and meta-analysis. *Cancer Prev Res (Phila)*. 3:1451-1461.

Deprez, J., D. Vertommen, D.R. Alessi, L. Hue, and M.H. Rider. 1997. Phosphorylation and activation of heart 6-phosphofructo-2-kinase by protein kinase B and other protein kinases of the insulin signaling cascades. *J Biol Chem*. 272:17269-17275.

Doege, H., A. Bocianski, H.G. Joost, and A. Schurmann. 2000a. Activity and genomic organization of human glucose transporter 9 (GLUT9), a novel member of the family of sugar-transport facilitators predominantly expressed in brain and leucocytes. *Biochem J*. 350 Pt 3:771-776.

Doege, H., A. Schurmann, G. Bahrenberg, A. Brauers, and H.G. Joost. 2000b. GLUT8, a novel member of the sugar transport facilitator family with glucose transport activity. *J Biol Chem*. 275:16275-16280.

Domchek, S.M., K.R. Auger, S. Chatterjee, T.R. Burke, Jr., and S.E. Shoelson. 1992. Inhibition of SH2 domain/phosphoprotein association by a nonhydrolyzable phosphonopeptide. *Biochemistry*. 31:9865-9870.

Dowling, R.J., I. Topisirovic, T. Alain, M. Bidinosti, B.D. Fonseca, E. Petroulakis, X. Wang, O. Larsson, A. Selvaraj, Y. Liu, S.C. Kozma, G. Thomas, and N. Sonenberg. 2010. mTORC1-mediated cell proliferation, but not cell growth, controlled by the 4E-BPs. *Science*. 328:1172-1176.

Dowling, R.J., M. Zakikhani, I.G. Fantus, M. Pollak, and N. Sonenberg. 2007. Metformin inhibits mammalian target of rapamycin-dependent translation initiation in breast cancer cells. *Cancer Res*. 67:10804-10812.

Drahota, Z., E. Palenickova, R. Endlicher, M. Milerova, J. Brejchova, M. Vosahlikova, P. Svoboda, L. Kazdova, M. Kalous, Z. Cervinkova, and M. Cahova. 2014. Biguanides inhibit complex I, II and IV of rat liver mitochondria and modify their functional properties. *Physiol Res*. 63:1-11.

Eissing, M., L. Ripken, G. Schreibelt, H. Westdorp, M. Ligtenberg, R. Netea-Maier, M.G. Netea, I.J.M. de Vries, and N. Hoogerbrugge. 2019. PTEN Hamartoma Tumor Syndrome and Immune Dysregulation. *Transl Oncol*. 12:361-367.

Evans, J.M., L.A. Donnelly, A.M. Emslie-Smith, D.R. Alessi, and A.D. Morris. 2005. Metformin and reduced risk of cancer in diabetic patients. *BMJ*. 330:1304-1305.

Faivre, S., G. Kroemer, and E. Raymond. 2006. Current development of mTOR inhibitors as anticancer agents. *Nat Rev Drug Discov*. 5:671-688.

Fantin, V.R., J. St-Pierre, and P. Leder. 2006. Attenuation of LDH-A expression uncovers a link between glycolysis, mitochondrial physiology, and tumor maintenance. *Cancer Cell*. 9:425-434.

Feldman, M.E., B. Apsel, A. Uotila, R. Loewith, Z.A. Knight, D. Ruggero, and K.M. Shokat. 2009. Active-site inhibitors of mTOR target rapamycin-resistant outputs of mTORC1 and mTORC2. *PLoS Biol*. 7:e38.

Flavahan, W.A., Q. Wu, M. Hitomi, N. Rahim, Y. Kim, A.E. Sloan, R.J. Weil, I. Nakano, J.N. Sarkaria, B.W. Stringer, B.W. Day, M. Li, J.D. Lathia, J.N. Rich, and A.B. Hjelmeland. 2013. Brain tumor initiating cells adapt to restricted nutrition through preferential glucose uptake. *Nat Neurosci*. 16:1373-1382.

Flaveny, C.A., K. Griffett, D. El-Gendy Bel, M. Kazantzis, M. Sengupta, A.L. Amelio, A. Chatterjee, J. Walker, L.A. Solt, T.M. Kamenecka, and T.P. Burris. 2015. Broad Anti-tumor Activity of a Small Molecule that Selectively Targets the Warburg Effect and Lipogenesis. *Cancer Cell*. 28:42-56.

Flier, J.S., M.M. Mueckler, P. Usher, and H.F. Lodish. 1987. Elevated levels of glucose transport and transporter messenger RNA are induced by ras or src oncogenes. *Science*. 235:1492-1495.

Foretz, M., S. Hebrard, J. Leclerc, E. Zarrinpashneh, M. Soty, G. Mithieux, K. Sakamoto, F. Andreelli, and B. Viollet. 2010. Metformin inhibits hepatic gluconeogenesis in mice independently of the LKB1/AMPK pathway via a decrease in hepatic energy state. *J Clin Invest*. 120:2355-2369.

Fresno Vara, J.A., E. Casado, J. de Castro, P. Cejas, C. Belda-Iniesta, and M. Gonzalez-Baron. 2004. PI3K/Akt signalling pathway and cancer. *Cancer Treat Rev*. 30:193-204.

Fruman, D.A., H. Chiu, B.D. Hopkins, S. Bagrodia, L.C. Cantley, and R.T. Abraham. 2017. The PI3K Pathway in Human Disease. *Cell*. 170:605-635.

Fryer, L.G., A. Parbu-Patel, and D. Carling. 2002. The Anti-diabetic drugs rosiglitazone and metformin stimulate AMP-activated protein kinase through distinct signaling pathways. *J Biol Chem*. 277:25226-25232.

Fujii, N., T. Hayashi, M.F. Hirshman, J.T. Smith, S.A. Habinowski, L. Kaijser, J. Mu, O. Ljungqvist, M.J. Birnbaum, L.A. Witters, A. Thorell, and L.J. Goodyear. 2000. Exercise induces isoform-specific increase in 5'AMP-activated protein kinase activity in human skeletal muscle. *Biochem Biophys Res Commun*. 273:1150-1155.

Fukumoto, H., S. Seino, H. Imura, Y. Seino, R.L. Eddy, Y. Fukushima, M.G. Byers, T.B. Shows, and G.I. Bell. 1988. Sequence, tissue distribution, and chromosomal localization of mRNA encoding a human glucose transporter-like protein. *Proc Natl Acad Sci U S A*. 85:5434-5438.

Gadalla, A.E., T. Pearson, A.J. Currie, N. Dale, S.A. Hawley, M. Sheehan, W. Hirst, A.D. Michel, A. Randall, D.G. Hardie, and B.G. Frenguelli. 2004. AICA riboside both activates AMP-activated protein kinase and competes with adenosine for the nucleoside transporter in the CA1 region of the rat hippocampus. *J Neurochem*. 88:1272-1282.

Gandin, V., K. Sikstrom, T. Alain, M. Morita, S. McLaughlan, O. Larsson, and I. Topisirovic. 2014. Polysome fractionation and analysis of mammalian translatomes on a genome-wide scale. *Journal of visualized experiments : JoVE*.

Garcia-Echeverria, C., and W.R. Sellers. 2008. Drug discovery approaches targeting the PI3K/Akt pathway in cancer. *Oncogene*. 27:5511-5526.

Garlich, J.R., P. De, N. Dey, J.D. Su, X. Peng, A. Miller, R. Murali, Y. Lu, G.B. Mills, V. Kundra, H.K. Shu, Q. Peng, and D.L. Durden. 2008. A vascular targeted pan phosphoinositide 3-kinase inhibitor prodrug, SF1126, with antitumor and antiangiogenic activity. *Cancer Res*. 68:206-215.

Giardiello, F.M., S.B. Welsh, S.R. Hamilton, G.J. Offerhaus, A.M. Gittelsohn, S.V. Booker, A.J. Krush, J.H. Yardley, and G.D. Luk. 1987. Increased risk of cancer in the Peutz-Jeghers syndrome. *N Engl J Med*. 316:1511-1514.

Gills, J.J., and P.A. Dennis. 2004. The development of phosphatidylinositol ether lipid analogues as inhibitors of the serine/threonine kinase, Akt. *Expert Opin Investig Drugs*. 13:787-797.

Gills, J.J., S. Holbeck, M. Hollingshead, S.M. Hewitt, A.P. Kozikowski, and P.A. Dennis. 2006. Spectrum of activity and molecular correlates of response to phosphatidylinositol ether lipid analogues, novel lipid-based inhibitors of Akt. *Mol Cancer Ther*. 5:713-722.

Gingras, A.C., B. Raught, S.P. Gygi, A. Niedzwiecka, M. Miron, S.K. Burley, R.D. Polakiewicz, A. Wyslouch-Cieszynska, R. Aebersold, and N. Sonenberg. 2001. Hierarchical phosphorylation of the translation inhibitor 4E-BP1. *Genes Dev*. 15:2852-2864.

Goldberg, S.F., M.E. Miele, N. Hatta, M. Takata, C. Paquette-Straub, L.P. Freedman, and D.R. Welch. 2003. Melanoma metastasis suppression by chromosome 6: evidence for a pathway regulated by CRSP3 and TXNIP. *Cancer Res*. 63:432-440.

Goldblatt, H., and G. Cameron. 1953. Induced malignancy in cells from rat myocardium subjected to intermittent anaerobiosis during long propagation in vitro. *J Exp Med*. 97:525-552.

Gorgens, S.W., T. Benninghoff, K. Eckardt, C. Springer, A. Chadt, A. Melior, J. Wefers, A. Cramer, J. Jensen, K.I. Birkeland, C.A. Drevon, H. Al-Hasani, and J. Eckel. 2017. Hypoxia in Combination With Muscle Contraction Improves Insulin Action and Glucose Metabolism in Human Skeletal Muscle via the HIF-1alpha Pathway. *Diabetes*. 66:2800-2807.

Gotlieb, W.H., J. Saumet, M.C. Beauchamp, J. Gu, S. Lau, M.N. Pollak, and I. Bruchim. 2008. In vitro metformin anti-neoplastic activity in epithelial ovarian cancer. *Gynecol Oncol*. 110:246-250.

Gottlob, K., N. Majewski, S. Kennedy, E. Kandel, R.B. Robey, and N. Hay. 2001. Inhibition of early apoptotic events by Akt/PKB is dependent on the first committed step of glycolysis and mitochondrial hexokinase. *Genes Dev*. 15:1406-1418.

Graff, J.R., B.W. Konicek, J.H. Carter, and E.G. Marcusson. 2008. Targeting the eukaryotic translation initiation factor 4E for cancer therapy. *Cancer Res*. 68:631-634.

Gravel, S.P., L. Hulea, N. Toban, E. Birman, M.J. Blouin, M. Zakikhani, Y. Zhao, I. Topisirovic, J. St-Pierre, and M. Pollak. 2014. Serine deprivation enhances antineoplastic activity of biguanides. *Cancer Res*. 74:7521-7533.

Grover-McKay, M., S.A. Walsh, E.A. Seftor, P.A. Thomas, and M.J. Hendrix. 1998. Role for glucose transporter 1 protein in human breast cancer. *Pathol Oncol Res*. 4:115-120.

Guertin, D.A., and D.M. Sabatini. 2007. Defining the role of mTOR in cancer. *Cancer Cell*. 12:9-22.

Haeusler, R.A., T.E. McGraw, and D. Accili. 2018. Biochemical and cellular properties of insulin receptor signalling. *Nat Rev Mol Cell Biol*. 19:31-44.

Han, K.S., and D.E. Ayer. 2013. MondoA senses adenine nucleotides: transcriptional induction of thioredoxin-interacting protein. *Biochem J*. 453:209-218.

Han, S.H., J.H. Jeon, H.R. Ju, U. Jung, K.Y. Kim, H.S. Yoo, Y.H. Lee, K.S. Song, H.M. Hwang, Y.S. Na, Y. Yang, K.N. Lee, and I. Choi. 2003. VDUP1 upregulated by TGF-beta1 and 1,25-dihydorxyvitamin D3 inhibits tumor cell growth by blocking cell-cycle progression. *Oncogene*. 22:4035-4046.

Hanahan, D., and R.A. Weinberg. 2000. The hallmarks of cancer. *Cell*. 100:57-70.

Hardie, D.G. 2011. AMP-activated protein kinase: an energy sensor that regulates all aspects of cell function. *Genes Dev*. 25:1895-1908.

Hardie, D.G., I.P. Salt, S.A. Hawley, and S.P. Davies. 1999. AMP-activated protein kinase: an ultrasensitive system for monitoring cellular energy charge. *Biochem J*. 338 (Pt 3):717-722.

Hatanaka, M. 1974. Transport of sugars in tumor cell membranes. *Biochim Biophys Acta*. 355:77-104.

Hawley, S.A., J. Boudeau, J.L. Reid, K.J. Mustard, L. Udd, T.P. Makela, D.R. Alessi, and D.G. Hardie. 2003. Complexes between the LKB1 tumor suppressor, STRAD alpha/beta and MO25 alpha/beta are upstream kinases in the AMP-activated protein kinase cascade. *J Biol*. 2:28.

Hawley, S.A., M. Davison, A. Woods, S.P. Davies, R.K. Beri, D. Carling, and D.G. Hardie. 1996. Characterization of the AMP-activated protein kinase kinase from rat liver and identification of threonine 172 as the major site at which it phosphorylates AMP-activated protein kinase. *J Biol Chem*. 271:27879-27887.

Hawley, S.A., A.E. Gadalla, G.S. Olsen, and D.G. Hardie. 2002. The antidiabetic drug metformin activates the AMP-activated protein kinase cascade via an adenine nucleotide-independent mechanism. *Diabetes*. 51:2420-2425.

Hawley, S.A., D.A. Pan, K.J. Mustard, L. Ross, J. Bain, A.M. Edelman, B.G. Frenguelli, and D.G. Hardie. 2005. Calmodulin-dependent protein kinase kinase-beta is an alternative upstream kinase for AMP-activated protein kinase. *Cell Metab*. 2:9-19.

Hawley, S.A., M.A. Selbert, E.G. Goldstein, A.M. Edelman, D. Carling, and D.G. Hardie. 1995. 5'-AMP activates the AMP-activated protein kinase cascade, and Ca2+/calmodulin activates the calmodulin-dependent protein kinase I cascade, via three independent mechanisms. *J Biol Chem*. 270:27186-27191.

Hay, N. 2005. The Akt-mTOR tango and its relevance to cancer. *Cancer Cell*. 8:179-183.

Hay, N., and N. Sonenberg. 2004. Upstream and downstream of mTOR. *Genes Dev*. 18:1926-1945.

Hemminki, A., D. Markie, I. Tomlinson, E. Avizienyte, S. Roth, A. Loukola, G. Bignell, W. Warren, M. Aminoff, P. Hoglund, H. Jarvinen, P. Kristo, K. Pelin, M. Ridanpaa, R. Salovaara, T. Toro, W. Bodmer, S. Olschwang, A.S. Olsen, M.R. Stratton, A. de la Chapelle, and L.A. Aaltonen. 1998. A serine/threonine kinase gene defective in Peutz-Jeghers syndrome. *Nature*. 391:184-187.

Henin, N., M.F. Vincent, H.E. Gruber, and G. Van den Berghe. 1995. Inhibition of fatty acid and cholesterol synthesis by stimulation of AMP-activated protein kinase. *FASEB J*. 9:541-546.

Hilgard, P., T. Klenner, J. Stekar, G. Nossner, B. Kutscher, and J. Engel. 1997. D-21266, a new heterocyclic alkylphospholipid with antitumour activity. *Eur J Cancer*. 33:442-446.

Hiraki, Y., O.M. Rosen, and M.J. Birnbaum. 1988. Growth factors rapidly induce expression of the glucose transporter gene. *J Biol Chem*. 263:13655-13662.

Hong, S.Y., F.X. Yu, Y. Luo, and T. Hagen. 2016. Oncogenic activation of the PI3K/Akt pathway promotes cellular glucose uptake by downregulating the expression of thioredoxin-interacting protein. *Cell Signal*. 28:377-383.

Horman, S., G. Browne, U. Krause, J. Patel, D. Vertommen, L. Bertrand, A. Lavoinne, L. Hue, C. Proud, and M. Rider. 2002. Activation of AMP-activated protein kinase leads to the phosphorylation of elongation factor 2 and an inhibition of protein synthesis. *Curr Biol*. 12:1419-1423.

Hosono, K., H. Endo, H. Takahashi, M. Sugiyama, E. Sakai, T. Uchiyama, K. Suzuki, H. Iida, Y. Sakamoto, K. Yoneda, T. Koide, C. Tokoro, Y. Abe, M. Inamori, H. Nakagama, and A. Nakajima. 2010. Metformin suppresses colorectal aberrant crypt foci in a short-term clinical trial. *Cancer Prev Res (Phila)*. 3:1077-1083.

Hsieh, A.C., Y. Liu, M.P. Edlind, N.T. Ingolia, M.R. Janes, A. Sher, E.Y. Shi, C.R. Stumpf, C. Christensen, M.J. Bonham, S. Wang, P. Ren, M. Martin, K. Jessen, M.E. Feldman, J.S. Weissman, K.M. Shokat, C. Rommel, and D. Ruggero. 2012. The translational landscape of mTOR signalling steers cancer initiation and metastasis. *Nature*. 485:55-61.

Hu, F.B., J.E. Manson, M.J. Stampfer, G. Colditz, S. Liu, C.G. Solomon, and W.C. Willett. 2001. Diet, lifestyle, and the risk of type 2 diabetes mellitus in women. *N Engl J Med*. 345:790-797.

Hurley, R.L., K.A. Anderson, J.M. Franzone, B.E. Kemp, A.R. Means, and L.A. Witters. 2005. The Ca2+/calmodulin-dependent protein kinase kinases are AMP-activated protein kinase kinases. *J Biol Chem*. 280:29060-29066.

Huy, H., H.Y. Song, M.J. Kim, W.S. Kim, D.O. Kim, J.E. Byun, J. Lee, Y.J. Park, T.D. Kim, S.R. Yoon, E.J. Choi, C.H. Lee, J.Y. Noh, H. Jung, and I. Choi. 2018. TXNIP regulates AKT-mediated cellular senescence by direct interaction under glucose-mediated metabolic stress. *Aging Cell*. 17:e12836.

Hwang, J., H.W. Suh, Y.H. Jeon, E. Hwang, L.T. Nguyen, J. Yeom, S.G. Lee, C. Lee, K.J. Kim, B.S. Kang, J.O. Jeong, T.K. Oh, I. Choi, J.O. Lee, and M.H. Kim. 2014. The structural basis for the negative regulation of thioredoxin by thioredoxin-interacting protein. *Nat Commun*. 5:2958.

Ibberson, M., M. Uldry, and B. Thorens. 2000. GLUTX1, a novel mammalian glucose transporter expressed in the central nervous system and insulin-sensitive tissues. *J Biol Chem*. 275:4607-4612.

Ihle, N.T., G. Paine-Murrieta, M.I. Berggren, A. Baker, W.R. Tate, P. Wipf, R.T. Abraham, D.L. Kirkpatrick, and G. Powis. 2005. The phosphatidylinositol-3-kinase inhibitor PX-866 overcomes resistance to the epidermal growth factor receptor inhibitor gefitinib in A-549 human non-small cell lung cancer xenografts. *Mol Cancer Ther*. 4:1349-1357.

Ingebritsen, T.S., H.S. Lee, R.A. Parker, and D.M. Gibson. 1978. Reversible modulation of the activities of both liver microsomal hydroxymethylglutaryl coenzyme A reductase and its inactivating enzyme. Evidence for regulation by phosphorylation-dephosphorylation. *Biochem Biophys Res Commun*. 81:1268-1277.

Inoki, K., T. Zhu, and K.L. Guan. 2003. TSC2 mediates cellular energy response to control cell growth and survival. *Cell*. 115:577-590.

Isakovic, A., L. Harhaji, D. Stevanovic, Z. Markovic, M. Sumarac-Dumanovic, V. Starcevic, D. Micic, and V. Trajkovic. 2007. Dual antiglioma action of metformin: cell cycle arrest and mitochondria-dependent apoptosis. *Cell Mol Life Sci*. 64:1290-1302.

Iversen, A.B., M.R. Horsman, S. Jakobsen, J.B. Jensen, C. Garm, N. Jessen, P. Breining, J. Frokiaer, and M. Busk. 2017. Results from (11)C-metformin-PET scans, tissue analysis and cellular drug-sensitivity assays questions the view that biguanides affects tumor respiration directly. *Sci Rep*. 7:9436.

Jean, S., and A.A. Kiger. 2014. Classes of phosphoinositide 3-kinases at a glance. *J Cell Sci*. 127:923-928.

Jenne, D.E., H. Reimann, J. Nezu, W. Friedel, S. Loff, R. Jeschke, O. Muller, W. Back, and M. Zimmer. 1998. Peutz-Jeghers syndrome is caused by mutations in a novel serine threonine kinase. *Nat Genet*. 18:38-43.

Jeon, J.H., K.N. Lee, C.Y. Hwang, K.S. Kwon, K.H. You, and I. Choi. 2005. Tumor suppressor VDUP1 increases p27(kip1) stability by inhibiting JAB1. *Cancer Res*. 65:4485-4489.

Jin, H.O., S.K. Seo, Y.S. Kim, S.H. Woo, K.H. Lee, J.Y. Yi, S.J. Lee, T.B. Choe, J.H. Lee, S. An, S.I. Hong, and I.C. Park. 2011. TXNIP potentiates Redd1-induced mTOR suppression through stabilization of Redd1. *Oncogene*. 30:3792-3801.

Joost, H.G., G.I. Bell, J.D. Best, M.J. Birnbaum, M.J. Charron, Y.T. Chen, H. Doege, D.E. James, H.F. Lodish, K.H. Moley, J.F. Moley, M. Mueckler, S. Rogers, A. Schurmann, S. Seino, and B. Thorens. 2002. Nomenclature of the GLUT/SLC2A family of sugar/polyol transport facilitators. *Am J Physiol Endocrinol Metab*. 282:E974-976.

Joost, H.G., and B. Thorens. 2001. The extended GLUT-family of sugar/polyol transport facilitators: nomenclature, sequence characteristics, and potential function of its novel members (review). *Mol Membr Biol*. 18:247-256.

Junien, J.L., G. Chomette, M. Guillaume, H. Wajcman, and J. Sterne. 1981. [Effect of long-term metformin treatment on the development of diabetes in genetically diabetic mice (DBM) (author's transl)]. *Diabete Metab*. 7:251-258.

Junn, E., S.H. Han, J.Y. Im, Y. Yang, E.W. Cho, H.D. Um, D.K. Kim, K.W. Lee, P.L. Han, S.G. Rhee, and I. Choi. 2000. Vitamin D3 up-regulated protein 1 mediates oxidative stress via suppressing the thioredoxin function. *J Immunol*. 164:6287-6295.

Kaadige, M.R., R.E. Looper, S. Kamalanaadhan, and D.E. Ayer. 2009. Glutamine-dependent anapleurosis dictates glucose uptake and cell growth by regulating MondoA transcriptional activity. *Proc Natl Acad Sci U S A*. 106:14878-14883.

Kaadige, M.R., J. Yang, B.R. Wilde, and D.E. Ayer. 2015. MondoA-Mlx transcriptional activity is limited by mTOR-MondoA interaction. *Mol Cell Biol*. 35:101-110.

Kauffmann-Zeh, A., P. Rodriguez-Viciana, E. Ulrich, C. Gilbert, P. Coffer, J. Downward, and G. Evan. 1997. Suppression of c-Myc-induced apoptosis by Ras signalling through PI(3)K and PKB. *Nature*. 385:544-548.

Keller, K., M. Strube, and M. Mueckler. 1989. Functional expression of the human HepG2 and rat adipocyte glucose transporters in Xenopus oocytes. Comparison of kinetic parameters. *J Biol Chem*. 264:18884-18889.

Kibbe, C., J. Chen, G. Xu, G. Jing, and A. Shalev. 2013. FOXO1 competes with carbohydrate response element-binding protein (ChREBP) and inhibits thioredoxin-interacting protein (TXNIP) transcription in pancreatic beta cells. *J Biol Chem*. 288:23194-23202.

Kim, J.W., P. Gao, Y.C. Liu, G.L. Semenza, and C.V. Dang. 2007. Hypoxia-inducible factor 1 and dysregulated c-Myc cooperatively induce vascular endothelial growth factor and metabolic switches hexokinase 2 and pyruvate dehydrogenase kinase 1. *Mol Cell Biol*. 27:7381-7393.

Kimura, N., C. Tokunaga, S. Dalal, C. Richardson, K. Yoshino, K. Hara, B.E. Kemp, L.A. Witters, O. Mimura, and K. Yonezawa. 2003. A possible linkage between AMP-activated protein kinase (AMPK) and mammalian target of rapamycin (mTOR) signalling pathway. *Genes Cells*. 8:65-79.

Knight, Z.A., B. Gonzalez, M.E. Feldman, E.R. Zunder, D.D. Goldenberg, O. Williams, R. Loewith, D. Stokoe, A. Balla, B. Toth, T. Balla, W.A. Weiss, R.L. Williams, and K.M. Shokat. 2006. A pharmacological map of the PI3-K family defines a role for p110alpha in insulin signaling. *Cell*. 125:733-747.

Knoll, S., K. Furst, B. Kowtharapu, U. Schmitz, S. Marquardt, O. Wolkenhauer, H. Martin, and B.M. Putzer. 2014. E2F1 induces miR-224/452 expression to drive EMT through TXNIP downregulation. *EMBO Rep*. 15:1315-1329.

Koenen, T.B., R. Stienstra, L.J. van Tits, J. de Graaf, A.F. Stalenhoef, L.A. Joosten, C.J. Tack, and M.G. Netea. 2011. Hyperglycemia activates caspase-1 and TXNIP-mediated IL-1beta transcription in human adipose tissue. *Diabetes*. 60:517-524.

Kohn, A.D., S.A. Summers, M.J. Birnbaum, and R.A. Roth. 1996. Expression of a constitutively active Akt Ser/Thr kinase in 3T3-L1 adipocytes stimulates glucose uptake and glucose transporter 4 translocation. *J Biol Chem*. 271:31372-31378.

Kordes, S., M.N. Pollak, A.H. Zwinderman, R.A. Mathot, M.J. Weterman, A. Beeker, C.J. Punt, D.J. Richel, and J.W. Wilmink. 2015. Metformin in patients with advanced pancreatic cancer: a double-blind, randomised, placebo-controlled phase 2 trial. *Lancet Oncol*. 16:839-847.

Krause, U., L. Bertrand, and L. Hue. 2002. Control of p70 ribosomal protein S6 kinase and acetyl-CoA carboxylase by AMP-activated protein kinase and protein phosphatases in isolated hepatocytes. *Eur J Biochem*. 269:3751-3759.

Kurth-Kraczek, E.J., M.F. Hirshman, L.J. Goodyear, and W.W. Winder. 1999. 5' AMP-activated protein kinase activation causes GLUT4 translocation in skeletal muscle. *Diabetes*. 48:1667-1671.

Kwon, H.J., Y.S. Won, H.W. Suh, J.H. Jeon, Y. Shao, S.R. Yoon, J.W. Chung, T.D. Kim, H.M. Kim, K.H. Nam, W.K. Yoon, D.G. Kim, J.H. Kim, Y.S. Kim, D.Y. Kim, H.C. Kim, and I. Choi. 2010. Vitamin D3 upregulated protein 1 suppresses TNF-alpha-induced NF-kappaB activation in hepatocarcinogenesis. *J Immunol*. 185:3980-3989.

Laderoute, K.R., K. Amin, J.M. Calaoagan, M. Knapp, T. Le, J. Orduna, M. Foretz, and B. Viollet. 2006. 5'-AMP-activated protein kinase (AMPK) is induced by low-oxygen and glucose deprivation conditions found in solid-tumor microenvironments. *Mol Cell Biol*. 26:5336-5347.

Lanczky, A., A. Nagy, G. Bottai, G. Munkacsy, A. Szabo, L. Santarpia, and B. Gyorffy. 2016. miRpower: a web-tool to validate survival-associated miRNAs utilizing expression data from 2178 breast cancer patients. *Breast Cancer Res Treat*. 160:439-446.

Landman, G.W., N. Kleefstra, K.J. van Hateren, K.H. Groenier, R.O. Gans, and H.J. Bilo. 2010. Metformin associated with lower cancer mortality in type 2 diabetes: ZODIAC-16. *Diabetes Care*. 33:322-326.

Laplante, M., and D.M. Sabatini. 2009. mTOR signaling at a glance. *J Cell Sci*. 122:3589-3594.

Laplante, M., and D.M. Sabatini. 2012. mTOR signaling in growth control and disease. *Cell*. 149:274-293.

Larsson, O., M. Morita, I. Topisirovic, T. Alain, M.J. Blouin, M. Pollak, and N. Sonenberg. 2012. Distinct perturbation of the translatome by the antidiabetic drug metformin. *Proc Natl Acad Sci U S A*. 109:8977-8982.

Lerner, A.G., J.P. Upton, P.V. Praveen, R. Ghosh, Y. Nakagawa, A. Igbaria, S. Shen, V. Nguyen, B.J. Backes, M. Heiman, N. Heintz, P. Greengard, S. Hui, Q. Tang, A. Trusina, S.A. Oakes, and F.R. Papa. 2012. IRE1alpha induces thioredoxin-interacting protein to activate the NLRP3 inflammasome and promote programmed cell death under irremediable ER stress. *Cell Metab*. 16:250-264.

Lheureux, S., C. Lecerf, M. Briand, M.H. Louis, S. Dutoit, A. Jebahi, F. Giffard, C.B. Fournier, A. Batalla, L. Poulain, and N. Aide. 2013. (18)F-FDG Is a Surrogate Marker of Therapy Response and Tumor Recovery after Drug Withdrawal during Treatment with a Dual PI3K/mTOR Inhibitor in a Preclinical Model of Cisplatin-Resistant Ovarian Cancer. *Transl Oncol*. 6:586-595.

Libby, G., L.A. Donnelly, P.T. Donnan, D.R. Alessi, A.D. Morris, and J.M. Evans. 2009. New users of metformin are at low risk of incident cancer: a cohort study among people with type 2 diabetes. *Diabetes Care*. 32:1620-1625.

Lin, S.C., and D.G. Hardie. 2018. AMPK: Sensing Glucose as well as Cellular Energy Status. *Cell Metab*. 27:299-313.

Lindhurst, M.J., J.C. Sapp, J.K. Teer, J.J. Johnston, E.M. Finn, K. Peters, J. Turner, J.L. Cannons, D. Bick, L. Blakemore, C. Blumhorst, K. Brockmann, P. Calder, N. Cherman, M.A. Deardorff, D.B. Everman, G. Golas, R.M. Greenstein, B.M. Kato, K.M. Keppler-Noreuil, S.A. Kuznetsov, R.T. Miyamoto, K. Newman, D. Ng, K. O'Brien, S. Rothenberg, D.J. Schwartzentruber, V. Singhal, R. Tirabosco, J. Upton, S. Wientroub, E.H. Zackai, K. Hoag, T. Whitewood-Neal, P.G. Robey, P.L. Schwartzberg, T.N. Darling, L.L. Tosi, J.C. Mullikin, and L.G. Biesecker. 2011. A mosaic activating mutation in AKT1 associated with the Proteus syndrome. *N Engl J Med*. 365:611-619.

Lindqvist, L.M., K. Tandoc, I. Topisirovic, and L. Furic. 2018. Cross-talk between protein synthesis, energy metabolism and autophagy in cancer. *Curr Opin Genet Dev*. 48:104-111.

Lindsley, C.W., S.F. Barnett, M.E. Layton, and M.T. Bilodeau. 2008. The PI3K/Akt pathway: recent progress in the development of ATP-competitive and allosteric Akt kinase inhibitors. *Curr Cancer Drug Targets*. 8:7-18.

Lindsten, T., J.A. Golden, W.X. Zong, J. Minarcik, M.H. Harris, and C.B. Thompson. 2003. The proapoptotic activities of Bax and Bak limit the size of the neural stem cell pool. *J Neurosci*. 23:11112-11119.

Liu, B., Z. Fan, S.M. Edgerton, X.S. Deng, I.N. Alimova, S.E. Lind, and A.D. Thor. 2009. Metformin induces unique biological and molecular responses in triple negative breast cancer cells. *Cell Cycle*. 8:2031-2040.

Liu, Y., J. Lau, W. Li, W. Tempel, L. Li, A. Dong, A. Narula, S. Qin, and J. Min. 2016. Structural basis for the regulatory role of the PPxY motifs in the thioredoxin-interacting protein TXNIP. *Biochem J*. 473:179-187.

Lochhead, P.A., I.P. Salt, K.S. Walker, D.G. Hardie, and C. Sutherland. 2000. 5-aminoimidazole-4-carboxamide riboside mimics the effects of insulin on the expression of the 2 key gluconeogenic genes PEPCK and glucose-6-phosphatase. *Diabetes*. 49:896-903.

Long, X., Y. Lin, S. Ortiz-Vega, K. Yonezawa, and J. Avruch. 2005. Rheb binds and regulates the mTOR kinase. *Curr Biol*. 15:702-713.

Luiken, J.J., S.L. Coort, J. Willems, W.A. Coumans, A. Bonen, G.J. van der Vusse, and J.F. Glatz. 2003. Contraction-induced fatty acid translocase/CD36 translocation in rat cardiac myocytes is mediated through AMP-activated protein kinase signaling. *Diabetes*. 52:1627-1634.

Maira, S.M., F. Stauffer, J. Brueggen, P. Furet, C. Schnell, C. Fritsch, S. Brachmann, P. Chene, A. De Pover, K. Schoemaker, D. Fabbro, D. Gabriel, M. Simonen, L. Murphy, P. Finan, W. Sellers, and C. Garcia-Echeverria. 2008. Identification and characterization of NVP-BEZ235, a new orally available dual phosphatidylinositol 3-kinase/mammalian target of rapamycin inhibitor with potent in vivo antitumor activity. *Mol Cancer Ther*. 7:1851-1863.

Malanga, D., M. Scrima, C. De Marco, F. Fabiani, N. De Rosa, S. De Gisi, N. Malara, R. Savino, G. Rocco, G. Chiappetta, R. Franco, V. Tirino, G. Pirozzi, and G. Viglietto. 2008. Activating E17K mutation in the gene encoding the protein kinase AKT1 in a subset of squamous cell carcinoma of the lung. *Cell Cycle*. 7:665-669.

Manning, B.D., and A. Toker. 2017. AKT/PKB Signaling: Navigating the Network. *Cell*. 169:381-405.

Marone, R., V. Cmiljanovic, B. Giese, and M.P. Wymann. 2008. Targeting phosphoinositide 3-kinase: moving towards therapy. *Biochim Biophys Acta*. 1784:159-185.

Martin, K.R., W. Zhou, M.J. Bowman, J. Shih, K.S. Au, K.E. Dittenhafer-Reed, K.A. Sisson, J. Koeman, D.J. Weisenberger, S.L. Cottingham, S.T. DeRoos, O. Devinsky, M.E. Winn, A.D. Cherniack, H. Shen, H. Northrup, D.A. Krueger, and J.P. MacKeigan. 2017. The genomic landscape of tuberous sclerosis complex. *Nat Commun*. 8:15816.

Masaki, S., H. Masutani, E. Yoshihara, and J. Yodoi. 2012. Deficiency of thioredoxin binding protein-2 (TBP-2) enhances TGF-beta signaling and promotes epithelial to mesenchymal transition. *PLoS One*. 7:e39900.

Masvidal, L., L. Hulea, L. Furic, I. Topisirovic, and O. Larsson. 2017. mTOR-sensitive translation: Cleared fog reveals more trees. *RNA Biol*. 14:1299-1305.

McLelland, J. 1985. Recovery from metformin overdose. *Diabet Med*. 2:410-411.

McVie-Wylie, A.J., D.R. Lamson, and Y.T. Chen. 2001. Molecular cloning of a novel member of the GLUT family of transporters, SLC2a10 (GLUT10), localized on chromosome 20q13.1: a candidate gene for NIDDM susceptibility. *Genomics*. 72:113-117.

Merrill, G.F., E.J. Kurth, D.G. Hardie, and W.W. Winder. 1997. AICA riboside increases AMP-activated protein kinase, fatty acid oxidation, and glucose uptake in rat muscle. *Am J Physiol*. 273:E1107-1112.

Miloslavski, R., E. Cohen, A. Avraham, Y. Iluz, Z. Hayouka, J. Kasir, R. Mudhasani, S.N. Jones, N. Cybulski, M.A. Ruegg, O. Larsson, V. Gandin, A. Rajakumar, I. Topisirovic, and O. Meyuhas. 2014. Oxygen sufficiency controls TOP mRNA translation via the TSC-Rheb-mTOR pathway in a 4E-BP-independent manner. *J Mol Cell Biol*. 6:255-266.

Minn, A.H., C. Hafele, and A. Shalev. 2005. Thioredoxin-interacting protein is stimulated by glucose through a carbohydrate response element and induces beta-cell apoptosis. *Endocrinology*. 146:2397-2405.

Monami, M., C. Lamanna, D. Balzi, N. Marchionni, and E. Mannucci. 2009. Sulphonylureas and cancer: a case-control study. *Acta Diabetol*. 46:279-284.

Morrison, J.A., L.A. Pike, S.B. Sams, V. Sharma, Q. Zhou, J.J. Severson, A.C. Tan, W.M. Wood, and B.R. Haugen. 2014. Thioredoxin interacting protein (TXNIP) is a novel tumor suppressor in thyroid cancer. *Mol Cancer*. 13:62.

Munday, M.R., D.G. Campbell, D. Carling, and D.G. Hardie. 1988. Identification by amino acid sequencing of three major regulatory phosphorylation sites on rat acetyl-CoA carboxylase. *Eur J Biochem*. 175:331-338.

Muoio, D.M. 2007. TXNIP links redox circuitry to glucose control. *Cell Metab*. 5:412-414.

Murakami, T., T. Nishiyama, T. Shirotani, Y. Shinohara, M. Kan, K. Ishii, F. Kanai, S. Nakazuru, and Y. Ebina. 1992. Identification of two enhancer elements in the gene encoding the type 1 glucose transporter from the mouse which are responsive to serum, growth factor, and oncogenes. *J Biol Chem*. 267:9300-9306.

Myers, A.P., and L.C. Cantley. 2010. Targeting a common collaborator in cancer development. *Sci Transl Med*. 2:48ps45.

Nie, W., W. Huang, W. Zhang, J. Xu, W. Song, Y. Wang, A. Zhu, J. Luo, G. Huang, Y. Wang, and X. Guan. 2015. TXNIP interaction with the Her-1/2 pathway contributes to overall survival in breast cancer. *Oncotarget*. 6:3003-3012.

Nishinaka, Y., A. Nishiyama, H. Masutani, S. Oka, K.M. Ahsan, Y. Nakayama, Y. Ishii, H. Nakamura, M. Maeda, and J. Yodoi. 2004. Loss of thioredoxin-binding protein-2/vitamin D3 up-regulated protein 1 in human T-cell leukemia virus type I-dependent T-cell transformation: implications for adult T-cell leukemia leukemogenesis. *Cancer Res*. 64:1287-1292.

Nishiyama, A., M. Matsui, S. Iwata, K. Hirota, H. Masutani, H. Nakamura, Y. Takagi, H. Sono, Y. Gon, and J. Yodoi. 1999. Identification of thioredoxin-binding protein-2/vitamin D(3) up-regulated protein 1 as a negative regulator of thioredoxin function and expression. *J Biol Chem*. 274:21645-21650.

Ohtake, F., H. Tsuchiya, Y. Saeki, and K. Tanaka. 2018. K63 ubiquitylation triggers proteasomal degradation by seeding branched ubiquitin chains. *Proc Natl Acad Sci U S A*. 115:E1401-E1408.

Oslowski, C.M., T. Hara, B. O'Sullivan-Murphy, K. Kanekura, S. Lu, M. Hara, S. Ishigaki, L.J. Zhu, E. Hayashi, S.T. Hui, D. Greiner, R.J. Kaufman, R. Bortell, and F. Urano. 2012. Thioredoxin-interacting protein mediates ER stress-induced beta cell death through initiation of the inflammasome. *Cell Metab*. 16:265-273.

Osthus, R.C., H. Shim, S. Kim, Q. Li, R. Reddy, M. Mukherjee, Y. Xu, D. Wonsey, L.A. Lee, and C.V. Dang. 2000. Deregulation of glucose transporter 1 and glycolytic gene expression by c-Myc. *J Biol Chem*. 275:21797-21800.

Pal, S.K., and D.I. Quinn. 2013. Differentiating mTOR inhibitors in renal cell carcinoma. *Cancer Treat Rev*. 39:709-719.

Parikh, H., E. Carlsson, W.A. Chutkow, L.E. Johansson, H. Storgaard, P. Poulsen, R. Saxena, C. Ladd, P.C. Schulze, M.J. Mazzini, C.B. Jensen, A. Krook, M. Bjornholm, H. Tornqvist, J.R. Zierath, M. Ridderstrale, D. Altshuler, R.T. Lee, A. Vaag, L.C. Groop, and V.K. Mootha. 2007. TXNIP regulates peripheral glucose metabolism in humans. *PLoS Med*. 4:e158.

Pause, A., G.J. Belsham, A.C. Gingras, O. Donze, T.A. Lin, J.C. Lawrence, Jr., and N. Sonenberg. 1994. Insulin-dependent stimulation of protein synthesis by phosphorylation of a regulator of 5'-cap function. *Nature*. 371:762-767.

Phay, J.E., H.B. Hussain, and J.F. Moley. 2000. Cloning and expression analysis of a novel member of the facilitative glucose transporter family, SLC2A9 (GLUT9). *Genomics*. 66:217-220.
Pirola, L., S. Bonnafous, A.M. Johnston, C. Chaussade, F. Portis, and E. Van Obberghen. 2003. Phosphoinositide 3-kinase-mediated reduction of insulin receptor substrate-1/2 protein expression via different mechanisms contributes to the insulin-induced desensitization of its signaling pathways in L6 muscle cells. *J Biol Chem*. 278:15641-15651.
Pollak, M. 2010. Metformin and other biguanides in oncology: advancing the research agenda. *Cancer Prev Res (Phila)*. 3:1060-1065.
Pollak, M. 2013. Potential applications for biguanides in oncology. *J Clin Invest*. 123:3693-3700.
Pollak, M. 2017. The effects of metformin on gut microbiota and the immune system as research frontiers. *Diabetologia*. 60:1662-1667.
Porta, C., C. Paglino, and A. Mosca. 2014. Targeting PI3K/Akt/mTOR Signaling in Cancer. *Front Oncol*. 4:64.
Proud, C.G. 2013. mTORC1 regulates the efficiency and cellular capacity for protein synthesis. *Biochem Soc Trans*. 41:923-926.
Puglisi, M., P. Thavasu, A. Stewart, J.S. de Bono, M.E. O'Brien, S. Popat, J. Bhosle, and U. Banerji. 2014. AKT inhibition synergistically enhances growth-inhibitory effects of gefitinib and increases apoptosis in non-small cell lung cancer cell lines. *Lung Cancer*. 85:141-146.
Racker, E. 1972. Bioenergetics and the problem of tumor growth. *Am Sci*. 60:56-63.
Rathmell, J.C., C.J. Fox, D.R. Plas, P.S. Hammerman, R.M. Cinalli, and C.B. Thompson. 2003. Akt-directed glucose metabolism can prevent Bax conformation change and promote growth factor-independent survival. *Mol Cell Biol*. 23:7315-7328.
Rathmell, J.C., M.G. Vander Heiden, M.H. Harris, K.A. Frauwirth, and C.B. Thompson. 2000. In the absence of extrinsic signals, nutrient utilization by lymphocytes is insufficient to maintain either cell size or viability. *Mol Cell*. 6:683-692.
Rea, S., and D.E. James. 1997. Moving GLUT4: the biogenesis and trafficking of GLUT4 storage vesicles. *Diabetes*. 46:1667-1677.
Riganti, C., E. Gazzano, M. Polimeni, E. Aldieri, and D. Ghigo. 2012. The pentose phosphate pathway: an antioxidant defense and a crossroad in tumor cell fate. *Free Radic Biol Med*. 53:421-436.
Rogers, S., S.E. Docherty, J.L. Slavin, M.A. Henderson, and J.D. Best. 2003. Differential expression of GLUT12 in breast cancer and normal breast tissue. *Cancer Lett*. 193:225-233.
Rogers, S., M.L. Macheda, S.E. Docherty, M.D. Carty, M.A. Henderson, W.C. Soeller, E.M. Gibbs, D.E. James, and J.D. Best. 2002. Identification of a novel glucose transporter-like protein-GLUT-12. *Am J Physiol Endocrinol Metab*. 282:E733-738.
Roux, P.P., and I. Topisirovic. 2018. Signaling Pathways Involved in the Regulation of mRNA Translation. *Mol Cell Biol*. 38.
Russell, R.R., 3rd, R. Bergeron, G.I. Shulman, and L.H. Young. 1999. Translocation of myocardial GLUT-4 and increased glucose uptake through activation of AMPK by AICAR. *Am J Physiol*. 277:H643-649.
Sabatini, D.M. 2006. mTOR and cancer: insights into a complex relationship. *Nat Rev Cancer*. 6:729-734.

Saha, A.K., P.R. Avilucea, J.M. Ye, M.M. Assifi, E.W. Kraegen, and N.B. Ruderman. 2004. Pioglitazone treatment activates AMP-activated protein kinase in rat liver and adipose tissue in vivo. *Biochem Biophys Res Commun*. 314:580-585.

Saitoh, M., H. Nishitoh, M. Fujii, K. Takeda, K. Tobiume, Y. Sawada, M. Kawabata, K. Miyazono, and H. Ichijo. 1998. Mammalian thioredoxin is a direct inhibitor of apoptosis signal-regulating kinase (ASK) 1. *EMBO J*. 17:2596-2606.

Sakamoto, K., A. McCarthy, D. Smith, K.A. Green, D. Grahame Hardie, A. Ashworth, and D.R. Alessi. 2005. Deficiency of LKB1 in skeletal muscle prevents AMPK activation and glucose uptake during contraction. *EMBO J*. 24:1810-1820.

Sancak, Y., C.C. Thoreen, T.R. Peterson, R.A. Lindquist, S.A. Kang, E. Spooner, S.A. Carr, and D.M. Sabatini. 2007. PRAS40 is an insulin-regulated inhibitor of the mTORC1 protein kinase. *Mol Cell*. 25:903-915.

Sanchez-Cespedes, M., P. Parrella, M. Esteller, S. Nomoto, B. Trink, J.M. Engles, W.H. Westra, J.G. Herman, and D. Sidransky. 2002. Inactivation of LKB1/STK11 is a common event in adenocarcinomas of the lung. *Cancer Res*. 62:3659-3662.

Sarbassov, D.D., D.A. Guertin, S.M. Ali, and D.M. Sabatini. 2005. Phosphorylation and regulation of Akt/PKB by the rictor-mTOR complex. *Science*. 307:1098-1101.

Saxton, R.A., and D.M. Sabatini. 2017. mTOR Signaling in Growth, Metabolism, and Disease. *Cell*. 168:960-976.

Schulze, P.C., J. Yoshioka, T. Takahashi, Z. He, G.L. King, and R.T. Lee. 2004. Hyperglycemia promotes oxidative stress through inhibition of thioredoxin function by thioredoxin-interacting protein. *J Biol Chem*. 279:30369-30374.

Segal, E.D., A. Yasmeen, M.C. Beauchamp, J. Rosenblatt, M. Pollak, and W.H. Gotlieb. 2011. Relevance of the OCT1 transporter to the antineoplastic effect of biguanides. *Biochem Biophys Res Commun*. 414:694-699.

Serra, V., B. Markman, M. Scaltriti, P.J. Eichhorn, V. Valero, M. Guzman, M.L. Botero, E. Llonch, F. Atzori, S. Di Cosimo, M. Maira, C. Garcia-Echeverria, J.L. Parra, J. Arribas, and J. Baselga. 2008. NVP-BEZ235, a dual PI3K/mTOR inhibitor, prevents PI3K signaling and inhibits the growth of cancer cells with activating PI3K mutations. *Cancer Res*. 68:8022-8030.

Shaked, M., M. Ketzinel-Gilad, Y. Ariav, E. Cerasi, N. Kaiser, and G. Leibowitz. 2009. Insulin counteracts glucotoxic effects by suppressing thioredoxin-interacting protein production in INS-1E beta cells and in Psammomys obesus pancreatic islets. *Diabetologia*. 52:636-644.

Sharma, C., H.X. Wang, Q. Li, K. Knoblich, E.S. Reisenbichler, A.L. Richardson, and M.E. Hemler. 2017. Protein Acyltransferase DHHC3 Regulates Breast Tumor Growth, Oxidative Stress, and Senescence. *Cancer Res*. 77:6880-6890.

Shaw, L.M. 2011. The insulin receptor substrate (IRS) proteins: at the intersection of metabolism and cancer. *Cell Cycle*. 10:1750-1756.

Shaw, R.J., M. Kosmatka, N. Bardeesy, R.L. Hurley, L.A. Witters, R.A. DePinho, and L.C. Cantley. 2004. The tumor suppressor LKB1 kinase directly activates AMP-activated kinase and regulates apoptosis in response to energy stress. *Proc Natl Acad Sci U S A*. 101:3329-3335.

Shaw, R.J., K.A. Lamia, D. Vasquez, S.H. Koo, N. Bardeesy, R.A. Depinho, M. Montminy, and L.C. Cantley. 2005. The kinase LKB1 mediates glucose homeostasis in liver and therapeutic effects of metformin. *Science*. 310:1642-1646.

Shen, L., J.M. O'Shea, M.R. Kaadige, S. Cunha, B.R. Wilde, A.L. Cohen, A.L. Welm, and D.E. Ayer. 2015. Metabolic reprogramming in triple-negative breast cancer through Myc suppression of TXNIP. *Proc Natl Acad Sci U S A*. 112:5425-5430.

Sheth, S.S., J.S. Bodnar, A. Ghazalpour, C.K. Thipphavong, S. Tsutsumi, A.D. Tward, P. Demant, T. Kodama, H. Aburatani, and A.J. Lusis. 2006. Hepatocellular carcinoma in Txnip-deficient mice. *Oncogene*. 25:3528-3536.

Shim, H., Y.S. Chun, B.C. Lewis, and C.V. Dang. 1998. A unique glucose-dependent apoptotic pathway induced by c-Myc. *Proc Natl Acad Sci U S A*. 95:1511-1516.

Shim, H., C. Dolde, B.C. Lewis, C.S. Wu, G. Dang, R.A. Jungmann, R. Dalla-Favera, and C.V. Dang. 1997. c-Myc transactivation of LDH-A: implications for tumor metabolism and growth. *Proc Natl Acad Sci U S A*. 94:6658-6663.

Shimobayashi, M., and M.N. Hall. 2014. Making new contacts: the mTOR network in metabolism and signalling crosstalk. *Nat Rev Mol Cell Biol*. 15:155-162.

Sonenberg, N., and A.G. Hinnebusch. 2009. Regulation of translation initiation in eukaryotes: mechanisms and biological targets. *Cell*. 136:731-745.

Stambolic, V., A. Suzuki, J.L. de la Pompa, G.M. Brothers, C. Mirtsos, T. Sasaki, J. Ruland, J.M. Penninger, D.P. Siderovski, and T.W. Mak. 1998. Negative regulation of PKB/Akt-dependent cell survival by the tumor suppressor PTEN. *Cell*. 95:29-39.

Stein, S.C., A. Woods, N.A. Jones, M.D. Davison, and D. Carling. 2000. The regulation of AMP-activated protein kinase by phosphorylation. *Biochem J*. 345 Pt 3:437-443.

Stoltzman, C.A., M.R. Kaadige, C.W. Peterson, and D.E. Ayer. 2011. MondoA senses non-glucose sugars: regulation of thioredoxin-interacting protein (TXNIP) and the hexose transport curb. *J Biol Chem*. 286:38027-38034.

Stoltzman, C.A., C.W. Peterson, K.T. Breen, D.M. Muoio, A.N. Billin, and D.E. Ayer. 2008. Glucose sensing by MondoA:Mlx complexes: a role for hexokinases and direct regulation of thioredoxin-interacting protein expression. *Proc Natl Acad Sci U S A*. 105:6912-6917.

Stuttfeld, E., C.H. Aylett, S. Imseng, D. Boehringer, A. Scaiola, E. Sauer, M.N. Hall, T. Maier, and N. Ban. 2018. Architecture of the human mTORC2 core complex. *Elife*. 7.

Suissa, S. 2017. Metformin to Treat Cancer: Misstep in Translational Research from Observational Studies. *Epidemiology*. 28:455-458.

Sullivan, J.E., K.J. Brocklehurst, A.E. Marley, F. Carey, D. Carling, and R.K. Beri. 1994. Inhibition of lipolysis and lipogenesis in isolated rat adipocytes with AICAR, a cell-permeable activator of AMP-activated protein kinase. *FEBS Lett*. 353:33-36.

Sullivan, L.B., D.Y. Gui, A.M. Hosios, L.N. Bush, E. Freinkman, and M.G. Vander Heiden. 2015. Supporting Aspartate Biosynthesis Is an Essential Function of Respiration in Proliferating Cells. *Cell*. 162:552-563.

Sullivan, W.J., P.J. Mullen, E.W. Schmid, A. Flores, M. Momcilovic, M.S. Sharpley, D. Jelinek, A.E. Whiteley, M.B. Maxwell, B.R. Wilde, U. Banerjee, H.A. Coller, D.B. Shackelford, D. Braas, D.E. Ayer, T.Q. de Aguiar Vallim, W.E. Lowry, and H.R. Christofk. 2018. Extracellular Matrix Remodeling Regulates Glucose Metabolism through TXNIP Destabilization. *Cell*. 175:117-132 e121.

Thompson, C.B. 2011. Rethinking the regulation of cellular metabolism. *Cold Spring Harb Symp Quant Biol*. 76:23-29.

Thoreen, C.C., S.A. Kang, J.W. Chang, Q. Liu, J. Zhang, Y. Gao, L.J. Reichling, T. Sim, D.M. Sabatini, and N.S. Gray. 2009. An ATP-competitive mammalian target of rapamycin

inhibitor reveals rapamycin-resistant functions of mTORC1. *J Biol Chem*. 284:8023-8032.
Thorens, B. 2015. GLUT2, glucose sensing and glucose homeostasis. *Diabetologia*. 58:221-232.
Tiainen, M., A. Ylikorkala, and T.P. Makela. 1999. Growth suppression by Lkb1 is mediated by a G(1) cell cycle arrest. *Proc Natl Acad Sci U S A*. 96:9248-9251.
Vander Heiden, M.G., L.C. Cantley, and C.B. Thompson. 2009. Understanding the Warburg effect: the metabolic requirements of cell proliferation. *Science*. 324:1029-1033.
Velasco, G., M.J. Geelen, and M. Guzman. 1997. Control of hepatic fatty acid oxidation by 5'-AMP-activated protein kinase involves a malonyl-CoA-dependent and a malonyl-CoA-independent mechanism. *Arch Biochem Biophys*. 337:169-175.
Veramendi, J., A.R. Fernie, A. Leisse, L. Willmitzer, and R.N. Trethewey. 2002. Potato hexokinase 2 complements transgenic Arabidopsis plants deficient in hexokinase 1 but does not play a key role in tuber carbohydrate metabolism. *Plant Mol Biol*. 49:491-501.
Vezina, C., A. Kudelski, and S.N. Sehgal. 1975. Rapamycin (AY-22,989), a new antifungal antibiotic. I. Taxonomy of the producing streptomycete and isolation of the active principle. *J Antibiot (Tokyo)*. 28:721-726.
Viale, A., P. Pettazzoni, C.A. Lyssiotis, H. Ying, N. Sanchez, M. Marchesini, A. Carugo, T. Green, S. Seth, V. Giuliani, M. Kost-Alimova, F. Muller, S. Colla, L. Nezi, G. Genovese, A.K. Deem, A. Kapoor, W. Yao, E. Brunetto, Y. Kang, M. Yuan, J.M. Asara, Y.A. Wang, T.P. Heffernan, A.C. Kimmelman, H. Wang, J.B. Fleming, L.C. Cantley, R.A. DePinho, and G.F. Draetta. 2014. Oncogene ablation-resistant pancreatic cancer cells depend on mitochondrial function. *Nature*. 514:628-632.
Waldhart, A.N., H. Dykstra, A.S. Peck, E.A. Boguslawski, Z.B. Madaj, J. Wen, K. Veldkamp, M. Hollowell, B. Zheng, L.C. Cantley, T.E. McGraw, and N. Wu. 2017. Phosphorylation of TXNIP by AKT Mediates Acute Influx of Glucose in Response to Insulin. *Cell Rep*. 19:2005-2013.
Wan, X., B. Harkavy, N. Shen, P. Grohar, and L.J. Helman. 2007. Rapamycin induces feedback activation of Akt signaling through an IGF-1R-dependent mechanism. *Oncogene*. 26:1932-1940.
Warburg, O., F. Wind, and E. Negelein. 1927. The Metabolism of Tumors in the Body. *J Gen Physiol*. 8:519-530.
Wieman, H.L., J.A. Wofford, and J.C. Rathmell. 2007. Cytokine stimulation promotes glucose uptake via phosphatidylinositol-3 kinase/Akt regulation of Glut1 activity and trafficking. *Mol Biol Cell*. 18:1437-1446.
Winder, W.W., and D.G. Hardie. 1996. Inactivation of acetyl-CoA carboxylase and activation of AMP-activated protein kinase in muscle during exercise. *Am J Physiol*. 270:E299-304.
Winder, W.W., and D.G. Hardie. 1999. AMP-activated protein kinase, a metabolic master switch: possible roles in type 2 diabetes. *Am J Physiol*. 277:E1-10.
Wojtaszewski, J.F., P. Nielsen, B.F. Hansen, E.A. Richter, and B. Kiens. 2000. Isoform-specific and exercise intensity-dependent activation of 5'-AMP-activated protein kinase in human skeletal muscle. *J Physiol*. 528 Pt 1:221-226.
Woods, A., K. Dickerson, R. Heath, S.P. Hong, M. Momcilovic, S.R. Johnstone, M. Carlson, and D. Carling. 2005. Ca2+/calmodulin-dependent protein kinase kinase-beta acts upstream of AMP-activated protein kinase in mammalian cells. *Cell Metab*. 2:21-33.
Wu, N., B. Zheng, A. Shaywitz, Y. Dagon, C. Tower, G. Bellinger, C.H. Shen, J. Wen, J. Asara, T.E. McGraw, B.B. Kahn, and L.C. Cantley. 2013. AMPK-dependent degradation of

TXNIP upon energy stress leads to enhanced glucose uptake via GLUT1. *Mol Cell*. 49:1167-1175.
Xu, G., J. Chen, G. Jing, and A. Shalev. 2013. Thioredoxin-interacting protein regulates insulin transcription through microRNA-204. *Nat Med*. 19:1141-1146.
Yang, H., W. Kong, L. He, J.J. Zhao, J.D. O'Donnell, J. Wang, R.M. Wenham, D. Coppola, P.A. Kruk, S.V. Nicosia, and J.Q. Cheng. 2008. MicroRNA expression profiling in human ovarian cancer: miR-214 induces cell survival and cisplatin resistance by targeting PTEN. *Cancer Res*. 68:425-433.
Yang, L., H.C. Dan, M. Sun, Q. Liu, X.M. Sun, R.I. Feldman, A.D. Hamilton, M. Polokoff, S.V. Nicosia, M. Herlyn, S.M. Sebti, and J.Q. Cheng. 2004. Akt/protein kinase B signaling inhibitor-2, a selective small molecule inhibitor of Akt signaling with antitumor activity in cancer cells overexpressing Akt. *Cancer Res*. 64:4394-4399.
Yao, R., and G.M. Cooper. 1995. Requirement for phosphatidylinositol-3 kinase in the prevention of apoptosis by nerve growth factor. *Science*. 267:2003-2006.
Yatscoff, R.W., D.F. LeGatt, and N.M. Kneteman. 1993. Therapeutic monitoring of rapamycin: a new immunosuppressive drug. *Ther Drug Monit*. 15:478-482.
Yoshihara, E., S. Masaki, Y. Matsuo, Z. Chen, H. Tian, and J. Yodoi. 2014. Thioredoxin/Txnip: redoxisome, as a redox switch for the pathogenesis of diseases. *Front Immunol*. 4:514.
Yu, F.X., T.F. Chai, H. He, T. Hagen, and Y. Luo. 2010. Thioredoxin-interacting protein (Txnip) gene expression: sensing oxidative phosphorylation status and glycolytic rate. *J Biol Chem*. 285:25822-25830.
Yu, F.X., and Y. Luo. 2009. Tandem ChoRE and CCAAT motifs and associated factors regulate Txnip expression in response to glucose or adenosine-containing molecules. *PLoS One*. 4:e8397.
Zakikhani, M., M.J. Blouin, E. Piura, and M.N. Pollak. 2010. Metformin and rapamycin have distinct effects on the AKT pathway and proliferation in breast cancer cells. *Breast Cancer Res Treat*. 123:271-279.
Zakikhani, M., R. Dowling, I.G. Fantus, N. Sonenberg, and M. Pollak. 2006. Metformin is an AMP kinase-dependent growth inhibitor for breast cancer cells. *Cancer Res*. 66:10269-10273.
Zamora-Leon, S.P., D.W. Golde, Concha, II, C.I. Rivas, F. Delgado-Lopez, J. Baselga, F. Nualart, and J.C. Vera. 1996. Expression of the fructose transporter GLUT5 in human breast cancer. *Proc Natl Acad Sci U S A*. 93:1847-1852.
Zech, R., S. Kiontke, U. Mueller, A. Oeckinghaus, and D. Kummel. 2016. Structure of the Tuberous Sclerosis Complex 2 (TSC2) N Terminus Provides Insight into Complex Assembly and Tuberous Sclerosis Pathogenesis. *J Biol Chem*. 291:20008-20020.
Zhang, J., Z. Gao, J. Yin, M.J. Quon, and J. Ye. 2008. S6K directly phosphorylates IRS-1 on Ser-270 to promote insulin resistance in response to TNF-(alpha) signaling through IKK2. *J Biol Chem*. 283:35375-35382.
Zhang, W., S. Patil, B. Chauhan, S. Guo, D.R. Powell, J. Le, A. Klotsas, R. Matika, X. Xiao, R. Franks, K.A. Heidenreich, M.P. Sajan, R.V. Farese, D.B. Stolz, P. Tso, S.H. Koo, M. Montminy, and T.G. Unterman. 2006. FoxO1 regulates multiple metabolic pathways in the liver: effects on gluconeogenic, glycolytic, and lipogenic gene expression. *J Biol Chem*. 281:10105-10117.

Zhou, G., R. Myers, Y. Li, Y. Chen, X. Shen, J. Fenyk-Melody, M. Wu, J. Ventre, T. Doebber, N. Fujii, N. Musi, M.F. Hirshman, L.J. Goodyear, and D.E. Moller. 2001. Role of AMP-activated protein kinase in mechanism of metformin action. *J Clin Invest*. 108:1167-1174.

Zhuo de, X., X.H. Niu, Y.C. Chen, D.Q. Xin, Y.L. Guo, and Z.B. Mao. 2010. Vitamin D3 up-regulated protein 1(VDUP1) is regulated by FOXO3A and miR-17-5p at the transcriptional and post-transcriptional levels, respectively, in senescent fibroblasts. *J Biol Chem*. 285:31491-31501.